

STRESS - STRAIN RELATIONSHIPS

FOR CONFINED CONCRETE : RECTANGULAR SECTIONS

A report submitted in partial fulfilment of
the requirements for the degree of Master of
Engineering at the University of Canterbury,
Christchurch, New Zealand.

by

BRYAN D. SCOTT

February 1980



SPECIMEN 12

12DH20 R10-98

$\dot{E} = .0167/S$

ABSTRACT

An experimental investigation into the behaviour of square, confined, reinforced concrete columns was undertaken. Thirty 450 mm square, 1200 mm high units were cast with varying amounts of longitudinal and lateral steel. These were subjected to concentric or eccentric axial loads to failure at slow or dynamic loading rates.

Confinement requirements of reinforced concrete columns are discussed and the results and analyses of experimental work presented.

Results include an assessment of the significance of loading rate, eccentricity, amount and distribution of longitudinal steel, and the amount of confining steel.

A general stress-strain curve for rectangular concrete sections loaded at seismic rates is proposed and compared with existing curves based on previous static loading tests.

ACKNOWLEDGEMENTS

The research for this report was carried out in the Department of Civil Engineering, University of Canterbury, under the overall guidance of its Head, Professor R. Park.

The project was supervised by Professor R. Park and Dr. M.J.N. Priestley, both of whom have given invaluable advice, and careful guidance. My thanks also to Professor S.M. Uzumeri (Toronto, Canada) for his introduction to this topic.

I wish to thank Mr. N.W. Prebble, Technical Officer, and all the technical staff of the Civil Engineering Department who have been associated with this project. Special thanks are due to Mr. A. Bell, Mr. G. Hill, and Mr. G. Clark for their contribution towards constructing, preparing and testing the specimens.

The financial assistance of the National Roads Board is gratefully acknowledged.

Thanks are also due to Mrs. V. Grey for her tracing and to Mrs. C. Gaerty for typing this text.

The special care and attention given by Ashby Bros. Ltd. to obtaining uniform concrete properties is gratefully acknowledged.

Finally a special thanks to my wife Gaile, for her support and encouragement.

TABLE OF CONTENTS

	<u>Page:</u>
ABSTRACT	i
ACKNOWLEDGEMENTS	ii
TABLE OF CONTENTS	iii
LIST OF FIGURES	vi
LIST OF TABLES	ix
NOTATION	x
 CHAPTER ONE :: INTRODUCTION	
1.1 General	1
1.2 Aim	2
1.3 Scope	2
1.4 Format	2
1.5 Previous Research	2
1.5.1 Chan (1955)	4
1.5.2 Roy and Sozen (1964)	4
1.5.3 Bertero and Felippa (1964)	7
1.5.4 Soliman and Yu (1967)	7
1.5.5 Kent and Park (1971)	9
1.5.6 Sargin (1971)	11
1.5.7 Vallenias, Bertero and Popov (1977)	12
1.5.8 Sheikh and Uzumeri (1978)	15
1.5.9 Modified Kent and Park (1979)	17
1.5.10 Summary	18
 CHAPTER TWO : CONFINEMENT REQUIREMENTS FOR PLASTIC HINGE ZONES IN REINFORCED CONCRETE COLUMNS	
2.0 Summary	20
2.1 The Codes Considered	20
2.1.1 ACI 318-77	21
2.1.2 SEAOC (1975)	21
2.1.3 ATC (1978)	22
2.1.4 ACI Committee 343	22
2.1.5 Japanese Practice	22
2.1.6 Ministry of Works and Development, Civil Division	22
2.1.7 Draft SANZ Concrete Design Code	23
2.2 Comparison of Code Requirements for A Typical Rectangular Column.	25

2.3	Conclusions	27
CHAPTER THREE : DESIGN AND CONSTRUCTION OF TEST UNITS		
3.0	Summary	28
3.1	Unit Size Criteria	28
3.2	Design of Test Units	28
3.2.1	Longitudinal Steel	28
3.2.2	Hoop Steel	29
3.3	Material Properties	32
3.3.1	Steel	32
3.3.2	Concrete	32
3.4	Construction	40
CHAPTER FOUR : INSTRUMENTATION AND TESTING PROCEDURE		
4.0	Summary	42
4.1	Instrumentation	42
4.1.1	Load Measurement	42
4.1.2	Longitudinal Concrete Strains	42
4.1.3	Hoop Reinforcement	43
4.2	Testing Procedure	44
4.2.1	Test Unit Preparation	44
4.2.2	Testing Procedure	45
CHAPTER FIVE : TEST RESULTS		
5.0	Summary	47
5.1	General Behaviour and Visual Observations	47
5.2	Presentation of Results	56
5.3	Discussion of Results	87
5.3.1	Rate of Loading	87
5.3.2	Confinement Ratio	92
5.3.3	Distribution of Longitudinal Steel	97
5.3.4	Ultimate Compression Strain	97
5.3.5	Strength of Longitudinal Steel	100
5.3.6	Eccentricity of Loading	100

CHAPTER SIX : CONCLUSIONS AND FUTURE RESEARCH

6.0 Summary	101
6.1 Conclusions	101
6.2 Recommendations for Future Research	102

APPENDIX A : REFERENCES	103
-------------------------	-----

LIST OF FIGURES

<u>Figure</u>	<u>Title</u>	<u>Page:</u>
1.1	Effect of Tie Spacing on Stress-Strain Relationship of Concrete (Roy and Sozen (1963)(10)	5
1.2	Stress-Strain Curve for Concrete Confined by Rectangular Ties as Proposed by Roy and Sozen (1964)(11)	6
1.3	Stress-Strain Relationship of Confined Concrete in Flexure (Soliman and Yu 1967) (15)	8
1.4	Stress-Strain Curve for Concrete Confined by Rectangular Hoops (Kent and Park 1971) (18)	10
1.5	Comparison of Analytical Curves with Experimental Results (Vallenas et al, 1977) (24)	13
1.6	Confined Concrete with Longitudinal Reinforcement - Analytical Curve and its Comparison with Experimental Results (Vallenas et al, 1977) (24)	13
1.7	Stress-Strain Curve for Confined Concrete in Square Columns (Sheikh and Uzumeri 1978) (2)	16
1.8	Stress-Strain Curve for Concrete Confined by Rectangular Hoops (Park, Priestley and Gill, 1979)(29)	17
2.1	Comparison of Code Hoop Steel Requirements for a Square Column (Park and Priestley 1979) (30)	26
3.1	Details of Test Units and Transverse Reinforcement	31
3.2	Stress-Strain Curve for DH24 Steel (Grade 380)	33
3.3	Stress-Strain Curve for DH20 Steel (Grade 380)	34
3.4	Stress-Strain Curve for D20 Steel (Grade 275)	35
3.5	Stress-Strain Curve for R10 Hoop Steel (Grade 275)	36
3.6	Stress-Strain Curve for R12 Hoop Steel (Grade 275)	37
3.7	Strength-Age Diagram of 200 x 100 mm Diameter Cylinders	38
3.8	Photographs of the Construction Sequence	41
4.1	Strain Gauge Locations	43
4.2	Preparation of Test Units, Testing Machine and Recording Instruments	46
5.1	Bending of the Support Bars	49
5.2	Unit 12 Photographs Showing Test Sequence	51
5.3	Unit 15 Photographs Showing Test Sequence	52

5.4	Photographs Showing Selected Features of Failure for Various Test Units	53
5.5	Photographs Showing Selected Features of Failure for Various Test Units	54
5.5(e)	Mid-Height Lateral Displacement Versus Average Longitudinal Strain	55
5.6	Unit 1 Axial Load, Slow Speed	58
5.7	Unit 2 Axial Load, Slow Speed	59
5.8	Unit 3 Axial Load, High Speed	60
5.9	Unit 4 Eccentric Load, Slow Speed	61
5.10	Unit 4 Eccentric Load, Slow Speed	62
5.11	Unit 5 Eccentric Load, High Speed	63
5.12	Unit 5 Eccentric Load, High Speed	64
5.13	Unit 6 Axial Load, Slow Speed	65
5.14	Unit 7 Axial Load, High Speed	66
5.15	Unit 8 Eccentric Load, Slow Speed	67
5.16	Unit 8 Eccentric Load, Slow Speed	68
5.17	Unit 9 Eccentric Load, High Speed	69
5.18	Unit 9 Eccentric Load, High Speed	70
5.19	Unit 11 Axial Load, High Speed	71
5.20	Unit 12 Axial Load, High Speed	72
5.21	Unit 13 Axial Load, High Speed	73
5.22	Unit 14 Axial Load, High Speed	74
5.23	Unit 15 Axial Load, High Speed	75
5.24	Unit 17 Axial Load, High Speed	76
5.25	Unit 18 Axial Load, High Speed	77
5.26	Unit 19 Axial Load, High Speed	78
5.27	Unit 20 Axial Load, High Speed	79
5.28	Unit 21 Axial Load, Slow Speed	80
5.29	Unit 22 Axial Load, High Speed	81
5.30	Unit 23 Axial Load, High Speed	82

5.31	Unit 24 Axial Load, High Speed	83
5.32	Unit 25 Axial Load, High Speed	84
5.33	Unit 26 Axial Load, High Speed	85
5.34	Unit 27 Axial Load, Medium Speed	86
5.35	Plain Concrete Units Loaded at Different Rates	89
5.36	8 Bar Units Loaded at Different Rates	90
5.37	12 Bar Units Loaded at Different Rates	91
5.38	Effect of Confinement Ratio for an 8 Bar Unit	94
5.39	Effect of Confinement Ratio for a 12 Bar Unit	95
5.40	Strength Increase Versus Confinement Ratio	96
5.41	Confinement Due to Distribution of Longitudinal Steel	98

LIST OF TABLES

<u>Table</u>	<u>Title</u>	<u>Page;</u>
1.1	Summary of Tests Reported by Different Researchers. (After Sheikh (1978)(2)	3, 4
3.1	Hoop Bar Diameter and Spacing of Hoop Sets	30
3.2	Yield and Ultimate Steel Stresses	32
3.3	Test Unit Properties	39
4.1	Calculated Eccentricities	45
5.1	Summary of Results	48
5.2	The Effect of Loading Rate on Peak Stress	88

NOTATION

A_c	= area of concrete section confined by hoops
A_g	= gross area of section
A_s	= area of longitudinal steel
A_{sb}	= area of rectangular hoop bar (one leg only)
A_{sh}	= total effective area of hoop bars and supplementary cross ties in the direction under consideration within spacing s_h
b or b'	= core dimension
c	= neutral axis depth at ultimate
c_1	= centre to centre distance between the longitudinal bars
d	= effective depth of section
d'	= nominal diameter of longitudinal bar
d''	= nominal diameter of transverse reinforcement
Δ	= displacement
E_c	= modulus of elasticity of concrete
ϵ	= strain
ϵ_c	= concrete strain
ϵ_{cu}	= ultimate concrete strain
$\epsilon_{s1}, \epsilon_{s2}$	= minimum and maximum average longitudinal strains corresponding to the maximum stress in concrete (2)
ϵ_y	= steel yield strain
$\epsilon_o, \epsilon_{oo}$	= concrete strain at maximum stress level
ϵ_{20c}	= concrete strain at 20% maximum stress (18)
ϵ_{50c}	= concrete strain at 50% maximum stress for confined concrete (18)
ϵ_{50h}	= $\epsilon_{50c} - \epsilon_{50u}$ (18)
ϵ_{50u}	= concrete strain at 50% maximum stress for unconfined concrete (18)
f_c	= stress in concrete
f'_c	= concrete cylinder strength
f'_s	= stress in transverse steel
f_y	= yield stress in longitudinal steel
f_{yh}	= yield stress of transverse steel
h	= depth of full section
I_{cr}	= cracked section modulus
k	= maximum stress ratio (24)
K_s	= ratio of the strength of confined concrete to the strength of plain concrete (2)

m	= cover concrete ratio for confined concrete
M	= moment
μ	= displacement ductility factor
n	= number of longitudinal bars in the specimen
NA	= neutral axis
P_e	= axial load due to gravity and seismic loading
P_o	= $0.85 f'_c (A_g - A_{st}) + f_y A_{st}$
P_{occ}	= $0.85 f'_c (A_c - A_s) (12)$
ρ_s	= volumetric transverse steel ratio
ρ_t	= longitudinal steel percentage
ϕ	= capacity reduction factor
Φ	= curvature
Φ_u	= section curvature at ultimate
Φ_y	= section curvature at yield
s or s_h	= spacing of hoop sets
Z	= slope of falling branch of concrete stress strain curve (18)

CHAPTER ONE

INTRODUCTION

1.1 GENERAL

For moment-curvature analysis of structural members and systems it is usually necessary to model the behaviour of the materials used. For reinforced concrete structures under monotonic loading suitable models exist for unconfined concrete and for steel, but limited information is available for concrete confined by transverse reinforcement.

The stress-strain curve for unconfined concrete is well known and generally accepted to finish at $\epsilon_{cu} = 0.003$, when crushing occurs. However under seismic loading high ductilities are often demanded of structures, which require ultimate concrete strains much greater than $\epsilon_{cu} = 0.003$. These strains and ductilities can be achieved by providing longitudinal and transverse reinforcement to effectively confine the core concrete. The confinement is provided by allowing the concrete to arch stirrup to stirrup vertically and bar to bar horizontally which is often assumed to confine the core as if by an equivalent uniform lateral fluid pressure.

A knowledge of the stress-strain curve for confined concrete is particularly important for columns with high axial load levels, when the moment curvature characteristics of the column are largely dependent on the concrete compressive strength and the stress strain relationship.

Early research on confined concrete was (generally) on small scale, concentrically and monotonically loaded units, often without cover or longitudinal reinforcement. The testing was generally carried out in load controlled testing machines at slow loading rates.

Behaviour under these conditions has been used to predict behaviour under seismic conditions, which are characterised by displacement control, rapid loading rates, repeated load application, and eccentricity of loading. Recently more realistically sized units have been used but not under simulated seismic conditions.

1.2 AIM

The aim of the study of this report was to examine experimentally the confinement requirements of Chapter 17 of DZ 3101⁽¹⁾, "Members subjected to flexure and axial load - additional seismic requirements", in order to further understand the behaviour of confined concrete in rectangular reinforced concrete columns in earthquake risk areas. To minimise interpretation problems inherent in extrapolating previous test data to seismic conditions, the study aimed at testing near full size models at rapid loading rates in a displacement controlled testing machine to more closely simulate seismic conditions.

1.3 SCOPE

Thirty large scale, about half to two-thirds full size, square column sections were designed to the revised provisions of Chapter 17 of DZ 3101, and confined to four different axial load levels, nominally 0.1, 0.25, 0.4, 0.7 of $f'_c A_g$. These were subjected to concentric or eccentric axial loads to failure at slow or dynamic loading rates.

1.4 FORMAT

The next section contains a brief review of previous research carried out in the field of the stress-strain behaviour of confined concrete. Chapter Two examines the various code provisions for confining steel. Chapter Three outlines the design and construction of the test units along with the properties of the materials used, while Chapter Four describes the instrumentation and testing procedure.

Test results are presented in Chapter Five in the form of load, confined concrete core stress/cylinder strength and hoop steel stress plotted against longitudinal strain. The results are summarised in Table 5.1 Trends in the results are also compared and discussed in Chapter Five. A summary and conclusions are given in Chapter Six along with suggestions for the direction of future research.

References are listed in Appendix A.

1.5 PREVIOUS RESEARCH

Theoretical and experimental research into the behaviour of confined concrete has been conducted by many researchers (References 2-28) at

various institutions throughout the world. Comprehensive literature surveys have been collated recently by Leslie (1974)⁽²⁵⁾ and Sheikh (1978)⁽²⁾. A summary of the work reviewed by Sheikh⁽²⁾ is given in Table 1.1. A brief description of the salient points from the more important researchers, based on Sheikh's survey⁽²⁾ is presented below. The work summarized will concern mainly square or rectangular column units confined by square or rectangular hoops. This report will not discuss results for spiral column tests.

TABLE 1.1 : Summary of the Tests Reported by Different Researchers
(Sheikh(1978)⁽²⁾)

Researcher	Details of the Specimens			
	Number	Size of the section mm	$\frac{A_{core}}{A_{gross}}$	Longitudinal Steel
King (1946)	164	89 x 89	0.54-0.61	4 corner bars
King (1946)	18	254 x 254	1.34-0.66	"
Chan (1955)	9	152 x 152	0.63-0.92	"
	7	152 x 152	0.92-0.96	"
	7	152 dia	0.97	4 bars
Bresler and Gilbert (1961)	2	203 x 203	0.61	6 bars
	2	203 x 203	"	8 bars
Pfister (1964)	4	305 x 305	0.42-0.53	12 bars
	3	203 x 457	0.36-0.49	12 bars
	4	254 x 305	0.49	6 bars
Roy and Sozen (1964)	45	127 x 127	0.86x0.9	4 corner bars
Bertero and Felippa (1964)	2	76 x 76		None
	5	"		4 corner bars
	2	108 x 108		None
	6	"		4 corner bars
Hudson (1966)	32	102 x 102	0.46-0.47	8 bars
	28	152 x 152	0.63-0.66	8 bars
Soliman and Yu (1967)	3	152 x 102	0.92-1.00	2 bars
	11	"	0.44-0.92	4 corner bars
	1	152 x 76	0.91	"
	1	152 x 127	0.93	"
Shah and Rangan (1970)	11	51 x 51	0.83	None
Somes (1970)	42	102 x 102	0.88-0.92	None
Sargin (1971)	41	127 x 127	0.64-0.96	None

TABLE 1.1 Continued.....

Burdette and Hilsdorf (1971)	16	127 x 127	0.72-1.00	None
	4	127 dia	1.00	"
Bunni (1975)	4	127 x 127	0.88-0.90	None
	50	"	0.88-0.95	4 corner bars
PCA (1977)	13	254 x 406	0.68-0.72	4 corner bars
	6	127 x 203	0.70	"
Bertero and Vallenias (1977)	3	254 x 254	0.78	8 bars
	3	229 x 229	0.96	"
	3	254 x 254	0.78	None
	3	229 x 228	0.96	"
Sheikh and Uzumeri (1978)	9	305 x 305	0.77	8 bars
	6	"	"	12 bars
	9	"	"	16 bars

1.5.1 Chan (1955)⁽⁶⁾

As part of some other investigations Chan reported the testing of 9 prisms 152 x 152 x 292 mm with bent-in hoops, 7 cylinders 152 mm diameter and 305 mm high with spiral reinforcement, and 7 prisms 152 x 92 x 1321 mm with welded hoops. These were loaded eccentrically or axially with a transverse load at the mid point. Chan's results for rectangular hoops, when compared with unconfined concrete, showed a strength increase of more than 50%, an increase in ultimate strain of about 500%, and that these increases were only 50% and 70% respectively of those for equivalent spiral reinforcement.

To determine the effect of confinement Chan ignored the hoop spacing, and considered only the volumetric ratio of hoop steel.

1.5.2 Roy and Sozen (1963)⁽¹⁰⁾, (1964)⁽¹¹⁾

Roy and Sozen developed an idealised bilinear stress-strain relationship for confined concrete from 45 tests carried out on 127 x 127 x 635 mm prisms with about 2% square hoop steel by volume. It was concluded that the ductility of confined concrete was closely related to the spacing of the hoops but the size of hoop bars and amount of longitudinal steel had little effect on concrete properties. It was concluded from the test results that the presence of square hoop steel increased the ductility

of concrete but not the concrete strength (peak stress) (See Figures 1.1 and 1.2).

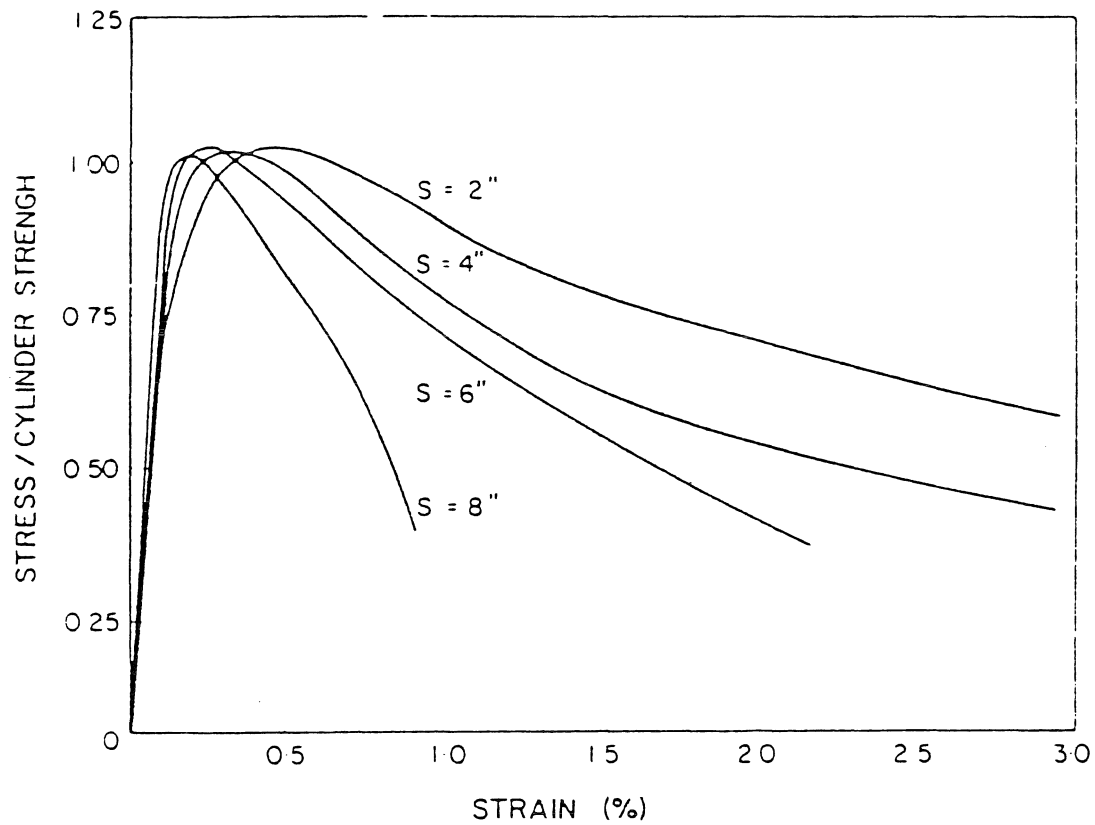


FIGURE 1.1 : Effect of Tie Spacing on Stress-Strain Relationship of Concrete (Roy and Sozen 1963)⁽¹⁰⁾

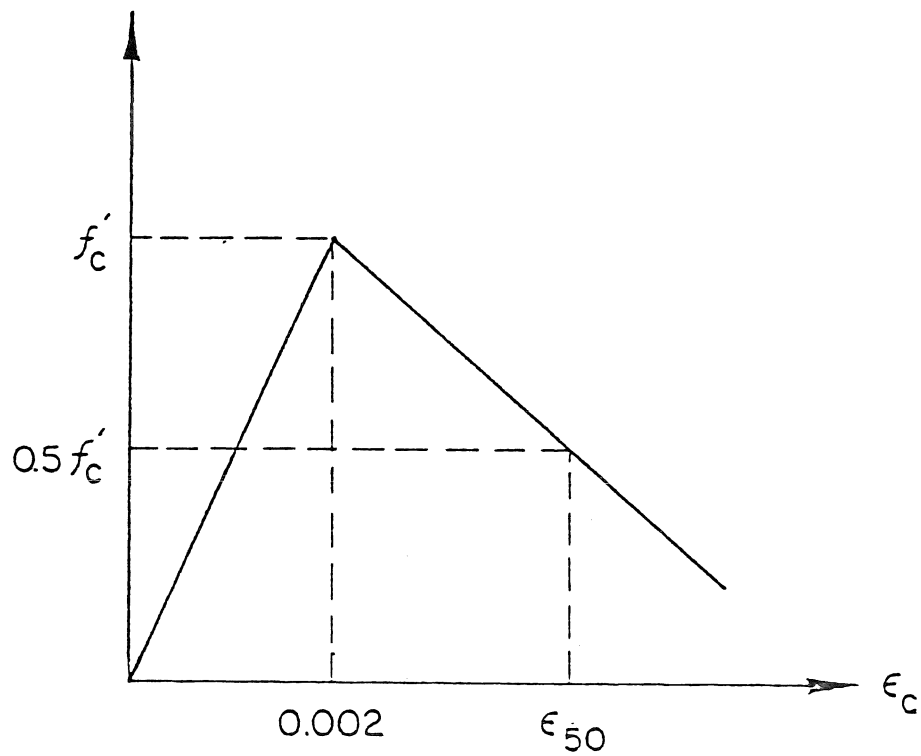


FIGURE 1.2 : Stress-Strain Curve for Concrete Confined by Rectangular Ties as proposed by Roy and Sozen (1964)⁽¹¹⁾

$$\epsilon_{50} = \frac{3}{4} \frac{\rho_s h}{s}$$

where h = overall depth of member

ρ_s = ratio of volume of transverse reinforcement to volume of concrete core

s = spacing of hoops

1.5.3 Bertero and Felippa (1964)⁽¹²⁾

In their discussion to Roy and Sozen's paper above⁽¹¹⁾, Bertero and Felippa reported the results of tests performed on 76 x 76 x 305 mm and 114 x 114 x 305 mm prisms with square hoop steel and/or longitudinal steel under concentric loading. Increases in concrete strength were found to be 13% to 26%, depending on the hoop steel volume. It was concluded that longitudinal steel alone did not enhance the concrete ductility. Hoops alone however did, and hoops with longitudinal steel provided even greater ductility enhancement.

1.5.4 Soliman and Yu (1967)⁽¹⁵⁾

Soliman and Yu conducted a study on the flexural stress-strain relationship of confined concrete. Fourteen units 152 x 102 x 1321 mm and one each 152 x 76 x 1321 mm and 152 x 127 x 1321 mm 2343 tested under the action of a major load and a minor load applied such that the neutral axis was kept constant near the tension side of the unit and parallel to the stronger axis throughout the entire range of loading.

An increase in concrete strength of up to 28% was observed by using closely spaced rectangular hoops. It is unclear whether this was based on gross concrete area or core concrete area. It appears also that no consideration has been given to the spalling of the cover concrete and that the stress-strain curve was based on the total concrete area initially under compression.

The stress-strain curve proposed by Soliman and Yu for confined concrete in flexure is shown in Figure 1.3 and the characteristics detailed below.

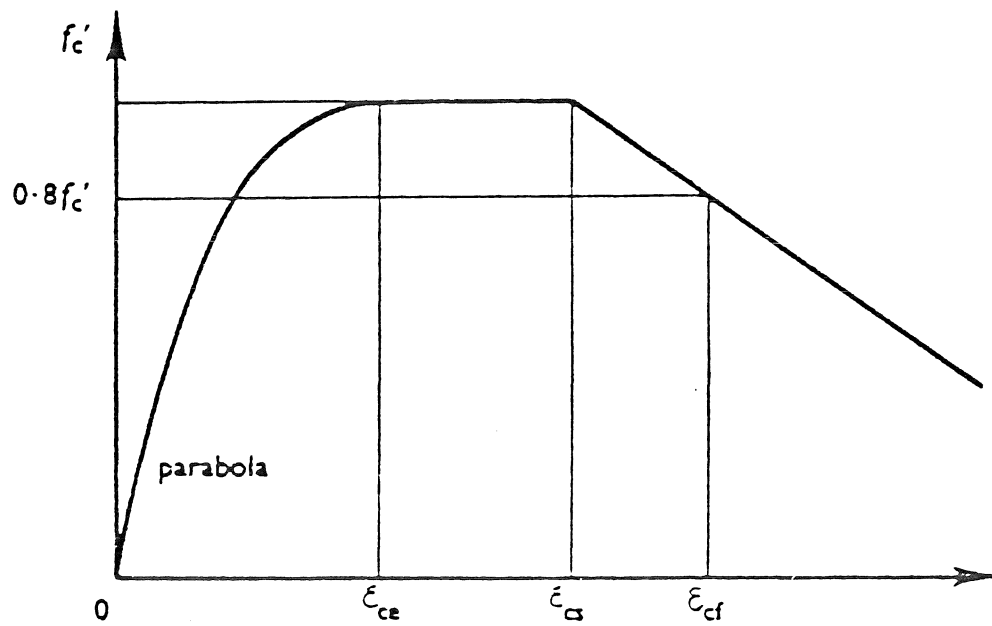


FIGURE 1.3 : Stress-Strain Relationship of Confined Concrete in Flexure (Soliman and Yu 1967)⁽¹⁵⁾

$$q'' = \left(1.4 \frac{A_{cc}}{A_c} - 0.45\right) \frac{A_{tie}(S_o - S)}{A_{tie} S + .0028 BS^2} \quad \dots \quad 1.1$$

$$f_{cmax} = 0.9 f'_c (1 + .05 q'') \quad \dots \quad 1.2$$

$$\epsilon_{ce} = 0.55 f'_c \times 10^{-6} \quad \dots \quad 1.3$$

$$\epsilon_{cs} = 0.0025 (1 + q'') \quad \dots \quad 1.4$$

$$\epsilon_{cf} = 0.0045 (1 + 0.85 q'') \quad \dots \quad 1.5$$

where for these equations

A_c = area of concrete in compression

A_{cc} = area of confined concrete in compression

A_{tie} = area of bar used for tie

B = width of bound concrete or 0.7 (depth of bound concrete) whichever is greater

f'_c = concrete cylinder strength

f_{cmax} = maximum stress in confined concrete

S = tie spacing

S_0 = tie spacing at which ties are not effective in confining the concrete, for the tests reported in the paper $S_0 = 10$ in.

In the q'' relation, the term $\frac{A_{cc}}{A_c}$ seems to be present in order to give the stress-strain relation for the gross concrete section which will result in a lower value of q'' and hence lower values of f_{cmax} , ϵ_{cs} and ϵ_{cf} .

1.5.5 Kent and Park (1971)⁽¹⁸⁾

In 1971 Kent and Park proposed the stress-strain curve, for concrete confined by rectangular hoops with the characteristics detailed below and shown in Figure 1.4.

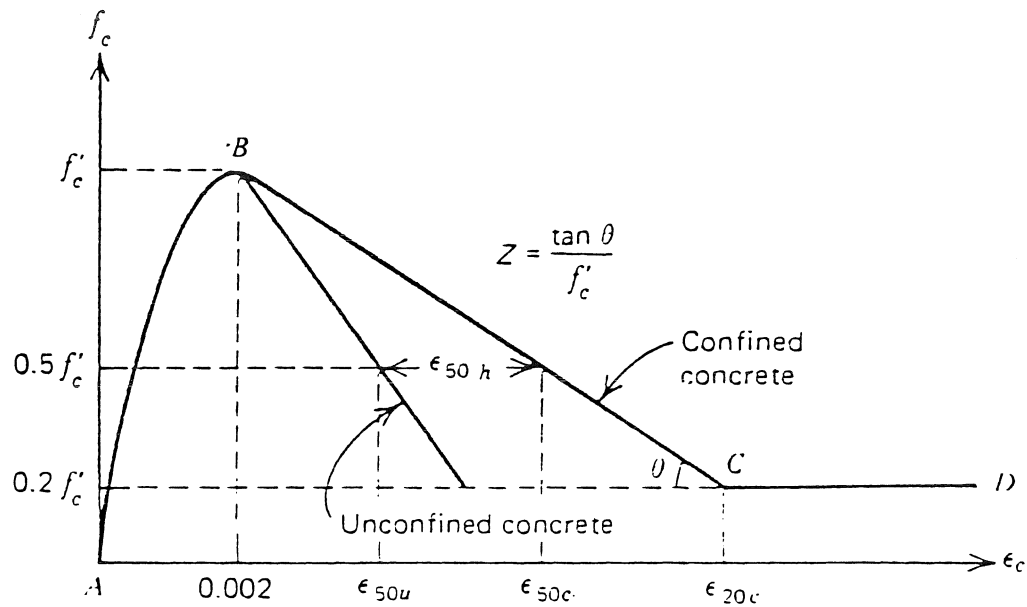


FIGURE 1.4 : Stress-Strain Curve for Concrete Confined by Rectangular Hoops (Kent and Park 1971)⁽¹⁸⁾

Region AB : for $\epsilon_c \leq \epsilon_0$

where $\epsilon_0 = .002$

$$f_c = f'_c \left(\frac{2\epsilon_c}{\epsilon_0} - \left(\frac{\epsilon_c}{\epsilon_0} \right)^2 \right) \quad \dots \quad 1.6$$

Region BC : for $\epsilon_0 \leq \epsilon_c \leq \epsilon_{20c}$... 1.7

$$f_c = f'_c \{1 - Z(\epsilon_c - \epsilon_0)\}$$

$$\text{where } Z = \frac{0.5}{\epsilon_{50u} + \epsilon_{50h} - \epsilon_{co}} \quad \dots \quad 1.8$$

$$\epsilon_{50u} = \frac{3 + 0.29f'_c}{145f'_c - 1000} \quad \dots \quad 1.9$$

$$\epsilon_{50h} = \frac{3}{4} \rho_s \sqrt{\frac{h''}{s}} \quad \dots \quad 1.10$$

where for these equations

f'_c = concrete cylinder strength in MPa,

and h'' = width of confined core,

Region CD $\epsilon_c \geq \epsilon_{20c}$

$$f_c = 0.2 f'_c \quad \dots \quad 1.11$$

This relationship was proposed on the basis of an analysis of existing experimental data. It incorporates many features of previous researchers but no increase in the strength of confined concrete was considered, although many researchers^(16, 12, 13, 15) observed a significant increase in concrete strength due to confinement by rectangular hoops. This assumption was based conservatively on the test results of Roy and Sozen (1964)⁽¹¹⁾ which indicated no significant increase in strength due to confinement by square hoops.

The falling branch was developed from the results of Roy and Sozen (1964)⁽¹¹⁾, Bertero and Felippa (1964)⁽¹⁷⁾ and Soliman and Yu (1967)⁽¹⁵⁾. It was assumed to be linear and follows the same format as suggested by Roy and Sozen (1964)⁽¹¹⁾.

It was also assumed that the stress-strain curve for the cover concrete was either the same as the unconfined concrete, or the confined concrete core, or somewhere in between, at strains less than 0.004. At strains greater than 0.004 the cover was considered to have spalled and to have zero strength.

1.5.6 Sargin (1971)^(19, 20)

Sargin tested 22 plain concrete and 41 laterally reinforced units. 18 plain and 31 laterally reinforced units were tested under concentric

loading and the remainder were tested under eccentric loading. All the specimens were 127 x 127 x 508 mm and contained no longitudinal reinforcement.

For concentrically loaded plain prisms the average concrete strength was about 98% of the cylinder strength and the strain, over a 254 mm gauge length, corresponding to the maximum stress was 0.0024. For eccentric loading these values were 100% and 0.003 measured over a 127 mm gauge length respectively.

These findings conflict with those of Sturman, Shah, and Winter (1965)⁽²⁶⁾ where they found the strength of concrete in eccentrically loaded units to be 20% higher than that of concentrically loaded units. Results reported by Hognestad et al (1955)⁽²⁷⁾ found excellent agreement between stress-strain curves for their eccentrically loaded prisms and concentrically loaded cylinders.

Sargin carried out a theoretical analysis of his results assuming that the increase in strength of the 'truly' confined concrete core is 4.1 times the lateral pressure, and that the hoops yield at or before the concrete reaches its maximum strength.

1.5.7 Vallenas, Bertero and Popov (1977)⁽²⁴⁾

This study reported the results of 12 reinforced concrete columns tested under axial load. The columns were 254 x 254 x 762 mm, with or without 8 longitudinal bars and diamond and square hoop sets. More than 20% increase in concrete core strength was observed in some columns. An increase in ductility of up to 300% was observed at the point of maximum strength and up to 1000% at a point on the descending branch of the curve where $f_c/f'_c = 0.85$. Results also showed that the addition of longitudinal steel enhanced the strength of the confined core concrete, on average by 7%. It was shown that none of the existing curves predicted the behaviour of their tests (Figure 1.5) and so Vallenas, Bertero and Popov suggested an improved stress-strain relationship as follows and shown in Figure 1.6.

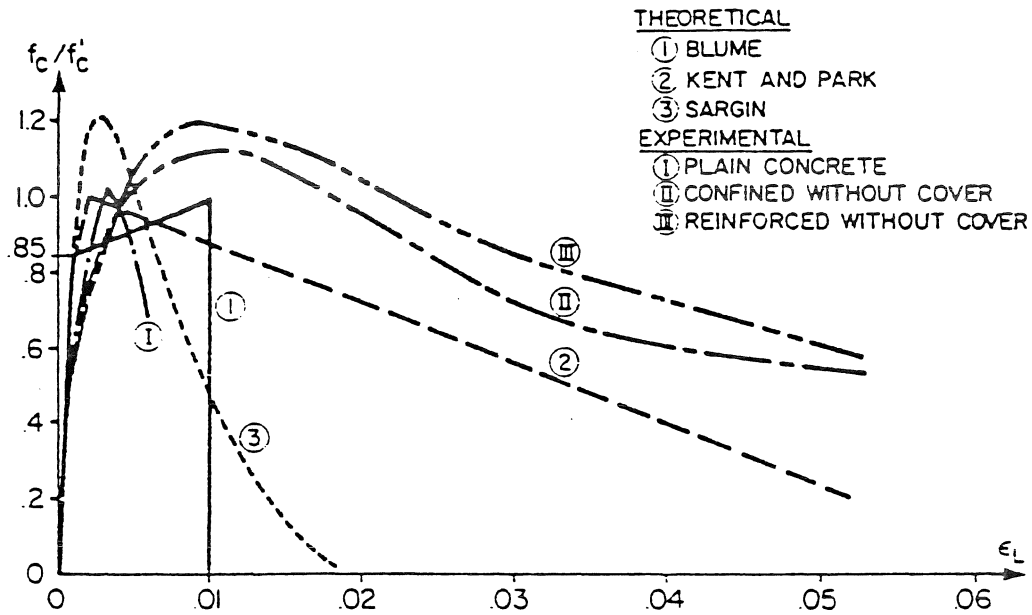


FIGURE 1.5 : Comparison of Analytical Curves with Experimental Results (Vallenas et al, 1977)⁽²⁴⁾

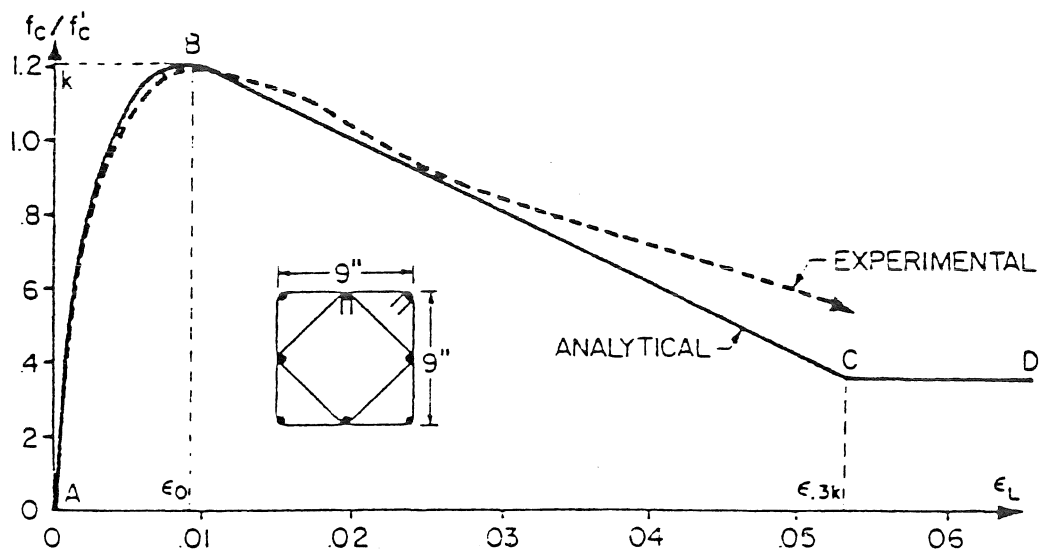


FIGURE 1.6 : Confined Concrete with Longitudinal Reinforcement - Analytical Curve and its Comparison with Experimental Results (Vallenas et al, 1977)⁽²⁴⁾

Region AB

$$\frac{f_c}{f'_c} = \frac{\frac{E_c \epsilon_0}{f'_c} \left(\frac{\epsilon_L}{\epsilon_0}\right) - k \left(\frac{\epsilon_L}{\epsilon_0}\right)^2}{1 + \left[\frac{E_c \epsilon_0}{k f'_c} - 2 \right] \left(\frac{\epsilon_L}{\epsilon_0}\right)} \quad \dots \quad 1.12$$

Region BC

$$\frac{f_c}{f'_c} = k \left[1 - Z \epsilon_0 \left(\frac{\epsilon_L}{\epsilon_0} - 1\right) \right] \quad \dots \quad 1.13$$

Region CD

$$\frac{f_c}{f'_c} = 0.3 k \quad \dots \quad 1.14$$

where

$$\epsilon_0 = .0024 + .006 \left(1 - \frac{.734(S)}{h''} \right) \frac{\rho_s f_{yh}}{\sqrt{f'_c}} \quad \dots \quad 1.15$$

$$k = 1 + .1096 \left(1 - .24 \frac{S}{h''} \right) \frac{(\rho_s + \frac{d''}{d} \rho) f_{yh}}{\sqrt{f'_c}} \quad \dots \quad 1.16$$

$$Z = \frac{0.5}{\frac{3}{4} \rho_s \sqrt{\frac{h''}{S}} + \left(\frac{3 + 0.29 f'_c}{145 f'_c - 1000} \right) - .002} \quad \dots \quad 1.17$$

where for these equations

d = diameter of longitudinal steel bar

d'' = diameter of tie bar

E_c = initial modulus of elasticity of concrete (MPa)

f_{yh} = yield strength of tie steel (MPa)

h'' = core dimension of rectangular tied column inside the hoop (mm)

k = ratio of maximum stress in the confined concrete to the cylinder strength

S = hoops spacing (mm)

ρ = volumetric ratio of the longitudinal steel

ρ_s = volumetric ratio of the tie steel

It is worth noting that these equations are dimensionally dependent and the equation for ϵ_0 appears to provide too large a strain increase. The result is that the stress at a strain of 0.002 is significantly less than f'_c . The equations also suggest that strength and ductility are not directly proportional to the confining force.

Gill, Park and Priestley (1979)⁽²⁸⁾ have shown that when applying the model to members under combined axial load and bending, results from moment-curvature analysis using Vallenias, Bertero and Popov's model have underestimated the moment when compared with both experimental results and other models e.g. Sheikh and Uzumeri⁽²⁾.

1.5.8 Sheikh and Uzumeri (1978)⁽²⁾

Sheikh and Uzumeri (1978)⁽²⁾ presented the results of 24 columns 305 x 305 x 1956 mm loaded in monotonic axial compression. Four different lateral steel arrangements, involving rectangular and/or octagonal hoops were used with 8, 12 or 16 longitudinal bars. Also examined were the volume spacing and characteristics of the hoop steel, and volume of longitudinal steel.

It was concluded that rectangular hoop reinforcement enhances the strength and ductility of confined concrete. The distribution of longitudinal steel around the core perimeter increased the efficiency of the confinement. A closer spacing of hoops resulted in higher concrete strength and ductility for the same amount of hoop reinforcement and vice versa. A higher steel strength and larger amount of hoop reinforcement resulted in higher strength and ductility.

The model developed by Shiekh and Uzumeri is detailed below and shown in Figure 1.7.

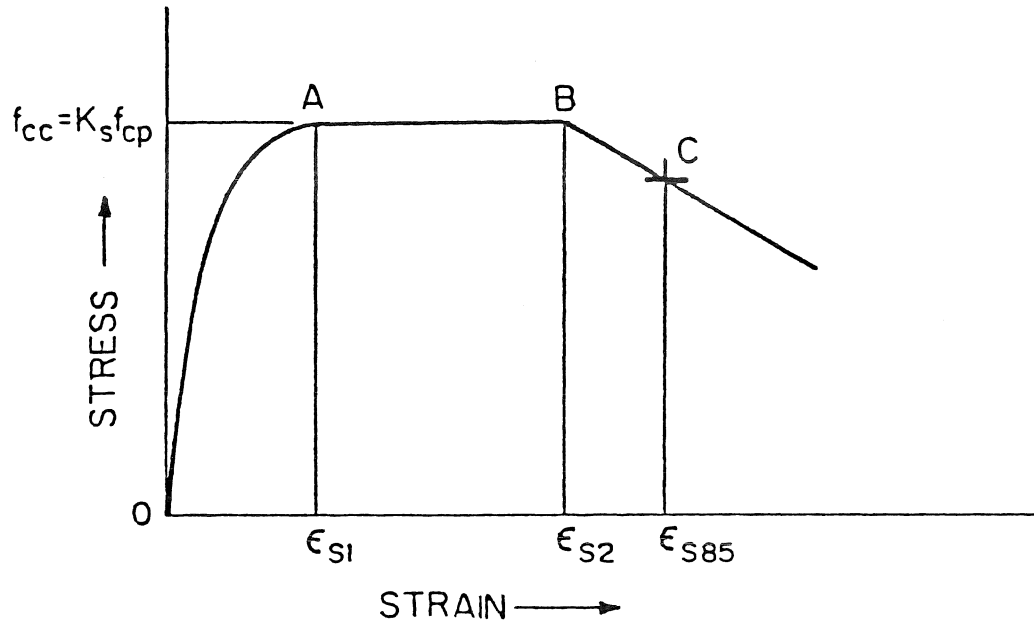


FIGURE 1.7 : Stress-Strain Curve for Confined Concrete in Square Columns (Sheikh and Uzumeri 1978) ⁽²⁾

$$K_s = 1.0 + \frac{1}{140P_{occ}} \left[\left(1 - \frac{n C^2}{5.5 b^2}\right) \left(1 - 0.5 \frac{S}{b}\right)^2 b^2 \right] \sqrt{\rho_s f'_s} \quad \dots \quad 1.18$$

(f'_s in MPa and P_{occ} in KN)

$$\epsilon_{s1} = 80 K_s f'_c \times 10^{-6} \quad (f'_c \text{ in MPa}) \quad \dots \quad 1.19$$

$$\frac{\epsilon_{s2}}{\epsilon_{s00}} = 1.0 + \frac{248}{C} \left[1 - 5(S/b)^2 \right] \frac{\rho_s f'_s}{\sqrt{f'_c}} \quad \dots \quad 1.20$$

(C in mm; f'_c and f'_s in MPa)

$$\epsilon_{s85} = 0.225 \rho_s \sqrt{b/S} + \epsilon_{s2} \quad \dots \quad 1.21$$

The units tested by Sheikh and Uzumeri, which were more realistically sized than previous tests, showed clearly the enhancement of strength and ductility due to confinement. The model however produces a flat plateau in the stress-strain curve due to the use of high yield strength hoops, ($f_{yh} = 520$ or 700 MPa). This meant that when maximum concrete core strength was reached the hoop steel was still below yield, allowing the

confining pressure to increase with subsequent increases of longitudinal and lateral strain. It is felt this may not be suitable for New Zealand conditions where lower grades of hoop steel (e.g. $f_{yh} = 275$ or 380 MPa) are commonly used which might not produce this plateau.

1.5.9 Modified Kent and Park (1979)⁽²⁹⁾

In the light of research results presented more recently by Gill, Park and Priestley (1979)⁽²⁸⁾ a modified form of the Kent and Park stress-strain relationship has been proposed by Park, Priestley and Gill (1979)⁽²⁹⁾ which accounts for the increase in the concrete core strength and strain at maximum stress.

The maximum stress reached is given by Kf'_c , where

$$K = 1 + \rho_s \frac{f_{yh}}{f'_c}$$

The maximum stress, Kf'_c , is assumed to occur at a strain of $0.002K$. The regions of the stress-strain curve are shown in Figure 1.8 and as detailed below.

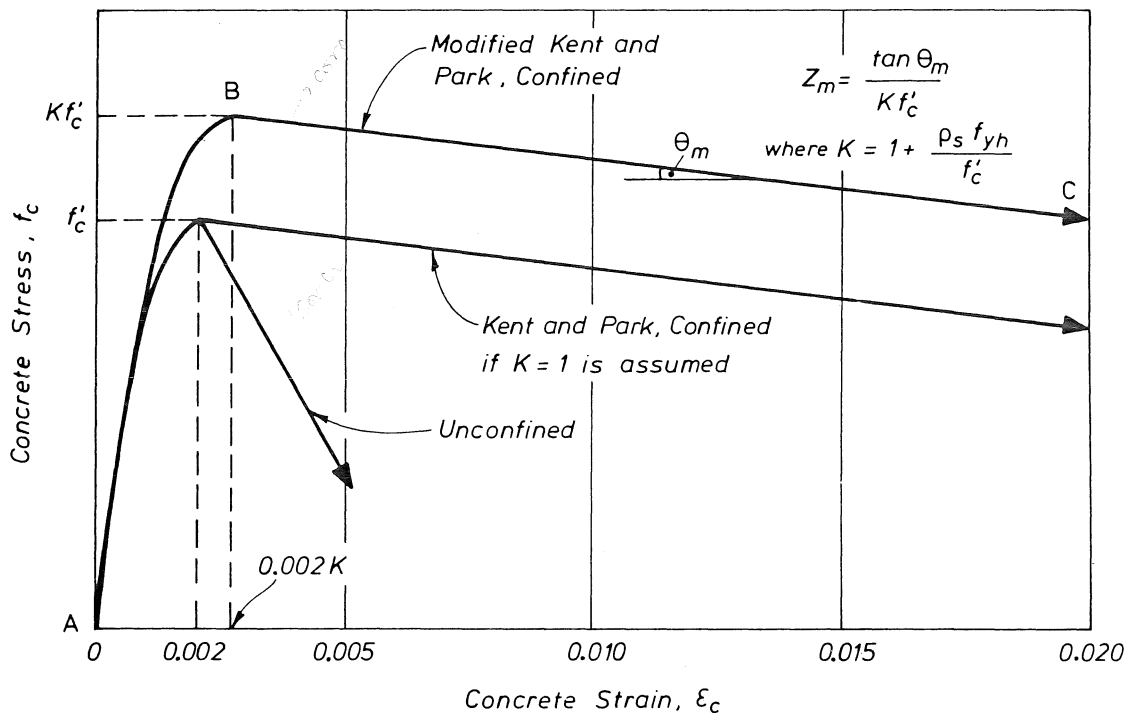


FIGURE 1.8 : Stress-Strain Curve for Concrete Confined by Rectangular Hoops (Park, Priestley and Gill, 1979)⁽²⁹⁾

Region AB ($\epsilon_c < 0.002K$)

$$f_c = Kf'_c \left[\frac{2\epsilon_c}{0.002K} + \left(\frac{\epsilon_c}{0.002K} \right)^2 \right] \quad \dots \quad 1.22$$

Region BC ($\epsilon_c > 0.002K$)

$$f_c = Kf'_c [1 - Z_m (\epsilon_c - 0.002K)] \quad \dots \quad 1.23$$

but not less than $0.2Kf'_c$, where

$$Z_m = \frac{0.5}{\frac{3 + 0.29f'_c}{145f'_c - 1000} + \frac{3}{4} \rho_s \sqrt{\frac{h''}{s_h}} - 0.002K} \quad \dots \quad 1.24$$

Gill, Park and Priestley note that the increase in peak stress may not be as much as observed in tests but the discrepancies seem to make little difference when using the model for moment-curvature analysis as Gill, Park and Priestley (1979)⁽²⁸⁾ have shown.

It should be noted that the basis of choosing $0.002K$ as the strain at peak stress is so that the second degree parabola defining the region AB maintains the same tangent modulus at zero stress (i.e. the same initial modulus of elasticity) regardless of the value of K . The relationship also assumes that rectangular hoops are only one half as effective as a circular spiral in enhancing the strength of the concrete.

1.5.10 Summary

There is a general agreement among researchers that the use of rectangular confining hoops does not significantly influence the rising branch of the stress-strain curve (i.e. the initial stiffness is unaltered) up to about $0.5 f'_c$. An increase in ductility is also a common conclusion but the amount is often a point of wide variance. There is disagreement as to whether enhancement of concrete strength occurs and if so, to what extent.

Most of the tests, as shown in Table 1.1, were conducted on small units, commonly 127×127 mm in section, with small core to gross area ratios and only 4 corner bars for longitudinal steel if any at all and simple

arrangements of rectangular hoops.

The definition of the core is another variable over which there has been much disagreement, brought about at least in part by the large variation in calculations of volumetric hoop steel ratio and gain in concrete strength which occur with small test models. Theoretically it is likely that the core may be defined to the centre-line of the outer hoops but from a practical standpoint and in keeping with current practice it will be taken in this study to the outside of the outer hoop. The behaviour of the cover concrete is another variable which is often ignored by researchers. Attempts have been made to overcome this problem by casting test units without cover, however Burdette and Hilsdorf (1971)⁽²¹⁾ showed that for columns without cover, shrinkage may result in an appreciable reduction in the strength increase due to confinement. In this study the behaviour of the cover has been taken as that for the large plain concrete units and its load carrying capacity at various strain levels calculated accordingly.

King (1946)⁽³⁾ concluded from comparative scaled up tests that the behaviour of large size columns would be very different from small scale models, and that a large number of parameters would require investigation before the results of small scale models could be used to predict the behaviour of full size units.

None of the previous experimental research was carried out at loading rates simulating those likely to occur during an earthquake. Generally tests were carried out on axially loaded units. Therefore, there must remain doubts about the validity of the proposed curves to seismically loaded columns subjected to combined axial load and bending moment.

It is beyond the scope of this report, but ideally a unified stress-strain curve is required that predicts the behaviour of concrete confined by arrangements of either circular spirals or rectangular hoops. Based on the assumption that most researchers adopt, that the confining force from the lateral reinforcement is equivalent to an applied lateral pressure, there is no reason why this generalised approach should not be possible.

CHAPTER TWO

CONFINEMENT REQUIREMENTS FOR PLASTIC HINGE ZONES IN REINFORCED CONCRETE COLUMNS

2.0 SUMMARY

This chapter reviews the requirements for confining steel in plastic hinge zones in rectangular columns, as specified in the seismic codes of various countries. In particular a comparison is made between New Zealand and overseas recommendations. This work is summarised from a paper by Park and Priestley (1979)⁽³⁰⁾.

2.1 THE CODES CONSIDERED

The overseas code requirements for reinforced concrete design considered in this section will be the A.C.I. Building Code⁽³¹⁾, the S.E.A.O.C. Code⁽³²⁾, the tentative provisions for buildings of the A.T.C.⁽³³⁾ and the A.C.I. Committee 343 report on the analysis and design of bridge structures⁽³⁴⁾. An indication of Japanese practice can be obtained from publications in English for example references 35 and 36. In New Zealand the Ministry of Works and Development have developed provisions for confinement of bridge piers^(37, 38) and the Standards Association of New Zealand has prepared a draft Concrete Design Code⁽¹⁾, which is now being redrafted into its final form. The summary given below will not include references to design of shear reinforcement, on the understanding that transverse hoops placed for confinement will act as shear reinforcement and that there may be cases where shear steel is the governing criteria. Generally the transverse steel for hoops is expressed as A_{sh} , the total area of hoop bars and supplementary cross ties in the direction under consideration within longitudinal spacing S_h . Sometimes ρ_s is used to define the total volumetric ratio of transverse steel in the section confining the concrete core.

2.1.1 ACI 318-77⁽³¹⁾

Confining steel consisting of hoop reinforcement is required over the end regions of columns adjacent to moment resisting connections over a length from the face of the connection equal to the greater of the overall thickness h (h being the larger sectional dimension for rectangular columns), one-sixth of the clear height of the column, or 450 mm.

For rectangular hoop reinforcement, with or without supplementary cross ties, if $P_e \leq \phi 0.4P_b$, the transverse steel should be designed as for beams but the hoop bar diameter should not be less than 10 mm and the spacing should not exceed $d/2$. If $P_e > \phi 0.4P_b$, and if a single rectangular hoop is used, the area of one leg of the hoop bar in the direction considered within spacing s_h should be at least equal to

$$A_{sb} = 1_h \rho_s s_h / 2 \quad \dots \quad 2.1$$

where ρ_s is calculated by the greater of Equations 2.2 and 2.3.

If $P_e \leq \phi 0.4P_b$, ρ_s is required to be at least equal to

$$\rho_s = 0.45 \left[\frac{A_g}{A_c} - 1 \right] \frac{f'_c}{f_{yh}} \quad \dots \quad 2.2$$

If $P_e > 0.4\phi P_b$, ρ_s should not be less than that given by Equation 2.2, or

$$\rho_s = 0.12 f'_c / f_{yh} \quad \dots \quad 2.3$$

with A_c taken as the area of concrete core measured to the outside of the peripheral hoop. The value of s_h used should not exceed 100 mm.

Supplementary cross ties of the same bar diameter as the hoop may be used to reduce the unsupported length l_h . The hoop and cross tie bar diameter should not be less than 10 mm for longitudinal bars 32 mm diameter or smaller, or 12 mm for larger longitudinal bars or bundled bars.

2.1.2 SEAOC (1975)⁽³²⁾

The potential plastic hinge zone is taken as in ACI 318-77.

For rectangular hoop reinforcement the total area of hoop bar and supplementary cross ties (if any) in the direction under consideration within spacing s_h should not be less than

$$A_{sh} = 0.3s_h h'' \frac{f'_c}{f_{yh}} \left[\frac{A_g}{A_c} - 1 \right] \quad \dots \quad 2.4$$

or

$$A_{sh} = 0.12s_h h'' f'_c / f_{yh} \quad \dots \quad 2.5$$

whichever is greater. The value of s_h used should not exceed 100 mm, and supplementary cross ties or legs of overlapping hoops should not be spaced at more than 360 mm between centres transversely.

2.1.3 ATC (1978)⁽³³⁾

The SEAOC provisions appear to have been followed for fully ductile frames.

2.1.4 ACI COMMITTEE 343⁽³⁴⁾

For rectangular hoop steel the transverse bar diameter is specified as in ACI 318-77. The quantity of transverse steel is not specified, but it is stated that the tie spacing should not exceed the least dimension of the member or 300 mm, except that when bars larger than 32 mm diameter are bundled the tie spacing should be reduced to one-half of that value.

2.1.5 JAPANESE PRACTICE^(35, 36)

No information was available to Park and Priestley (1979)⁽³⁰⁾ regarding current Japanese practice for bridges. However, AIJ requirements for buildings⁽³⁶⁾ specify a minimum rectangular hoop diameter of 9 mm with spacing not to exceed the lesser of 150 mm, one-half of the smaller column dimension, or 7.5 longitudinal bar diameters.

2.1.6 N.Z. MINISTRY OF WORKS AND DEVELOPMENT, CIVIL DIVISION^(37, 38)

Until recently the design of confining reinforcement for bridge columns was governed by the MWD provisions^(37, 38). This involves sufficient confining steel to ensure that the available structure displacement ductility factor μ is at least 6, based on the following steps:

- (1) The ratio of the structure displacement ductility factor, μ , to curvature ductility factor, ϕ_u/ϕ_y , within the plastic hinge region is calculated. The ratio depends on geometric considerations, and the plastic hinge length which is taken to be that given by Baker's formula⁽³⁹⁾.

- (2) Calculate the yield curvature ϕ_y , and hence the required ultimate curvature ϕ_u .
- (3) Calculate the "ultimate" compression strain ϵ_{cu} corresponding to ϕ_u , based on a conservative idealisation for the stress-strain curve of confined concrete.
- (4) Calculate the required volumetric ratio of confining reinforcement.

For rectangular hoops and supplementary cross ties ρ_s is obtained using

$$\epsilon_{cu} = 0.0021 \left\{ 1 + 150\rho_s + (0.7 - 10\rho_s) \frac{d}{c} \right\} \quad \dots \quad 2.6$$

Equation 2.6 is based on the work of Baker and Amarakone⁽³⁹⁾ and Chan⁽⁶⁾, but was made significantly less conservative than the results of that work in the light of the findings of more recent tests (see the December 1977 amendment⁽³⁷⁾).

It is understood that the MWD will be adopting the requirements of the new SANZ Concrete Design Code (at present in draft form⁽¹⁾) when that SANZ code is available in its final form.

2.1.7 DRAFT SANZ CONCRETE DESIGN CODE⁽¹⁾

The confinement provisions of the draft SANZ Concrete Design Code, DZ3101, are based on the ACI/SEAOC requirements modified to take account of the effect of axial load level.

(a) First Draft

In the first draft of DZ3101, issued for comment in 1978, the potential plastic hinge regions were specified as in ACI 318-77. The total area of rectangular hoop reinforcement, including supplementary cross ties if any, in the direction under consideration in potential plastic hinge regions, when $P_e \leq 0.6f'_cA_g$, was required to be not less than

$$A_{sh} = 0.3s_h h'' \left[\frac{A_g}{A_c} - 1 \right] \frac{f'_c}{f_y} \left[0.33 + 1.67 \frac{P_e}{f'_c A_g} \right] \quad \dots \quad 2.7$$

nor

$$A_{sh} = 0.12s_h h'' \frac{f'_c}{f_{yh}} \left[0.33 + 1.67 \frac{P_e}{f'_c A_g} \right] \quad \dots \quad 2.8$$

where P_e was not to be taken as less than $0.1f'_c A_g$. The diameter of hoop or tie bar was to be at least 10 mm, and the maximum centre spacing of hoop sets was not to exceed the smaller of one-fifth of the smaller member section dimension, 150 mm, or six times the diameter of the longitudinal bars. The yield force of the hoop bar or supplementary cross tie was to be at least one-sixteenth of the yield force of the longitudinal bar or bars it was to restrain. Other rules were also given to ensure adequate lateral support of the longitudinal bars. These equations were based on theoretical moment-curvature analyses⁽²⁵⁾ conducted using the stress-strain model proposed by Kent and Park (1971)⁽¹⁸⁾.

(b) Revised Draft

The potential plastic hinge region for $P_e \leq \phi 0.3f'_c A_g$ is now recommended as not less than the longer column section dimension in the case of a rectangular section, or where the moment exceeds 0.8 of the maximum moment at that end of the member. When $P_e > \phi 0.3f'_c A_g$ the potential plastic hinge region is increased to 1.5 times the above value.

In potential plastic hinge regions when rectangular hoops, with or without supplementary cross ties, are used and either $P_e \leq \phi 0.7f'_c A_g$ or $P_e \leq \phi 0.7P_o$, the total area of transverse steel within spacing s_h should not be less than

$$A_{sh} = 0.3 s_h h'' \left[\frac{A_g}{A_c} - 1 \right] \frac{f'_c}{f_{yh}} \left(0.5 + 1.25 \frac{P_e}{\phi f'_c A_g} \right) \quad \dots \quad 2.9$$

nor

$$A_{sh} = 0.12 s_h h'' \frac{f'_c}{f_{yh}} \left(0.5 + 1.25 \frac{P_e}{\phi f'_c A_g} \right) \quad \dots \quad 2.10$$

When the load P_e has been obtained using a capacity design procedure, the value of the strength reduction factor ϕ in all the above equations can be taken as unity.

These modifications of Equations 2.7 and 2.8 were made on the basis of the test results on near full scale columns obtained by Gill, Park and Priestley (1979)⁽²⁸⁾.

2.2 COMPARISON OF CODE REQUIREMENTS FOR A TYPICAL RECTANGULAR COLUMN

The difference between the confinement ratios required by the above codes is illustrated in Figure 2.1 for a typical 700 mm square column confined by an arrangement of square and octagonal hoops such as would be used in a building.

Figure 2.1 illustrates that the Japanese requirements apparently result in very low quantities of hoop steel.

The step change in the ACI 318 requirements has again been taken to occur at $P_e = 0.1f'_c A_g$ in Figure 2.1, which is a reasonable approximation for $0.4\phi P_b$. The SEAOC and ATC recommendations do not permit a reduction in the hoop content at low axial load levels. The SANZ (revised draft) quantity shows a linear increase in hoop content with axial load from 50% of the SEAOC moment at zero axial load to 1.38 times the SEAOC amount at $P_e = 0.7f'_c A_g$. Using the arrangement of one square hoop plus one octagonal hoop per set, shown in the column section in Figure 2.1, the total effective area of hoop bars per set, A_{sh} , is taken as twice the area of the square hoop leg plus 1.414 (i.e. twice $1/\sqrt{2}$) times the area of the octagonal hoop leg. Hence if both hoops are of the same size bar with leg area A_{sb} , the value of A_{sh} would be $3.414A_{sb}$. The SEAOC code requirements for the column shown in Figure 2.1 could be met using 16 mm diameter square and octagonal hoop bar with the hoop sets placed at 88 mm centres. The longitudinal steel used in this example consisted of twelve 32 mm diameter bars.

As illustrated in Figure 5, the MWD approach requires substantially more hoop steel than does the other approaches at high axial load levels. At low axial load levels only very small quantities of confining steel are again required because of the high emphasis of the d/c ratio on ϵ_{cu} in Equation 2.6. For example, Equation 8 indicates that $\epsilon_{cu} = 0.010$ will be available if $c/d < 0.19$ even if $\rho_s = 0$. Also there are large differences between the hoop requirements for various μ_{pier} demands in Figure 2.1.

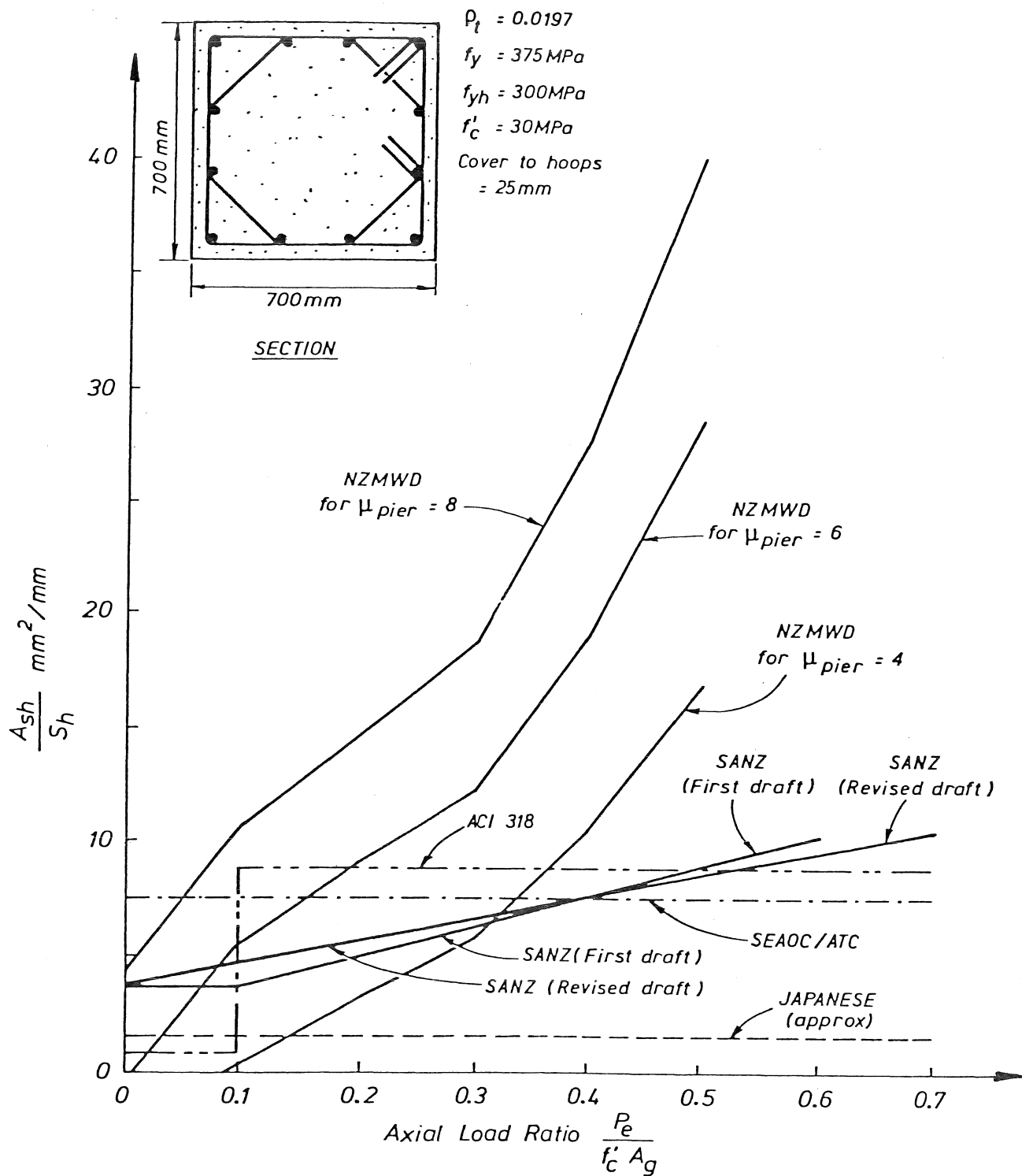


FIGURE 2.1 : Comparison of Code Hoop Steel Requirements for a Square Column (Park and Priestley (1979))⁽³⁰⁾

2.3 CONCLUSIONS

The various overseas and New Zealand code recommendations for transverse confining steel in potential plastic hinge regions of columns and piers in seismic design show vast differences in the required quantities of transverse steel and it is evident that this is still a matter of some controversy.

Recent tests on near full scale reinforced concrete columns containing spiral steel or rectangular hoop steel, under simulated seismic loading, at the University of Canterbury, have shown that the quantities of confining steel recommended in the draft SANZ Concrete Design Code, with slight modifications mainly to take into account the effect of the possible increase of actual concrete strength over a specified f'_c and to avoid the spread of plastic hinging into less heavily confined regions, will result in available displacement ductility factors for columns of at least 8.

The provisions for confining steel which have been used by the Ministry of Works and Development for ductile bridge piers appear to be very conservative when axial load levels are high and are in need of revision to avoid the use of excessive quantities of confining steel. This observation is made not only from comparison with the quantity of confining steel required by the draft SANZ Concrete Design Code but also in the light of the results of the column tests recently conducted at the University of Canterbury. At low axial load levels the MWD confinement provisions may be unconservative but the requirements of transverse steel for shear will govern in that case and result in a greater quantity of transverse steel being placed.

CHAPTER THREE

DESIGN AND CONSTRUCTION OF TEST UNITS

3.0 SUMMARY

This chapter describes the design of the test units, the properties of the materials used and the construction method employed.

3.1 UNIT SIZE CRITERIA

In 1978 the University of Canterbury installed a 10 MN Dartec Universal Testing Machine in the Civil Engineering Department, which now permits the testing of large scale building components at rapid loading rates.

Considerable effort was made to test as large a unit as possible, in order to avoid the complications caused by scale effects that have been noted by other researchers (e.g. King (1946)⁽³⁾ and Sheikh and Uzumeri (1978)⁽²⁾). The 10 MN capacity of the Dartec testing machine was the dominant factor in determining unit size. Other factors which influenced final column dimensions were the expected enhancement of concrete strength due to confinement and rapid loading rates; a realistic longitudinal steel ratio; the expected yield and ultimate strengths of the longitudinal steel; the ease of formwork construction and a suitable height to core dimension ratio. Based on these considerations a unit size of 450 x 450 x 1200 was chosen.

3.2 DESIGN OF TEST UNITS

3.2.1 Longitudinal Steel

The use of high strength steel (Grade 380) in reinforced concrete building columns is becoming increasingly common. The early strain hardening of the steel improves the performance of the column at high strains by compensating for the loss of capacity due to spalling cover concrete. This approach applies principally where column moments are induced from overstrength beam drive and there is a desire to prevent column hinging. However if columns are the fundamental earthquake resisting elements, as

in a bridge where plastic hinging must occur in the piers, the column overstrength may be very high with Grade 380 steel, resulting in excessive shear forces. To model current building practice 18 of the 30 units were constructed with Grade 380 longitudinal steel.

It has been shown that distribution of longitudinal steel has a marked effect on ductility⁽⁴⁰⁾ and confinement⁽²⁴⁾, and so two longitudinal steel distributions were chosen to represent current practice. The longitudinal steel was also selected to conform with NZS DZ3101⁽¹⁾ and the volume of steel to be similar between units. The final choices for longitudinal reinforcement were 8 DH 24 bars with $\rho_t = 0.0186$, or 12 DH 20 or 12 D 20 bars with $\rho_t = 0.0179$ as shown in Figure 3.1, where D signifies Grade 275 deformed bar (nominal $f_y = 275$ MPa) and DH signifies Grade 380 deformed bar (nominal $f_y = 380$ MPa).

3.2.2 Hoop Steel

The hoop steel was designed to conform with a proposed modification of NZS DZ 3101⁽¹⁾ for Special Transverse Hoop Reinforcement in Potential Plastic Hinge Zones, as detailed in Chapter Two.

The equations used in their modified form, restated here from Chapter Two, were:

$$A_{sh} = 0.35 h'' \left(\frac{A_g}{A_c} - 1 \right) \frac{f'_c}{f_{yh}} \left(0.5 + \frac{1.25 P_e}{f'_c A_g} \right) \quad \dots \quad 3.1$$

$$\text{or} \quad A_{sh} = 0.12 S_h h'' \frac{f'_c}{f_{yh}} \left(0.5 + \frac{1.25 P_e}{f'_c A_g} \right) \quad \dots \quad 3.2$$

whichever is greater, where P_e is not greater than $0.7 f'_c A_g$.

Four levels of confinement were chosen to cover the range of axial loads, P_e . These were P_e equal to 0.1, 0.25, 0.4, and 0.7 of $f'_c A_g$. Confinement to an axial load level of $0.25 f'_c A_g$ was chosen to be typical of current practice and to be representative when considering the effect of the other variables.

Equation 3.2 governs the hoop steel quantity because of the test unit dimensions chosen and from this equation the required spacing of the hoops was determined for a given transverse bar area. All hoop steel was plain bar Grade 275. The hoop bar diameter and spacings are given in Table 3.1.

TABLE 3.1 : Hoop Bar Diameter and Spacing of Hoop Sets

$\frac{P_e}{f'_c A_g}$	Hoop Bar Diameter mm	Hoop Spacing mm
0.1	10	98
0.25	10	72
0.4	12	88
0.7	12	64

The hoop spacing was reduced by half for 200 mm at each end of the test unit to ensure that failure occurred in the 800 mm long central region. The configuration of hoop sets is shown in Figure 3.1

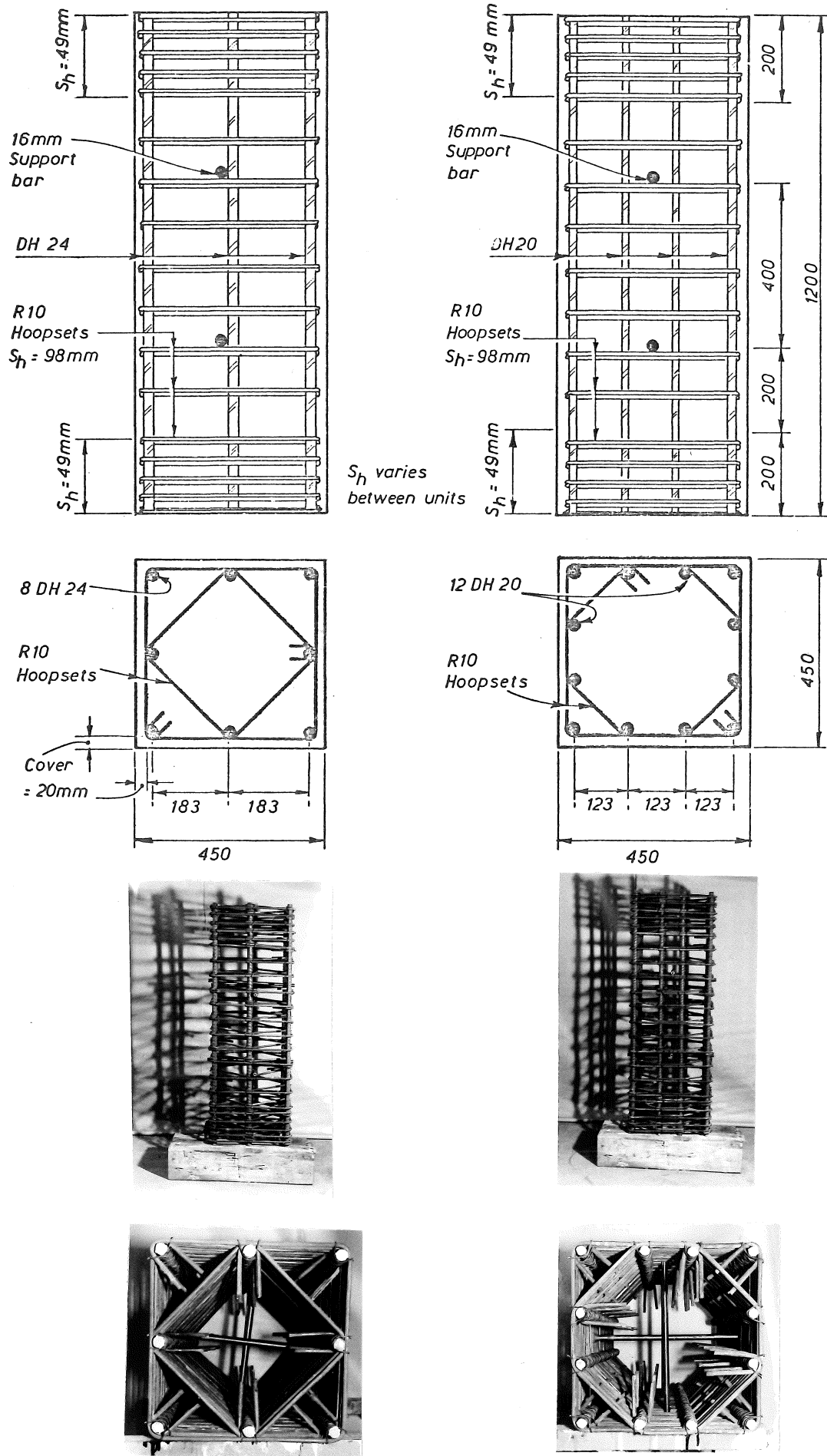


FIGURE 3,1 ; Details of Test Units and Transverse Reinforcement

3.3 MATERIAL PROPERTIES

3.3.1 Steel

The reinforcement for each bar size was chosen from a single supply batch to ensure uniform properties. Three randomly selected samples of each diameter bar were subjected to full extensometer tensile testing in order to establish the stress-strain relationships for the steel.

This assumes that the static stress-strain curve for steel in tension can be applied to steel in dynamic compression. For these test units the longitudinal steel carries a maximum load of about 1.5 MN so that an error of 10% due to any discrepancy between tension and compression yield, or from dynamic loading rates represents only 2% error in concrete core stress.

Table 3.2 summarises the yield and ultimate stresses while Figures 3.2 - 3.6 show the measured stress-strain curves.

TABLE 3.2 : Yield and Ultimate Steel Stresses

Bar	Yield Stress (MPa)	Ultimate Stress (MPa)
DH 24	394	646
DH 20	434	708
D 20	272	416
R 12	296	424
R 10	309	436

3.3.2 Concrete

The concrete used in all specimens was delivered ready-mixed with a target strength at 28 days of 25 MPa, a slump of 75 mm and maximum aggregate size of 20 mm.

Cylinders 200 x 100 mm diameter were cast with each pour and tested at 7, 14, 28, and 42 days, and also during testing. Cylinders were cured in the fog room at 20°C in 100% relative humidity while the test specimens were covered with hessian and polythene with the top surface kept moist for 7 days before stripping the formwork. They were then allowed to stand for another 5 weeks (6 in total) before testing.

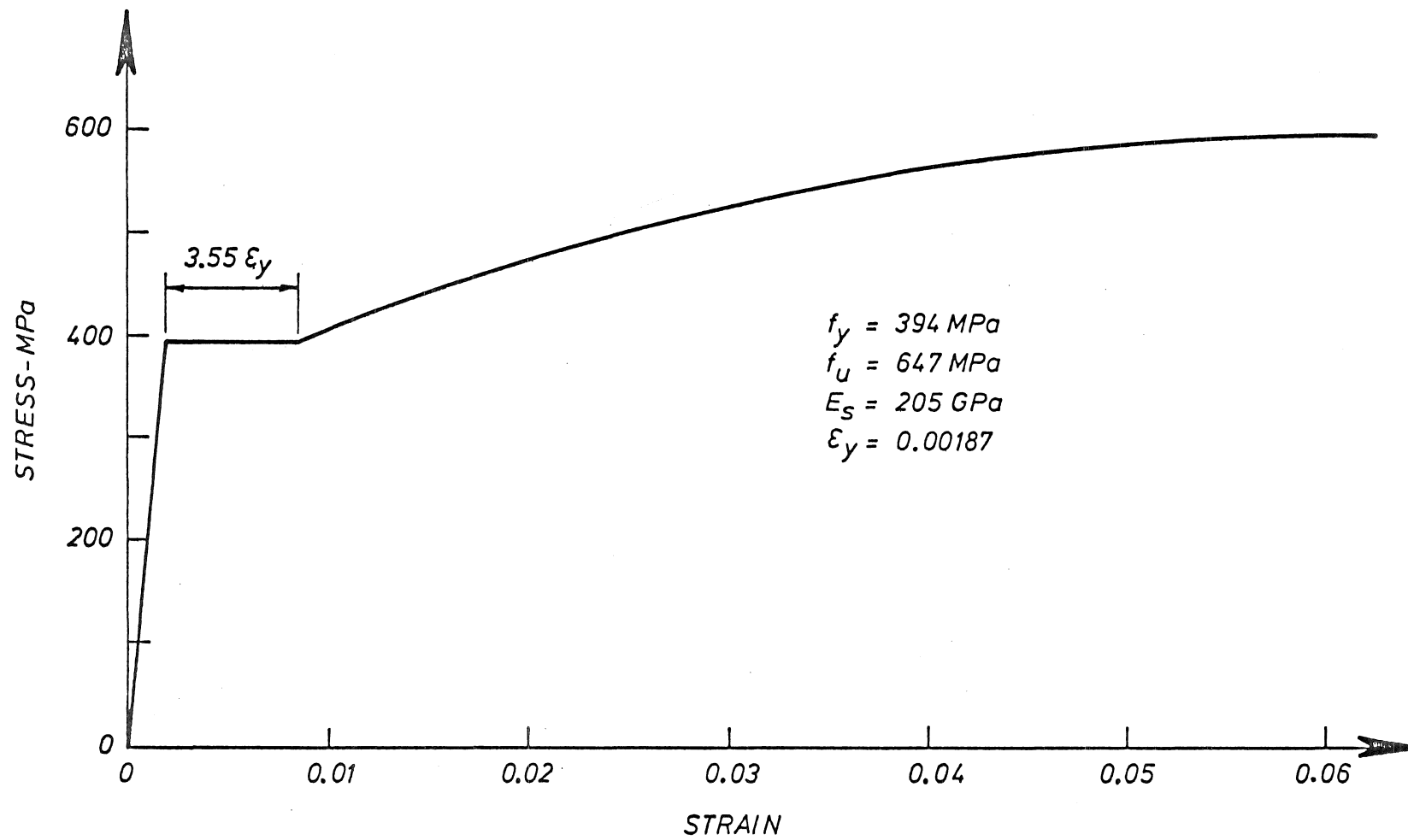


FIGURE 3.2 : STRESS-STRAIN CURVE FOR DH24 STEEL (GRADE 380)

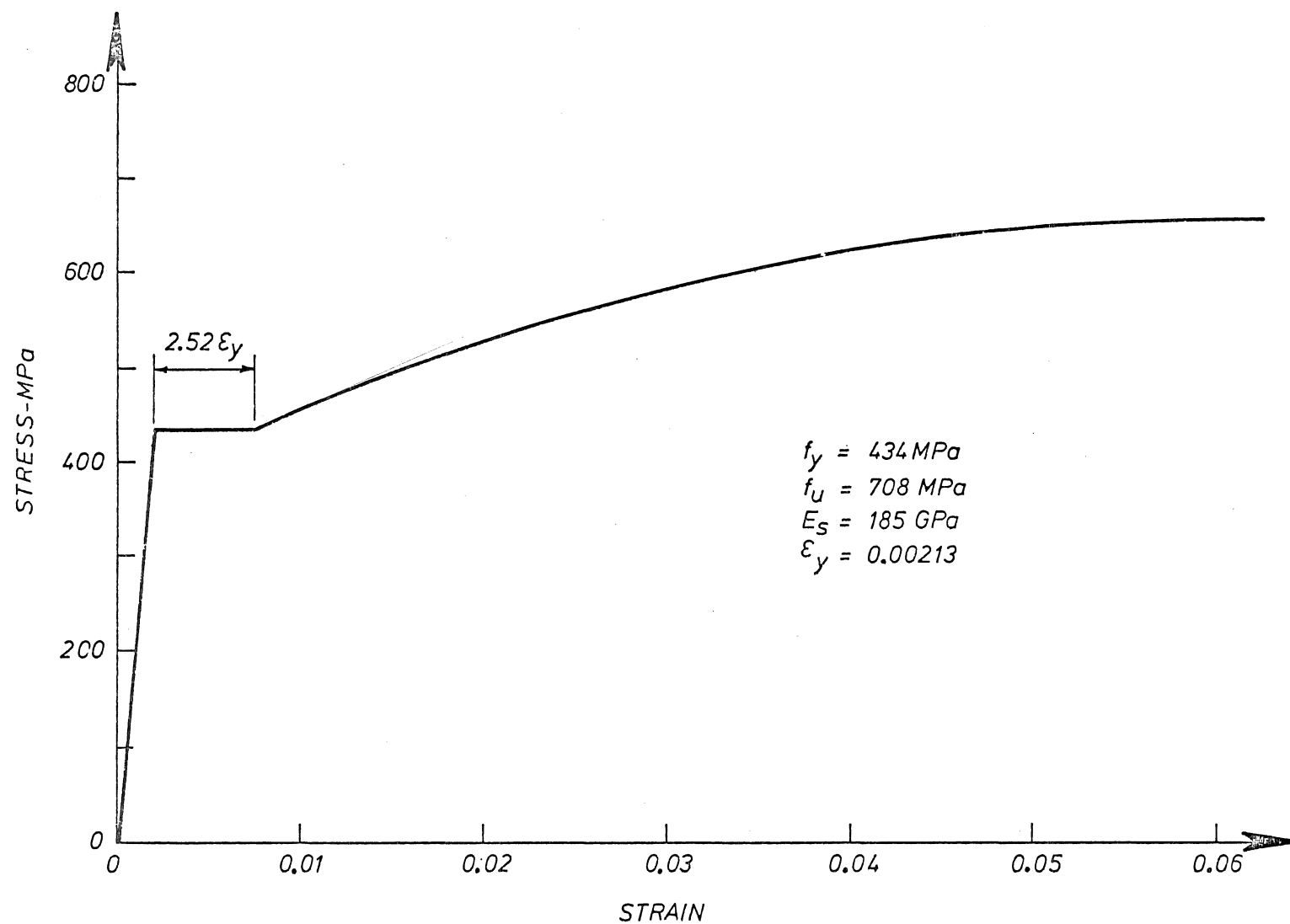


FIGURE 3.3 : STRESS-STRAIN CURVE FOR DH20 STEEL (GRADE 380)

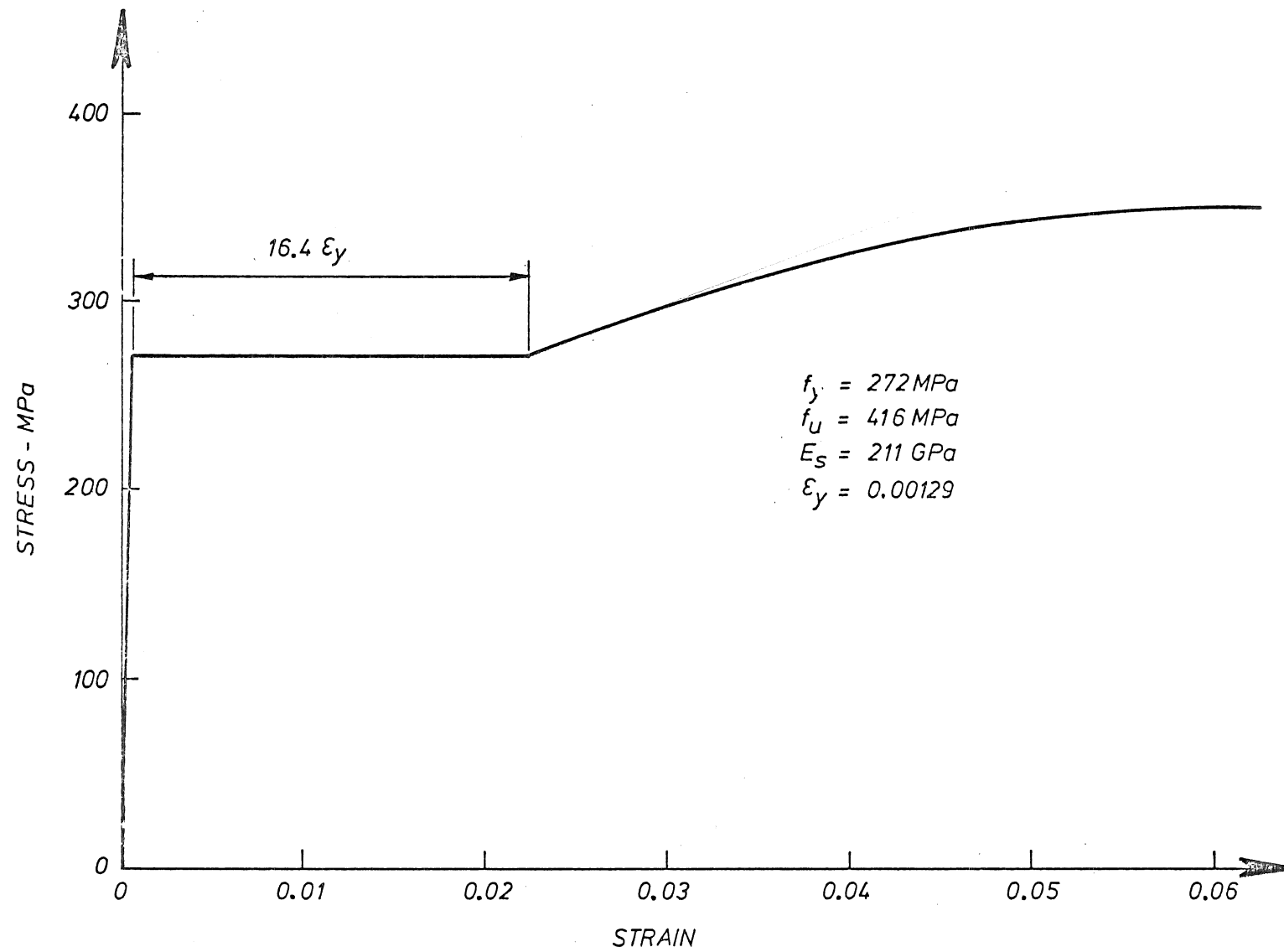


FIGURE 3.4 : STRESS-STRAIN CURVE FOR D20 STEEL (GRADE 275)

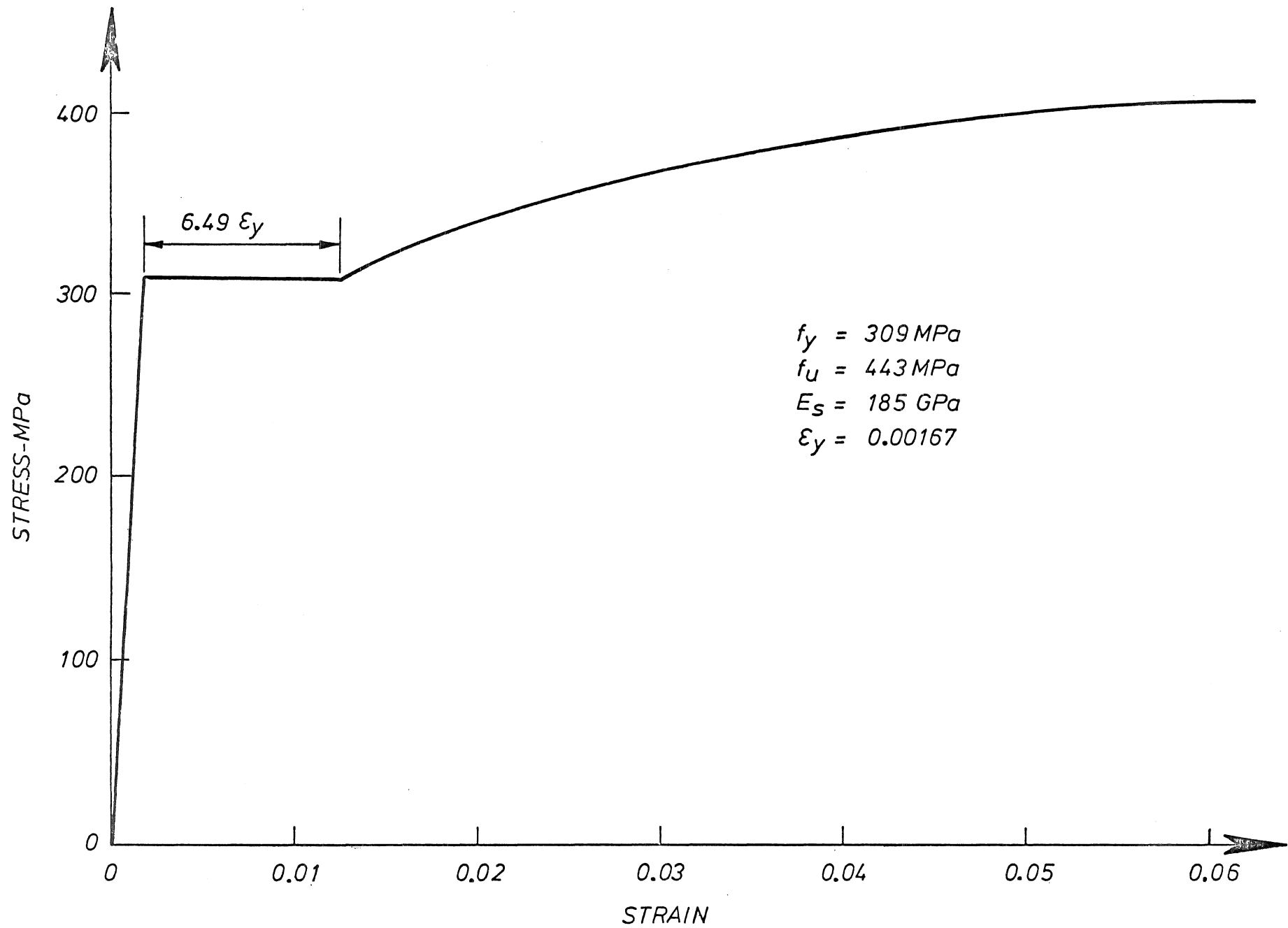


FIGURE 3.5 : STRESS-STRAIN CURVE FOR R10 HOOP STEEL (GRADE 275)

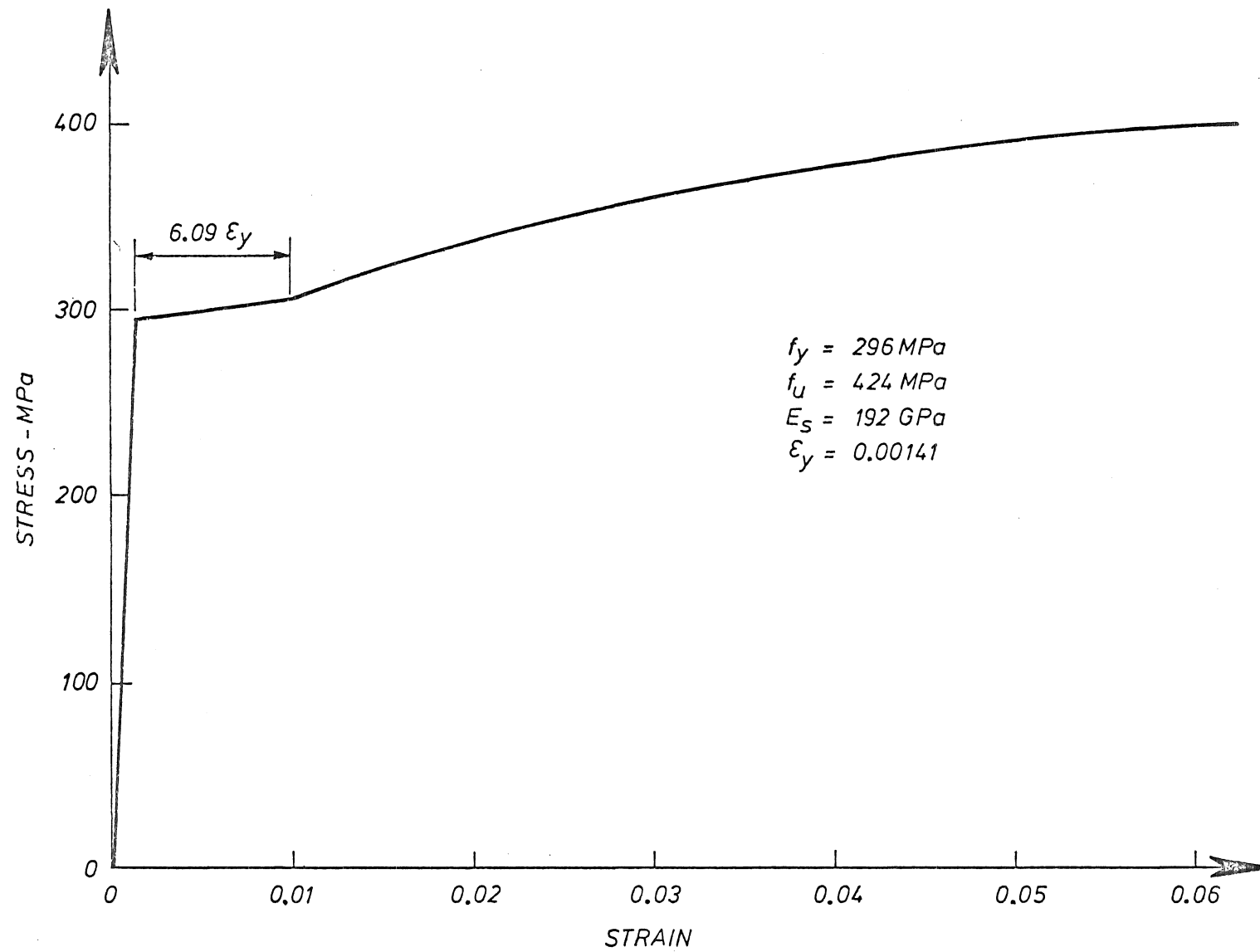


FIGURE 3.6 : STRESS-STRAIN CURVE FOR R12 HOOP STEEL (GRADE 275)

Figure 3.7 shows the strength-age properties of the three batches of concrete as measured by standard 200 x 100 mm diameter cylinder tests. The average cylinder strength measured at 6 weeks is given in Table 3.3, which also summarises reinforcement details for all units. It will be noted that strength at 6 weeks was very close to the target value of 25 MPa for all three batches.

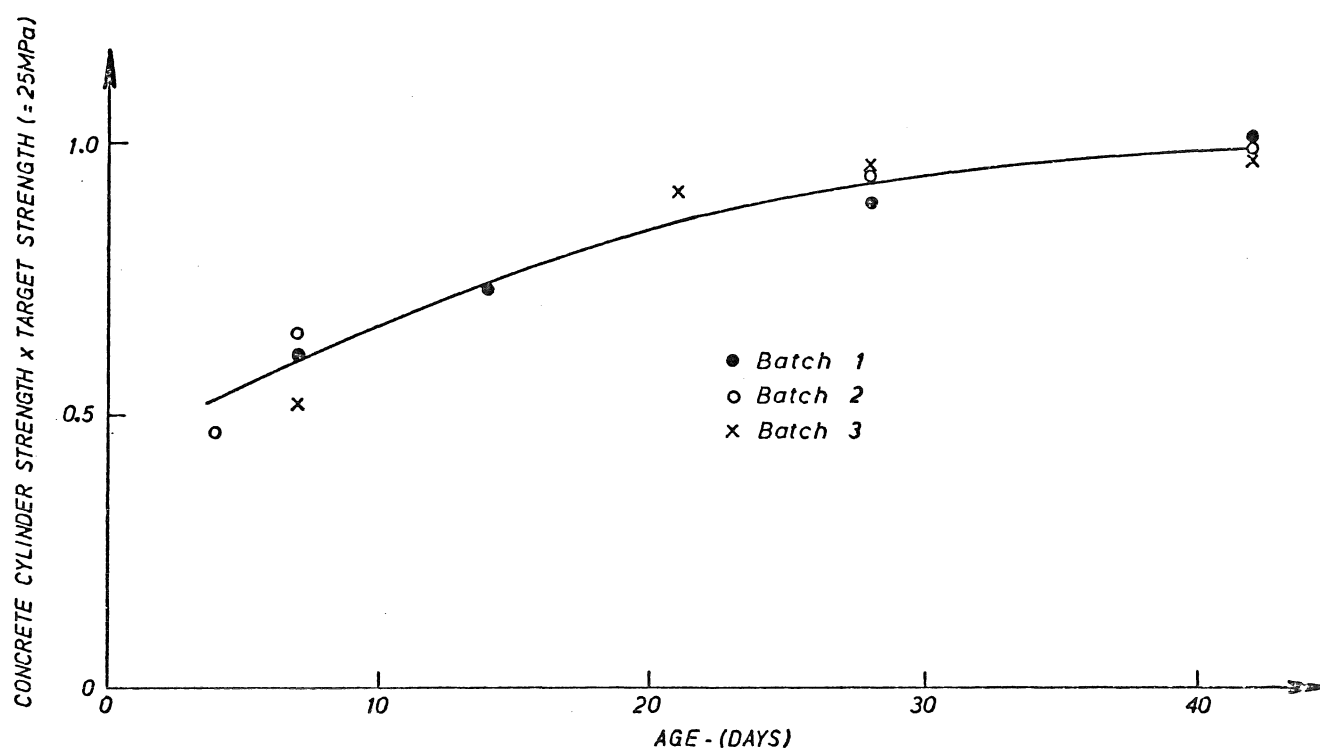
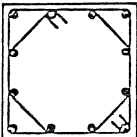
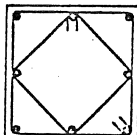
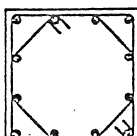
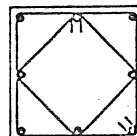
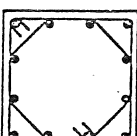


FIGURE 3.7 : STRENGTH-AGE DIAGRAM OF 200 x 100MM DIAMETER CYLINDERS

TABLE 3.3 : Test Unit Properties

Batch No, And (MPa) Cylinder Strength	Specimen Number	Number and Diameter of Longitudinal Bars (mm)	Yield Strength (MPa)	Hoop Diameter and Spacing (mm)	Yield Strength (MPa)	Volume of Hoop Steel	Hoop Type
1 ~ 25.3	1	0		0		0	
	2	12 ~ 20	434	10 ~ 72	309	,0182	
	3	"	"	"	"	"	
	4	"	"	"	"	"	
	5	"	"	"	"	"	
	6	8 ~ 24	394	"	"	,0174	
	7	"	"	"	"	"	
	8	"	"	"	"	"	
	9	"	"	"	"	"	
	10	"	"	"	"	"	
2 ~ 24.8	11	0		0		0	
	12	12 ~ 20	434	10 ~ 98	309	,0140	
	13	"	"	10 ~ 72	"	,0182	
	14	"	"	12 ~ 88	296	,0224	
	15	"	"	12 ~ 64	"	,0309	
	16	"	"	10 ~ 72	309	,0182	
	17	8 ~ 24	394	10 ~ 98	"	,0134	
	18	"	"	10 ~ 72	"	,0174	
	19	"	"	12 ~ 88	296	,0213	
	20	"	"	12 ~ 64	"	,0293	
3 ~ 24.2	21	0		0		0	
	22	12 ~ 20	272	10 ~ 98	309	,0140	
	23	"	"	10 ~ 72	"	,0182	
	24	"	"	12 ~ 88	"	,0224	
	25	"	"	12 ~ 64	"	,0309	
	26	0		0		0	
	27	"		"		"	
	28	"		"		"	
	29	"		"		"	
	30	"		"		"	

3.4 CONSTRUCTION

The height of the test units was chosen to be 1200 mm for two reasons. Firstly this gave a suitable aspect ratio of 3 to 1 height to core dimension, and secondly the 18 mm construction plywood was produced in a 2400 x 1200 mm module. This meant that test units could be cast in batches of ten in two moulds, each with five test units. The formwork was supported by 38 x 38 x 4.7 mm angle at all exterior joints and at the third points of height on each side. The test units were tied at these levels with 10 mm bolts into 16 mm diameter rods that were to be used as lifting points and also during testing as supports for the linear potentiometers used for longitudinal strain measurement.

The construction sequence consisted of tying the cages, fixing the strain gauges to the transverse reinforcement and placing the cages in the painted and oiled moulds. The cages were fixed in position by the bolted tie rods.

The ready mixed concrete was placed in 3 lifts and well vibrated. Eighteen 200 x 100 mm test cylinders were cast and vibrated on a vibration table with each pour. Figure 3.8 shows some aspects of the construction sequence.

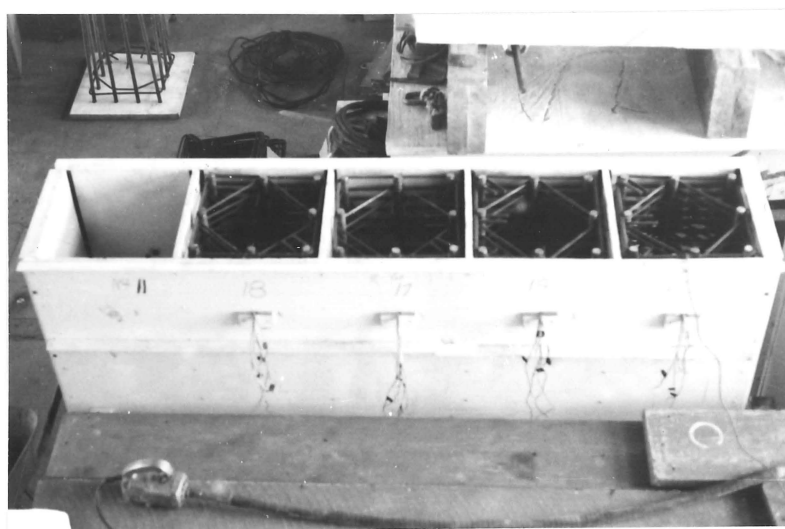
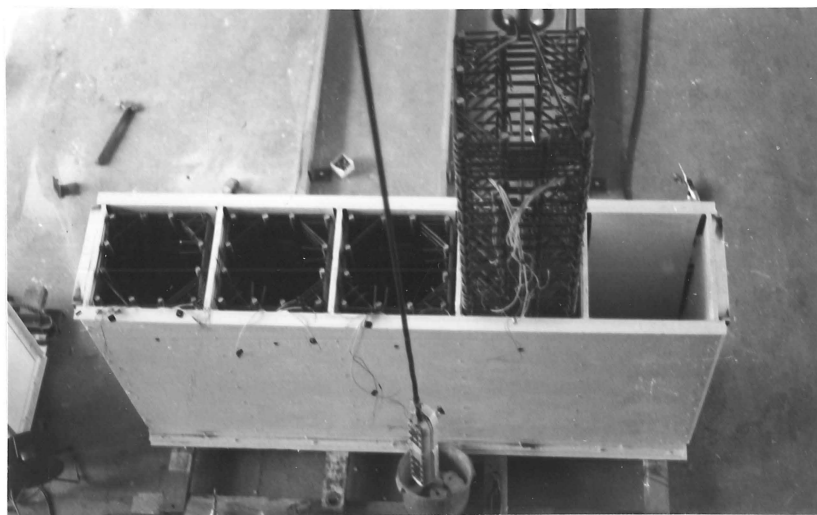


FIGURE 3.8 : Photographs of the Construction Sequence

CHAPTER FOUR

INSTRUMENTATION AND TESTING PROCEDURE

4.0 SUMMARY

To obtain the strain and load measurements for analysis various instruments were required to record the data. This chapter details the instruments used and describes the testing procedure.

4.1 INSTRUMENTATION

Two methods of recording data were used, depending upon the loading rate. For dynamic loading rates all measurements were recorded electronically and synchronised with a 2HZ timing signal generator. For 'slow' loading rates all measurements were recorded manually while loading continued at the preset rate.

4.1.1 Load Measurement

Two methods of load measurement were employed. The first (Pressure Load), as part of the Dartec testing machine equipment, measured load across the pressure transducer valves of the machine hydraulics to a precision of 1 kN. The second (Strain Load) measured load from strain gauges installed on the columns of the Dartec machine. Pressure load was recorded on three Hewlett-Packard X-Y (Type 7035B) Plotters, plotted against Dartec displacement, sum of East and West, and sum of North and South potentiometer strains respectively. Strain load was recorded along with Dartec displacement against time on a two channel Hewlett-Packard chart recorder, (Type 7402A).

4.1.2 Longitudinal Concrete Strains

These were also recorded by two methods. The first was the Dartec machine stroke displacement to give an overall unit strain. The second method recorded linear potentiometer displacement over a central 400 mm gauge length from four 50 mm Sakae 20 FLP 50A 10 Kohm linear potentiometers. By allowing for the flexibility of the Dartec machine quite good agreement

was found between the two records. As well as being recorded in pair summation plotted against load, as described above, individual potentiometer readings were recorded on a 20 channel Bryans Southern Ultra-violet Chart Recorder.

4.1.3 Hoop Reinforcement

To measure strains on hoop reinforcement, electrical resistance strain gauges were fixed to the underside of the transverse reinforcement. In general six gauges were located on each unit at three different levels within the test region, as shown in Figure 4.1. For tests carried out at slow loading rates additional strain gauges were used to obtain further information.

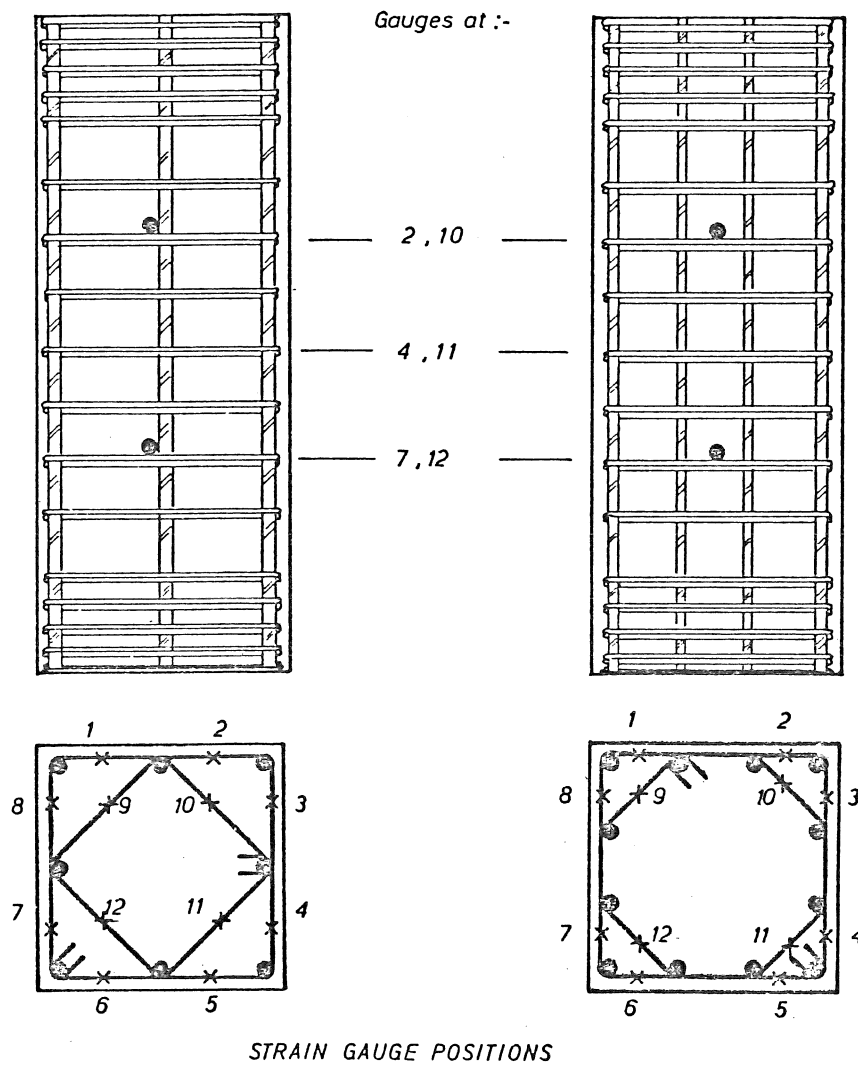


FIGURE 4.1 : Strain Gauge Locations

To affix the strain gauges, gauge sites were smoothed with emery paper and cleaned thoroughly with Methyl Ethyl Keytone. 5 mm KFC-5-C1-11 strain gauges were used throughout, applied with Kyowa CC-15A cement and joined to Showa 5FC-5T self-adhesive terminals. The strain gauges were water-proofed with at least four layers of Shinkoh SN/4 compound and mechanical protection was provided by two layers of Scotch 3M vinyl mastic. All strain gauge leads were threaded through electrical "spaghetti" which was double tied to the stirrups close to the strain gauge site and which provided mechanical protection to the strain gauge leads. The strain readings were recorded individually on the Bryans-Southern Recorder for tests carried out at dynamic loading rates. For tests at slow loading rates, load, Dartec displacement and strains, both longitudinal and transverse, were recorded manually. Potentiometers were connected to a Hewlett-Packard Digital Volt Meter and strain gauges to calibrated Budd P350 strain indicator, respectively.

4.2 TESTING PROCEDURE

4.2.1 Test Unit Preparation

In preparation for testing the units were checked for vertical plumb, and if necessary, vertically aligned by placing washers under the appropriate corners. The units were then set in plaster, firstly on a 20 mm steel base plate and then at the top against the cross head of the machine, to ensure even load distribution to the units. Installation and testing of the units was carried out with the spherical seating, normally located at the top platten, removed. It was felt that a more uniform compression field with lower tendency for buckling of the units at high strains would result from the rigid contact at top and bottom.

For eccentrically loaded units a roller bearing was installed at top and bottom of the test unit, to load the units at a predetermined eccentricity, 49 mm for 12 bar units and 33 mm for 8 bar units. These eccentricities were calculated from a laminar analysis using a stress-strain curve at various strain gradients. The intention of the eccentric loading was to produce a strain gradient varying from zero at the outside of the confined core on one side to a maximum at the other. However, as the required eccentricity, based on the stress-strain curve obtained from the appropriate concentrically loaded unit (unit 2 or 6), was a function of the maximum compression strain (see Table 4.1) this could only be obtained

approximately. The chosen eccentricities satisfy the required strain gradient at a peak compression strain of 0.01. Note that no allowance was made for additional eccentricity resulting from flexural deformation of the units (P - Δ effect). Results presented in Chapter Five show this to be a significant factor.

Potentiometers were mounted on the brackets and strain gauges wired to the appropriate recorder. The Dartec machine and recorders were even calibrated for load, strain and displacement. A preload of 2 MN was used for load calibration.

4.2.2 Testing Procedure

For the bulk of the tests which were performed at the rapid loading rate of 20 mm /s, equal to an average strain rate of 0.0167 /s, a countdown had to be given to approximately synchronise starting the time clock, camera (recording at 4 frames per second), the video tape (for 3 tests), the Hewlett-Packard two channel recorder, the Bryans-Southern recorder, and the Dartec machine operation. The stroke controls of the test machine were set to ramp longitudinal displacement at 20 mm/s to a maximum displacement of 50 mm, corresponding to an average longitudinal strain of 0.0417 and a test duration of 2.5 seconds. This was sufficient to ensure the failure criterion of first hoop fracture was met in all but one eccentrically loaded unit. Eccentric units had a stroke limit of only 30 mm to protect the potentiometers.

Test preparation and instrumentation can be seen in Figure 4.2.

TABLE 4.1 : Calculated eccentricities

MAX. STRAIN	8 BAR UNIT e mm	12 BAR UNIT e mm
.001	90	95
.004 (before spalling)	64	73
.004 (after spalling)	56	63
.01	33	49
.02	24	40

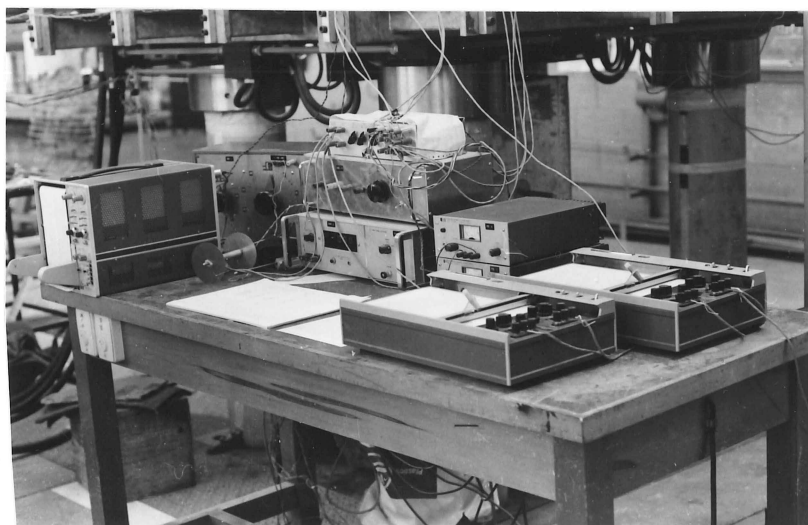
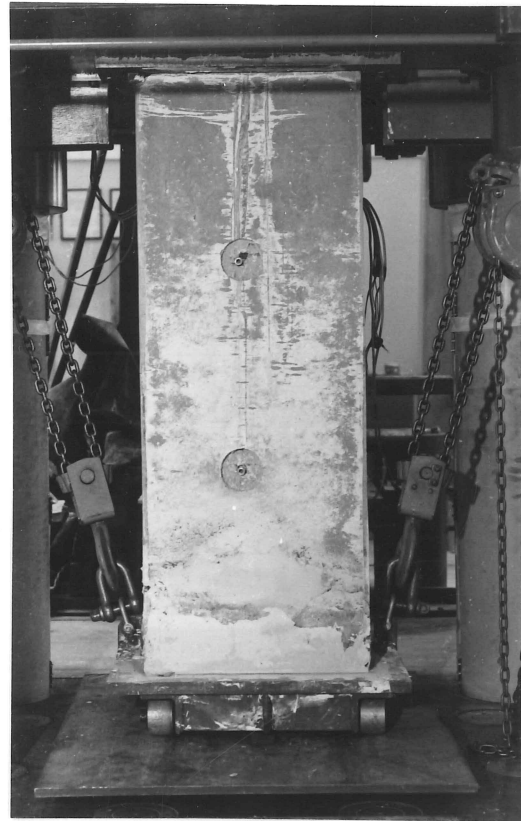


FIGURE 4.2 : Preparation of Test Units, Testing Machine and Recording Instruments.

CHAPTER FIVE

TEST RESULTS

5.0 SUMMARY

This chapter presents the results from the 25 tests performed, describes the visual observations made and discusses trends in behaviour. Graphic results are given for each unit and all are summarised in Table 5.1.

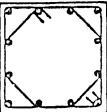
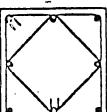
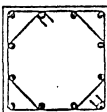
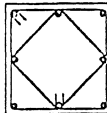


5.1 GENERAL BEHAVIOUR AND VISUAL OBSERVATIONS

The appearance of vertical cover cracks was always the first sign of any distress in the test units. These spread rapidly as cover crushing occurred causing the cover to spall in quite large slabs. As expected, this was particularly evident for units with closely spaced hoops. With the cover gone load still continued to increase a small amount and then began to decrease as the core concrete started to arch between the hoops and longitudinal bars as its outer edges fell away. The load decreased until buckling of the longitudinal bars occurred. This was invariably associated with fracture of the hoops at or near the buckle. As the hoops snapped the core concrete in the vicinity was reduced to fine rubble and flowed, or was ejected from the core. The test ceased at the end of the 50 mm stroke travel.

In spite of the precautions taken to ensure axially of the applied load some strain gradient was evident in both the strain readings and the inclined failure plane.

It was also found after testing that the horizontal bars supporting the linear potentiometers had often deformed near one end, about 50 mm from the longitudinal bars inside the core, indicating that initially plane sections were not remaining plane for the duration of the test. This occurred despite the fact that the end sections remained plane and parallel. To compound the problem further this phenomenon did not occur in all tests. It was noticed that the horizontal bars bent only if they were near a buckle in the longitudinal bars as shown in Figure 5.1,

TABLE 5.1 : SUMMARY OF RESULTS

BATCH NUMBER AND CYLINDER STRENGTH (MPa)	UNIT NUMBER	NUMBER AND DIAMETER OF LONGITUDINAL BARS (mm)	HOOP DIAMETER AND SPACING (mm)	VOLUME OF HOOP STEEL	HOOP SET SHAPES	TYPE OF LOAD	RATE OF LOADING Strain/s mm/s 1200	PEAK LOAD (MN)	AVERAGE STRAIN AT PEAK LOAD	MAXIMUM CORE STRESS $\frac{f_{cc}}{f'_c}$	STRAIN AT MAXIMUM CORE STRESS	AVERAGE STRAIN AT FIRST HOOP FRACTURE	PEAK COMP'N STRAIN AT FIRST HOOP FRACTURE
1 — 25.3	1	0	0	0		Concentric	.000033	4.38	.0018	0.86	.0018	~	
	2	12 ~ 20	10 ~ 72	.0182		"	"	7.07	.0036	1.24	.0052	.0052	
	3	"	"	"		"	.0167	8.41	.0030	1.54	.0040	.0215	
	4	"	"	"		Eccentric	.000033	5.49	.0027			.0274	.0743
	5	"	"	"		"	.0167	6.40	.0033			.0188	.0609
	6	8 ~ 24	"	.0174		Concentric		6.72	.0041	1.22	.0044	.0325	
	7	"	"	"		"	.0167	7.85	.0032	1.47	.0038	.0271	
	8	"	"	"		Eccentric		5.54	.0044			.0206	.0649
	9	"	"	"		"	.0167	6.65	.0026			-	-
	10	"	"	"		Not Tested	~	-	-	-	-	-	-
2 — 24.8	11	0	0	0		Concentric	.0167	5.75	.0012	1.17	.0012	-	-
	12	12 ~ 20	10 ~ 98	.0140		"	"	8.50	.0025	1.55	.003	.0167	
	13	"	10 ~ 72	.0182		"	"	8.65	.0035	1.65	.004	.0203	
	14	"	12 ~ 88	.0224		"	"	8.80	.0033	1.67	.0045	.0289	
	15	"	12 ~ 64	.0309		"	"	9.40	.0052	1.86	.0055	.0304	
	16	"	10 ~ 72	.0182		Not Tested	~	-	-	-	-	-	-
	17	8 ~ 24	10 ~ 98	.0134		Concentric	.0167	7.90	.0027	1.48	.004	.0214	
	18	"	10 ~ 72	.0174		"	"	8.50	.0025	1.60	.0025	.0287	
	19	"	12 ~ 88	.0213		"	"	8.40	.0032	1.62	.0035	.0359	
	20	"	12 ~ 64	.0293		"	"	8.80	.0039	1.75	.004	.0382	
3 — 24.2	21	0	0	0		"	.000033	4.78	.0018	0.97	.0018	-	
	22	12 ~ 20	10 ~ 98	.0140		"	"	7.30	.0017	1.41	.0028	.0238	
	23	"	10 ~ 72	.0182		"	"	7.45	.0021	1.49	.0030	.0287	
	24	"	12 ~ 88	.0224		"	"	7.80	.0023	1.57	.0035	.0284	
	25	"	12 ~ 64	.0309		"	"	8.50	.0030	1.79	.0040	.0323	
	26	0	0	0		"	.000033	6.20	.0010	1.27	.0010	-	-
	27	"	"	"		"	.00167	5.40	.0006	1.10	.0006	-	-
	28	"	"	"		Not Tested		-	-	-	-	-	-
	29	"	"	"		"		-	-	-	-	-	-
	30	"	"	"		"		-	-	-	-	-	-

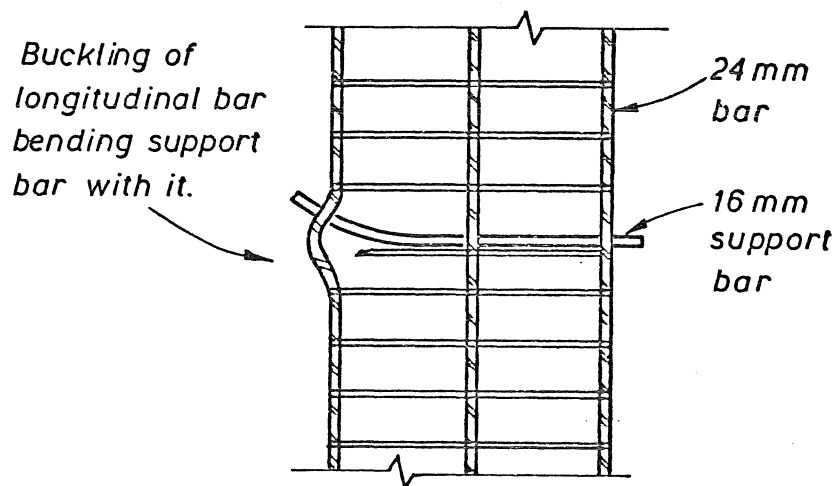


FIGURE 5.1 : Bending of the Support Bars

It appears that very high localised strains associated with longitudinal bar buckling caused local section distortion. However, as this phenomenon occurred towards the end of testing, errors in longitudinal strain are not considered to be great.

The problem of defining an 'ultimate' concrete strain has recently received some attention (e.g. Park, Priestley, and Gill⁽²⁹⁾), Baker and Amerazone⁽⁴¹⁾ and Corley⁽⁴¹⁾ both list expressions for ultimate compressive strain, but experimental studies by Potangaroa, Park and Priestley⁽⁴²⁾ and Gill, Park and Priestley⁽²⁸⁾ have indicated these expressions to be very conservative. In this series of tests marked strength degradation of the core was always initiated by fracture of an internal hoop. Generally a considerable number of hoops fractured before testing was complete, and

the concrete was still able to carry a significant load after fracture of (say) 3 or 4 hoops. It thus seems to be a reasonably conservative decision to define the ultimate compressive strain as the strain at which fracture of a hoop first occurs.

It should be noted that fracture of the outer (rectangular) hoops occurred later, if at all, than fracture of the inner hoops. This was due to bond loss on the outer stirrups, from loss of cover, resulting in an averaging of strain over the core thickness.

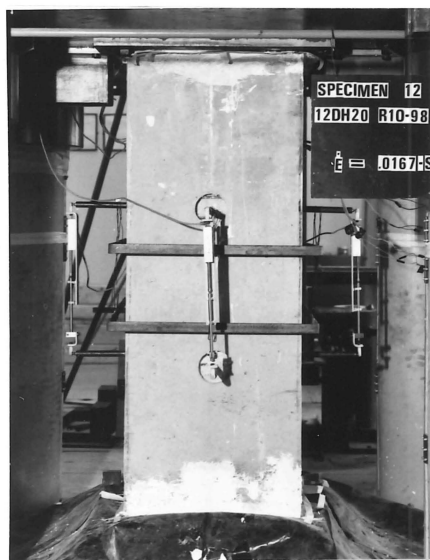
Fracture of an inner hoop and subsequent local degradation of the core also caused a loss of anchorage bond to the outer hoops, resulting in a tendency to unwind rather than fracture.

The series of photographs included in this section show typical behaviour during testing. Figures 5.2 and 5.3 show time sequences of photographs for two units (12 and 15 respectively) taken at high speed with a Nikon SLR camera with a motorised drive unit at approximately 0.35 second intervals. Figures 5.4 and 5.5 show selected features of the tests performed. The horizontal metal bands seen in these figures at the centre of the units were made loose fitting (25 mm clearance all round) to provide protection to the potentiometers but in no way provide any confinement.

Figure 5.3 shows vertical cracking of the cover has occurred by $t = 0.39$ s just before a peak load of 8.5 MN was reached and by the next frame at $t = .79$ s load has fallen to 6.4 MN. The next photograph at $t = 1.13$ occurs just before first hoop fracture and the explosive frame at $t = 1.48$ is the third hoop to fracture. By the last sequential photograph at $t = 2.22$ s six hoops have fractured and two more will do so before the end of the test. The final photograph shows the condition of the core at the end of testing.

Figure 5.3 shows a similar sequence of photos to Figure 5.2. In this series for unit 15 the effect of a higher confinement steel content can be seen. Vertical cover cracks do not appear until $t = 0.79$ s, which, in this case, coincides with a peak load of 9.4 MN. The higher load demand on the Dartec machine has slowed the loading rate from 20 mm/s to 15 mm/s, so first hoop fracture does not occur until $t = 2.88$ s while still carrying a load of 7.5 MN. Falling slabs of cover can be seen at $t = 2.53, 2.83, 3.10$ s. As they fall from the top of the unit. Slabs of cover from the central test region can be seen held in place by the protective bands.

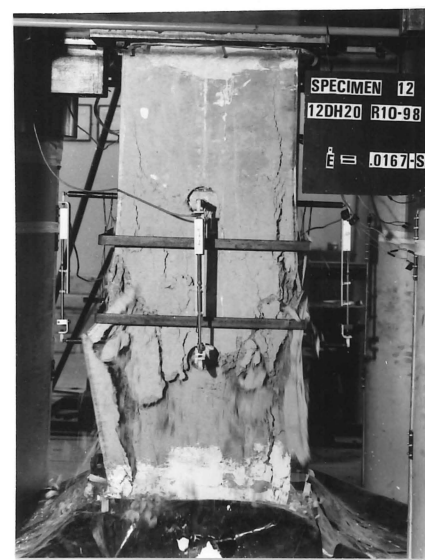
FIGURE 5.2 : Unit 12 Photographs Showing Test Sequence



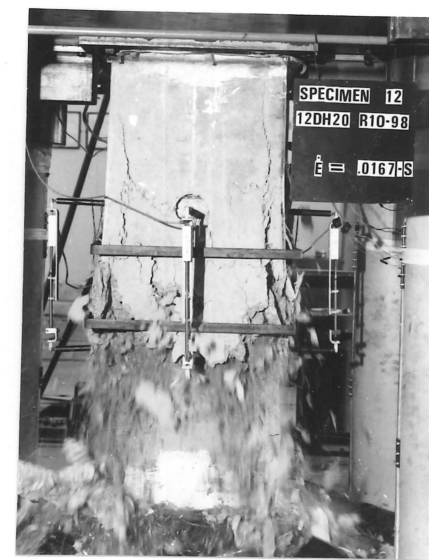
$t = 0$



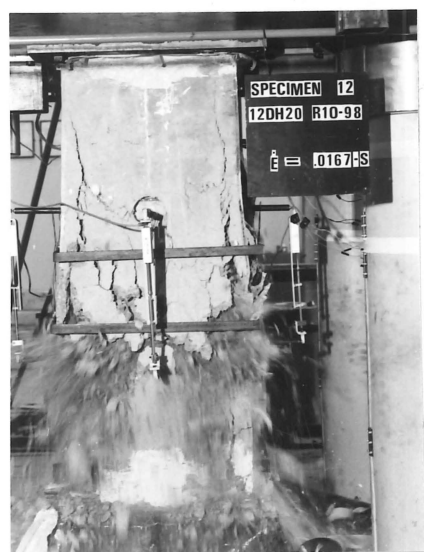
$t = 0.39$



$t = 0.79$



$t = 1.13$



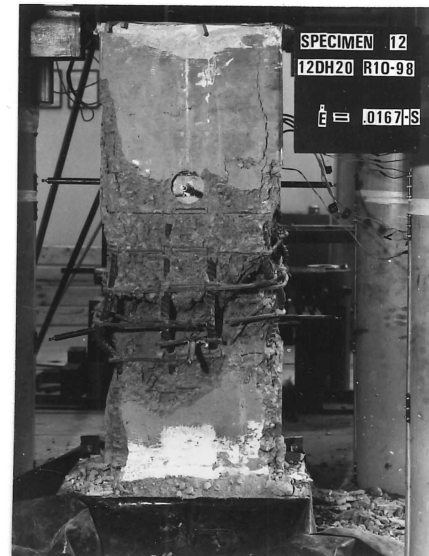
$t = 1.48$



$t = 1.85$



$t = 2.22$

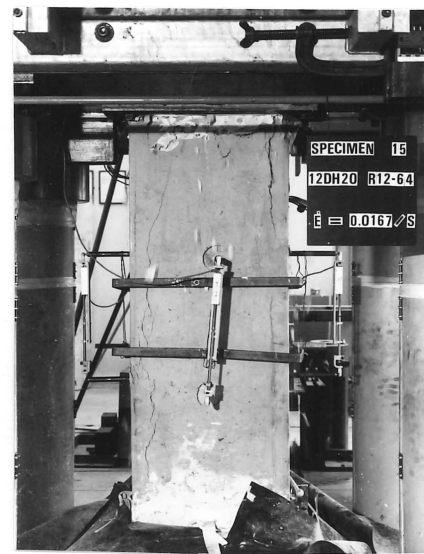


End of Test

FIGURE 5.3 : Unit 15 Photographs Showing Test Sequence



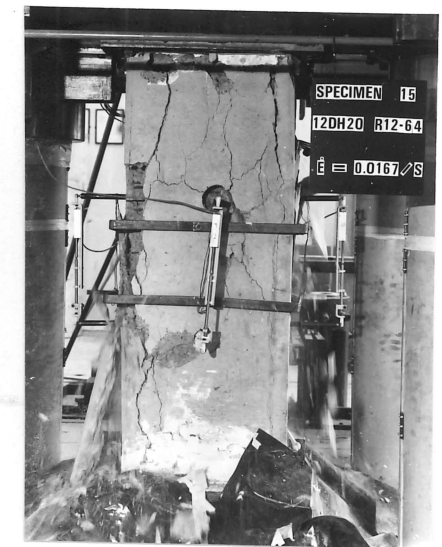
$t = 0.19$



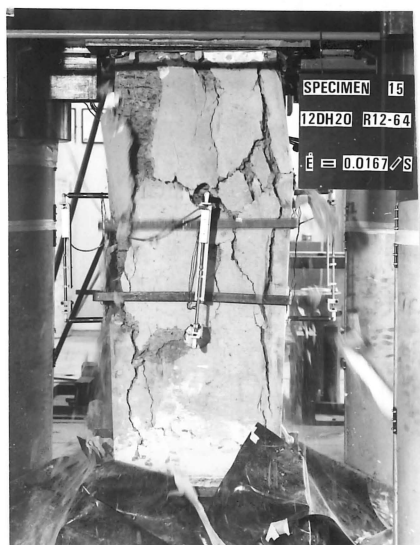
$t = 0.79$



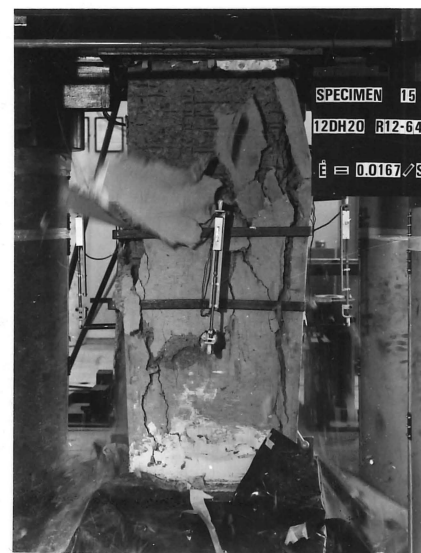
$t = 1.39$



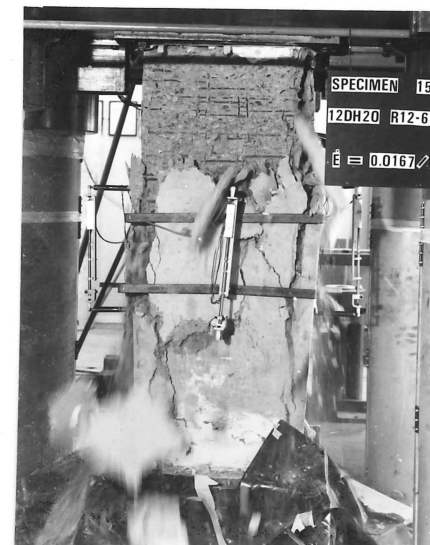
$t = 1.92$



$t = 2.53$



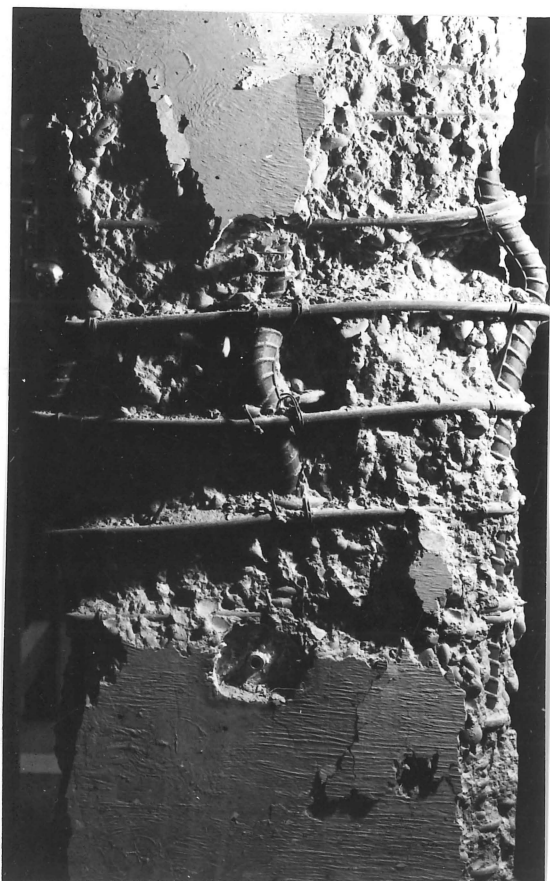
$t = 2.83$



$t = 3.10$



End of Test



(a)



(b)

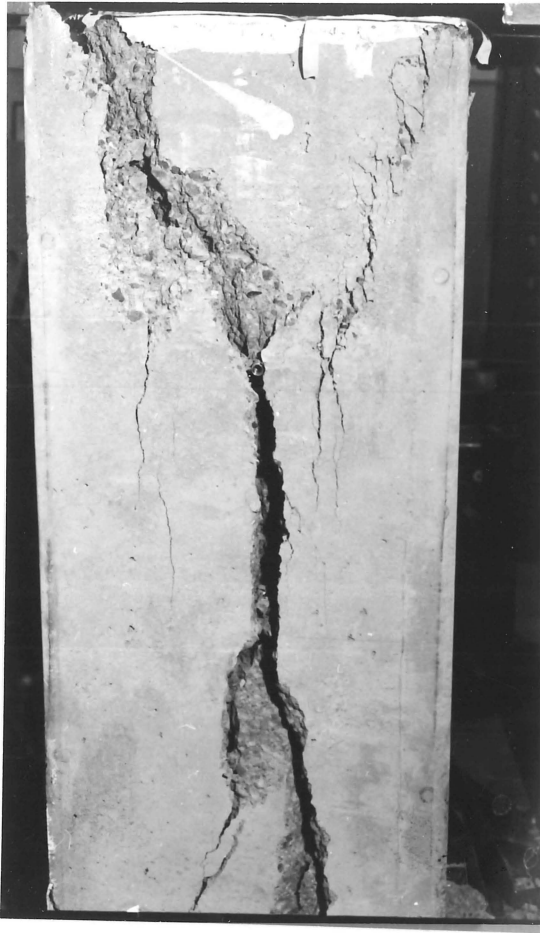


(c)

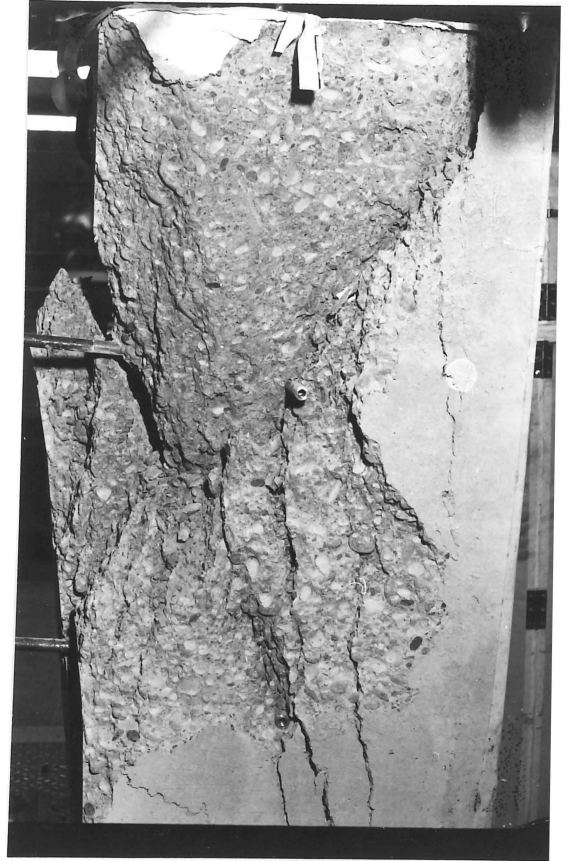


(d)

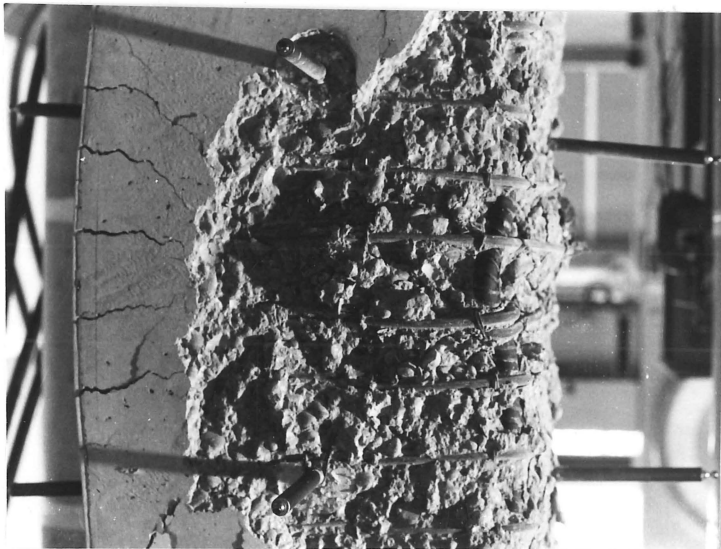
FIGURE 5.4 : Photographs Showing Selected Features of Failure For Various Units



(a)



(b)

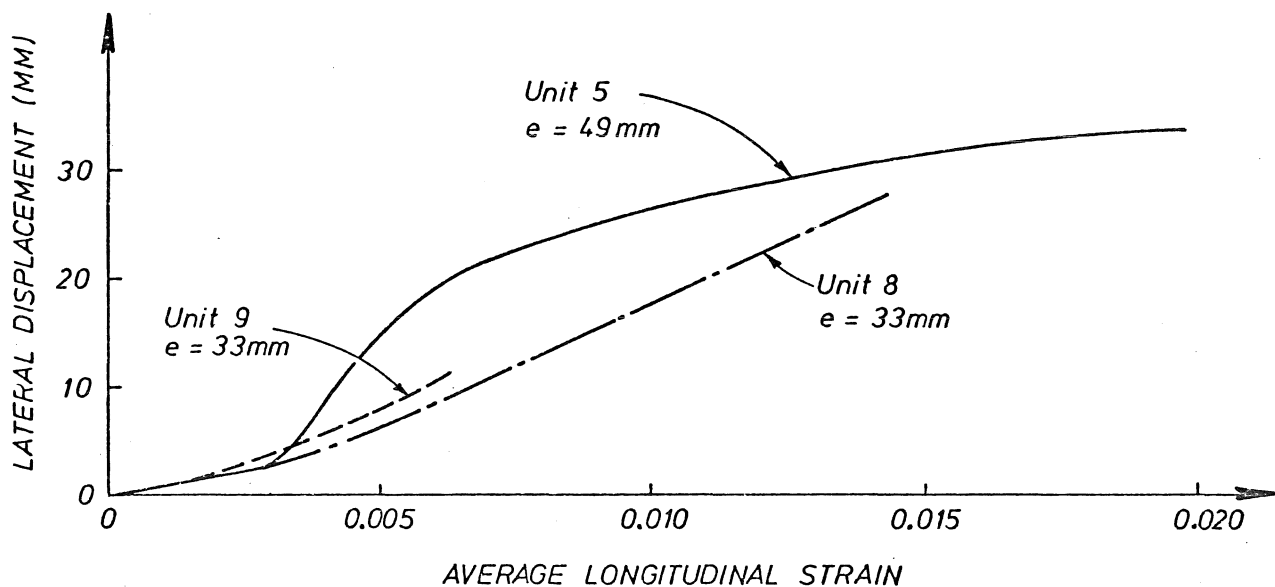


(c)



(d)

FIGURE 5.5 : Photographs Showing Selected Features of Failure for Various Test Units



MID-HEIGHT LATERAL DISPLACEMENT VERSUS AVERAGE LONGITUDINAL STRAIN

FIGURE 5.5 (e) :

Figure 5.4(a) shows unit 17 after testing and is typical of all units tested axially. Failure has occurred in the central region, longitudinal bars have buckled and in this case for lightly confined units the core has deteriorated rather badly;

Figure 5.4(b) shows a close-up of the fracture of three hoops from unit 12 (see also Figure 5.2). Note also the loss of anchorage to the outer hoops and the bending of the horizontal potentiometer bars.

Figure 5.4(c) depicts the double buckling of a 20 mm dia Grade 380 longitudinal bar and Figure 5.4(d) shows a close-up view of the excellent condition of Unit 15 (see also Figure 5.3) after testing,

Unit 11, the plain unit tested at high speed can be seen in Figure 5.5(a) and (b). The cone failure at each end joined by a large vertical crack

was typical of all plain units tested. The failure was always brittle and sudden with rapid loss of load capacity.

The eccentrically loaded units 4 and 5 can be seen in Figures 5.5(c) and (d) respectively. Note the buckling of the longitudinal bars on the compression face and the large evenly spaced tension cracks on the opposite face. These cracks are slightly inclined due to the shear induced by the moment gradient resulting from high, but variable $P - \Delta$ moments. As $P - \Delta$ moments are a maximum at mid-height and zero at top and bottom, a moment gradient with height, and thus a shear force distribution, is involved.

Figure 5.5(e) shows the significance and magnitude of the central deflection as it relates to the applied eccentricity and longitudinal strain.

5.2 PRESENTATION OF RESULTS

Results are presented graphically for all units tested, in Figures 5.6 to 5.34 which show three graphs per unit. These show (a) Load versus longitudinal strain curves, (b) Hoop steel stress versus longitudinal strain, and (c) core concrete stress versus longitudinal strain. On all of these is indicated the longitudinal strain at which the first hoop snapped. The load-strain curves show the sequential fracture of ties as steps of decreasing load. The cover concrete and steel components of the load are shown individually and summed so that the remaining load carried by the core is defined. The load carried by the cover was calculated from the stress strain relationships of unit one, tested at the slow rate. The results from unit eleven, tested at the fast rate, were not available until much later in the series. For this reason unit one is compared with all units rather than unit eleven. If there was a difference of $0.15 f'_c$ in stress at a given strain between units one and eleven, the difference in load carried by the cover would be 0.13 MN. The load and stress carried by the core is then in error by less than 2%. It was found that if the cut-off strain for cover contribution was taken as 0.003 or 0.004, the stress strain curve peaked at that strain. It therefore seemed reasonable to use the stress-strain curve for unit one to a strain of .01 to model the behaviour of the cover. From this graph the core stress-strain curve was calculated by subtracting the components described above from the total load. Also shown on the stress-strain curve is the appropriate Modified Kent and Park stress-strain relationship detailed in Chapter One. The Hoop steel stress-strain curve shows an average of the hoop steel stresses and indicates when the hoops have yielded relative to

the longitudinal strain.

For the eccentrically loaded units (4, 5, 8 and 9) the first graph for each (Figures 5.9, 5.11, 5.15 and 5.17) shows the load strain curves for tension and compression strains at the outside of the core and for an average of these. Note that initially both sides were in compression and as the longitudinal strain increased, lateral displacement increased, resulting in an effective increase in eccentricity of load ($P - \Delta$ effect). This effected a change in strain gradient resulting in the crack patterns seen in Figure 5.5 (c) and (d). The second graph for each of the eccentrically loaded units (Figures 5.10, 5.12, 5.16, and 5.18) shows a comparison of theoretical and experimental load and movement plotted against average strain. The theoretical curve was found from a laminar analysis using nine 50 mm strips. Assuming an average strain over the strip, the stress at that strain was found from the corresponding unit with the same longitudinal and transverse steel and loaded axially at the same rate. The cover contribution was treated in the same manner as for axially loaded units.

Five units (10, 16, 28, 29, 30) shown in Table 5.1 as 'not tested' were left for future comparison of age effects.

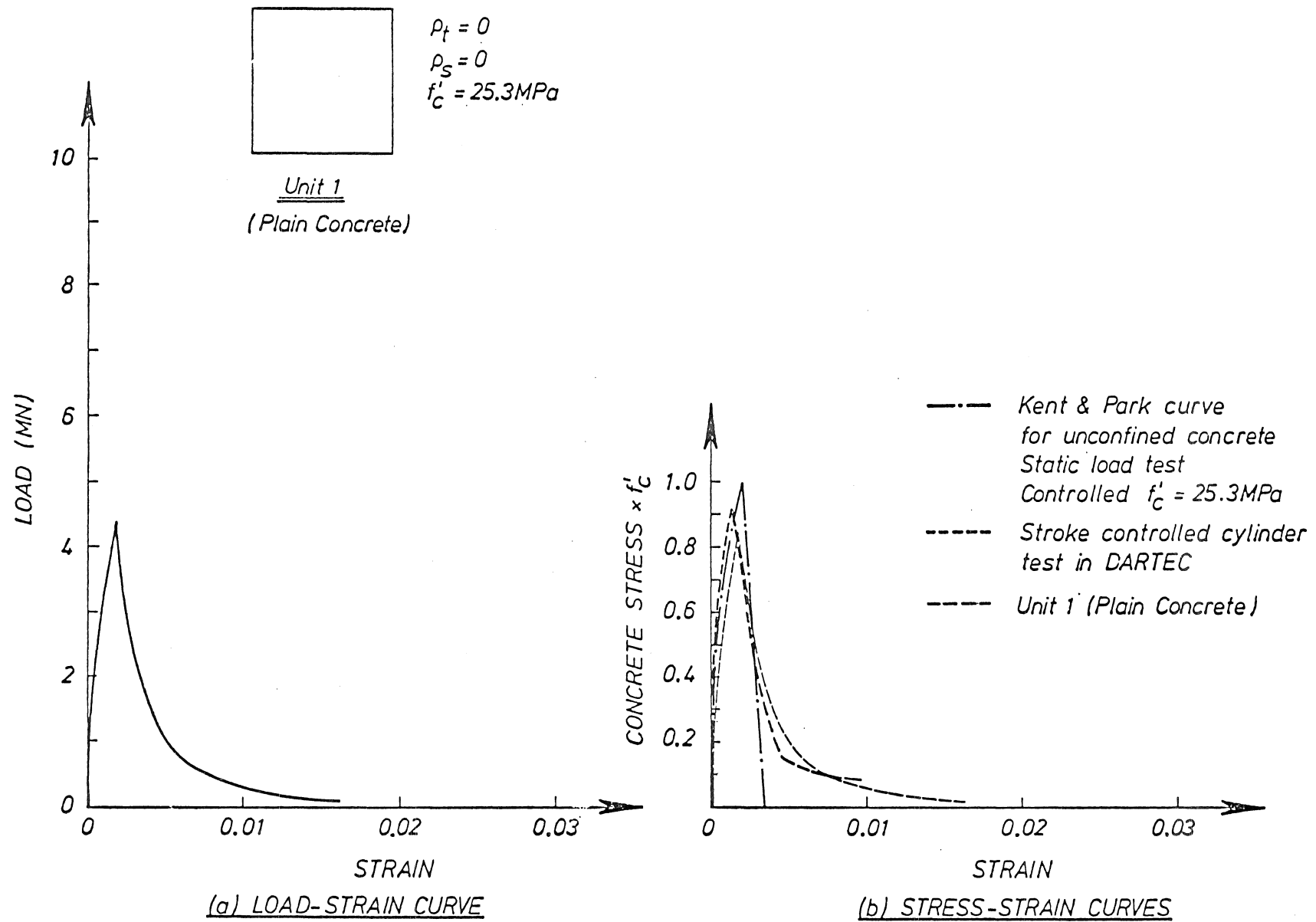


FIGURE 5.6 : UNIT 1 AXIAL LOAD, SLOW SPEED

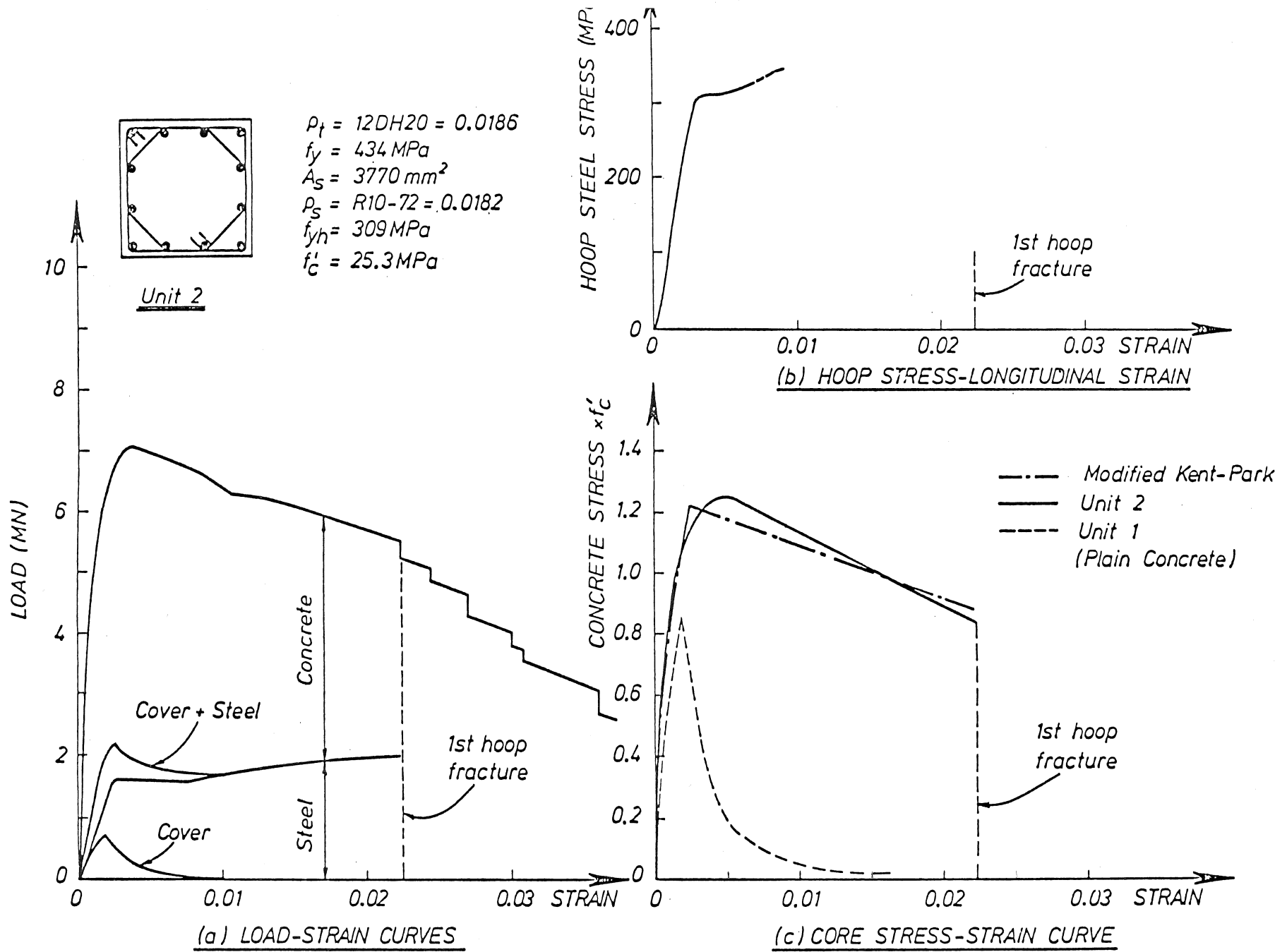


FIGURE 5.7 : UNIT 2 AXIAL LOAD, SLOW SPEED

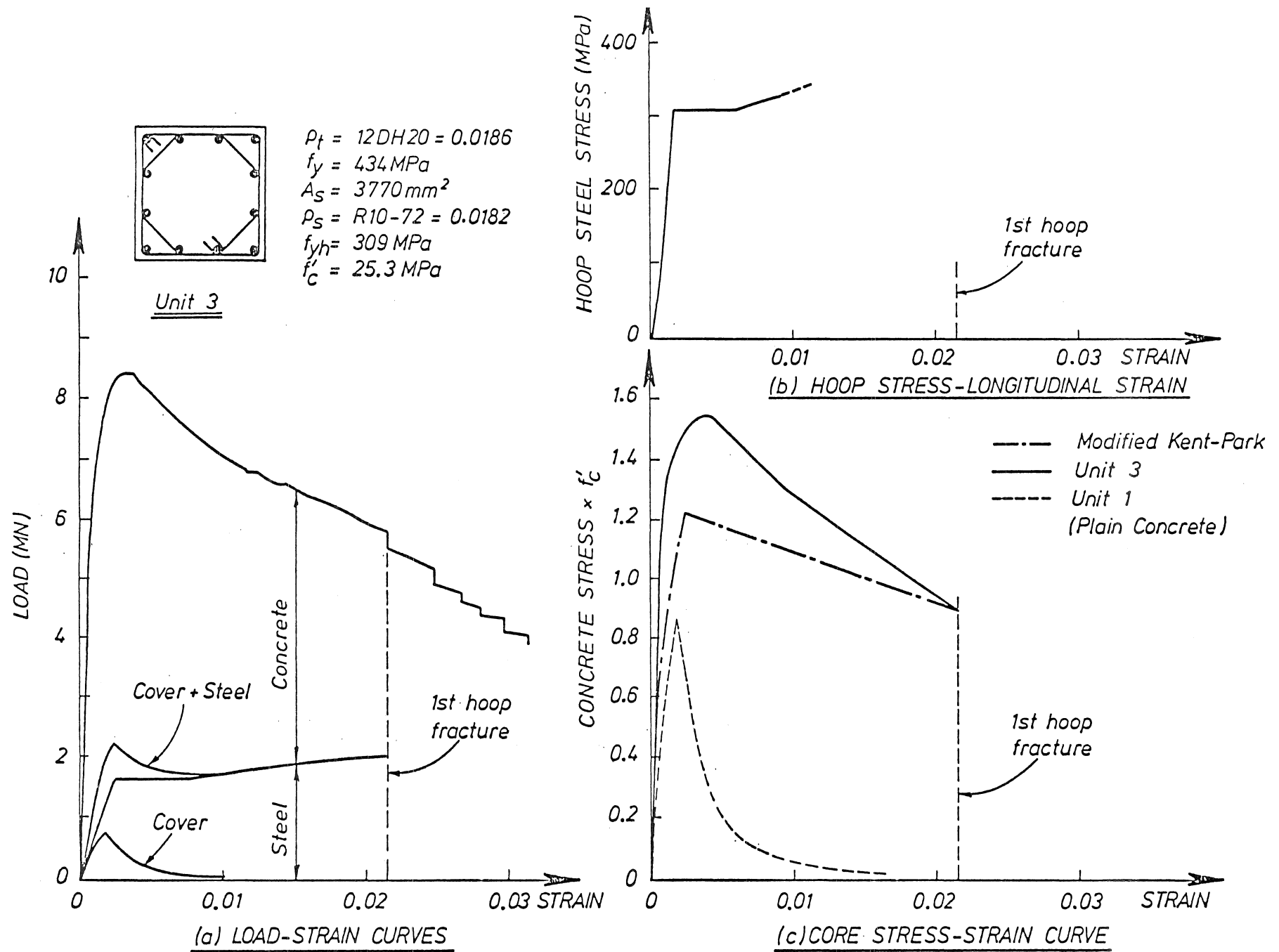


FIGURE 5.8 : UNIT 3 AXIAL LOAD, HIGH SPEED

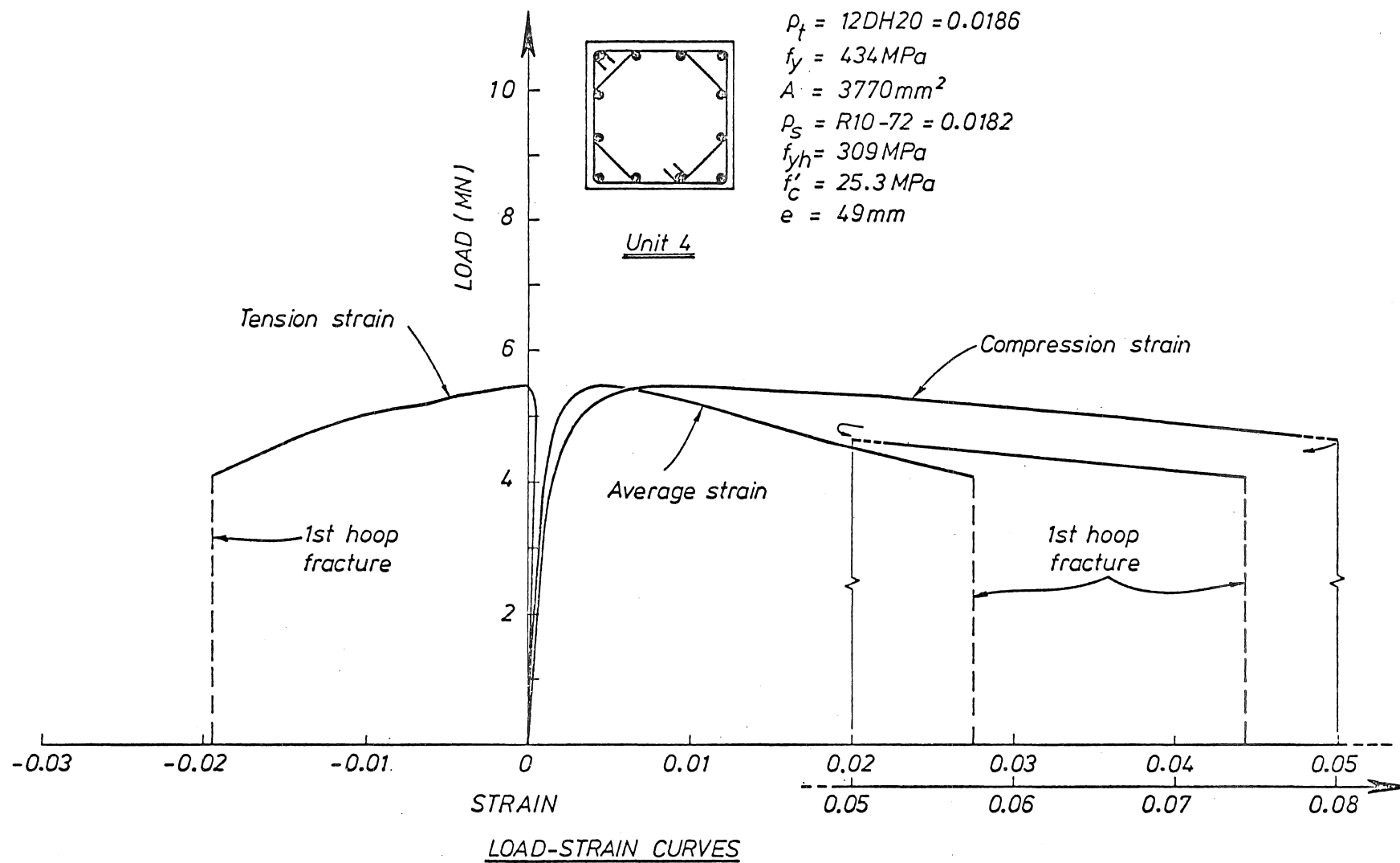


FIGURE 5.9 : UNIT 4 ECCENTRIC LOAD, SLOW SPEED

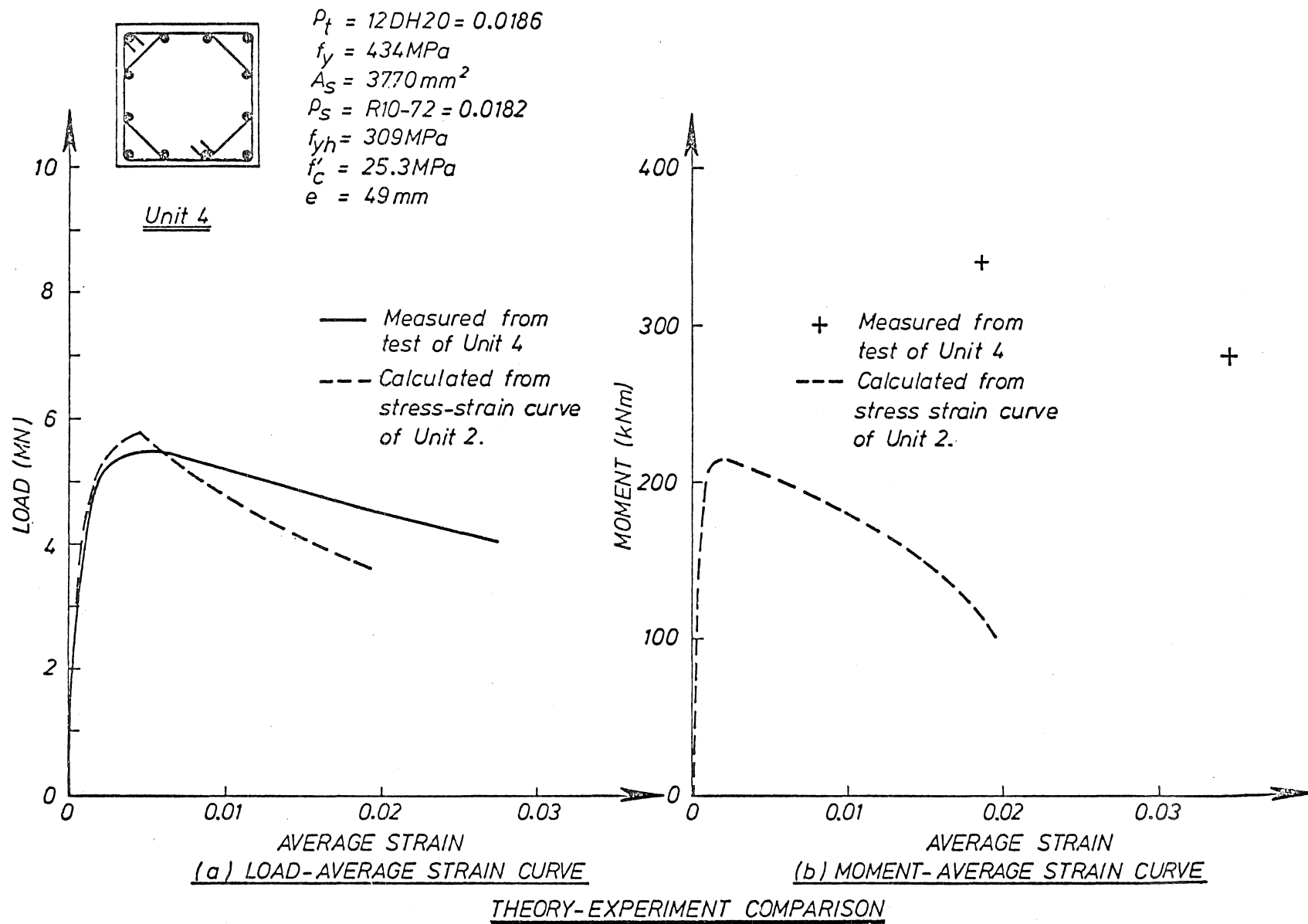


FIGURE 5.10 : UNIT 4 ECCENTRIC LOAD, SLOW SPEED

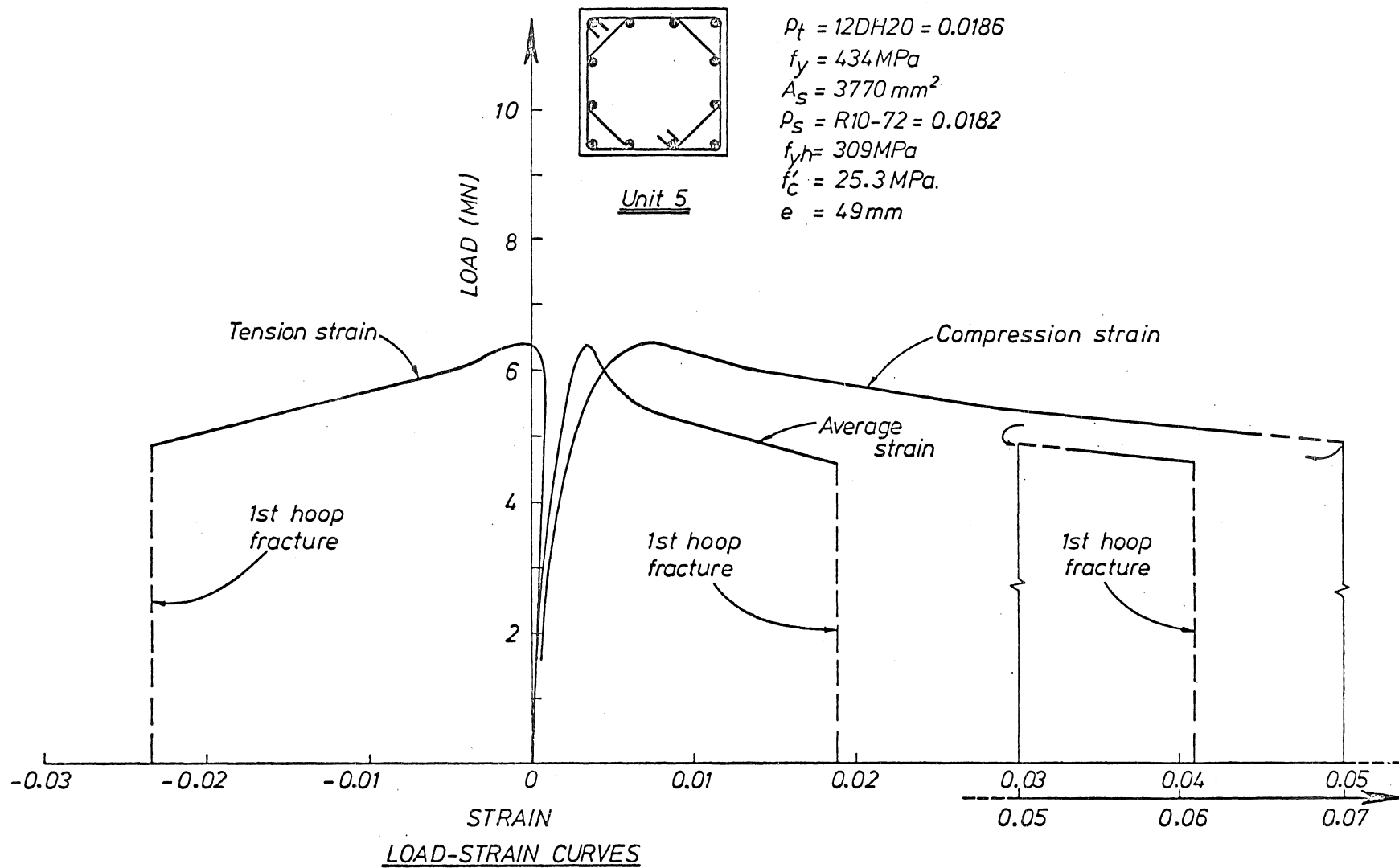


FIGURE 5.11 : UNIT 5 ECCENTRIC LOAD, HIGH SPEED

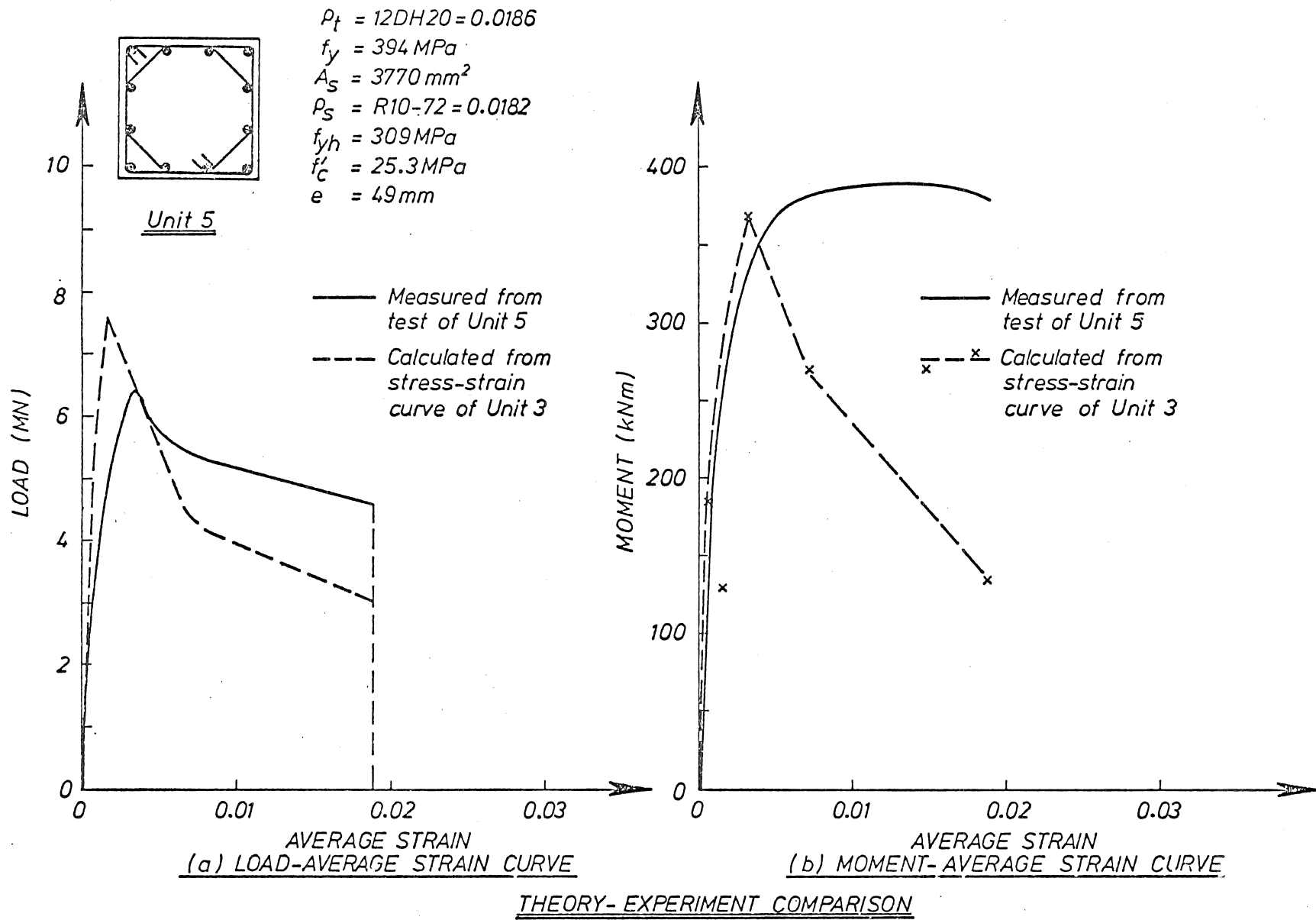


FIGURE 5.12 : UNIT 5 ECCENTRIC LOAD, HIGH SPEED

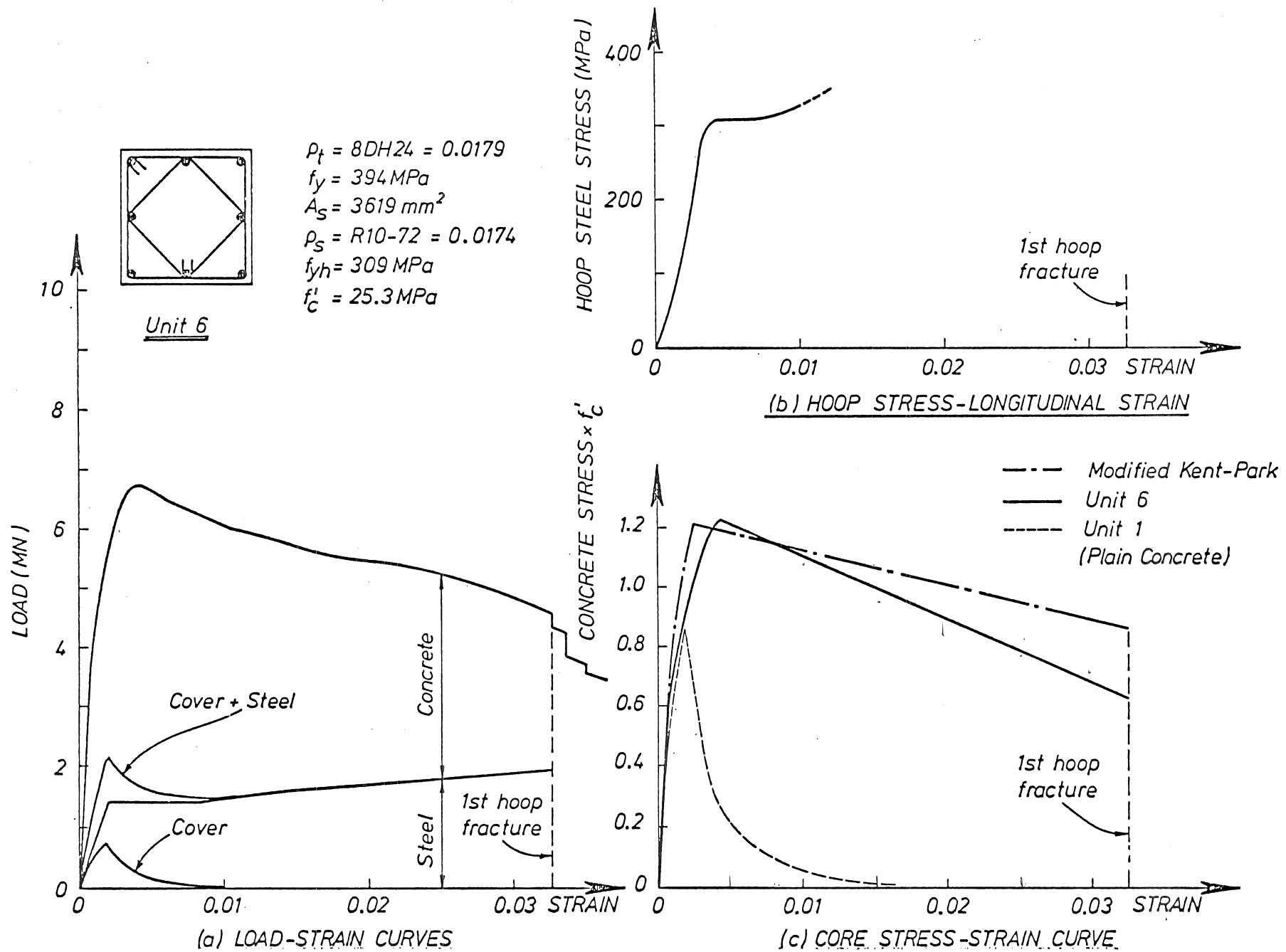


FIGURE 5.13 : UNIT 6 AXIAL LOAD, SLOW SPEED

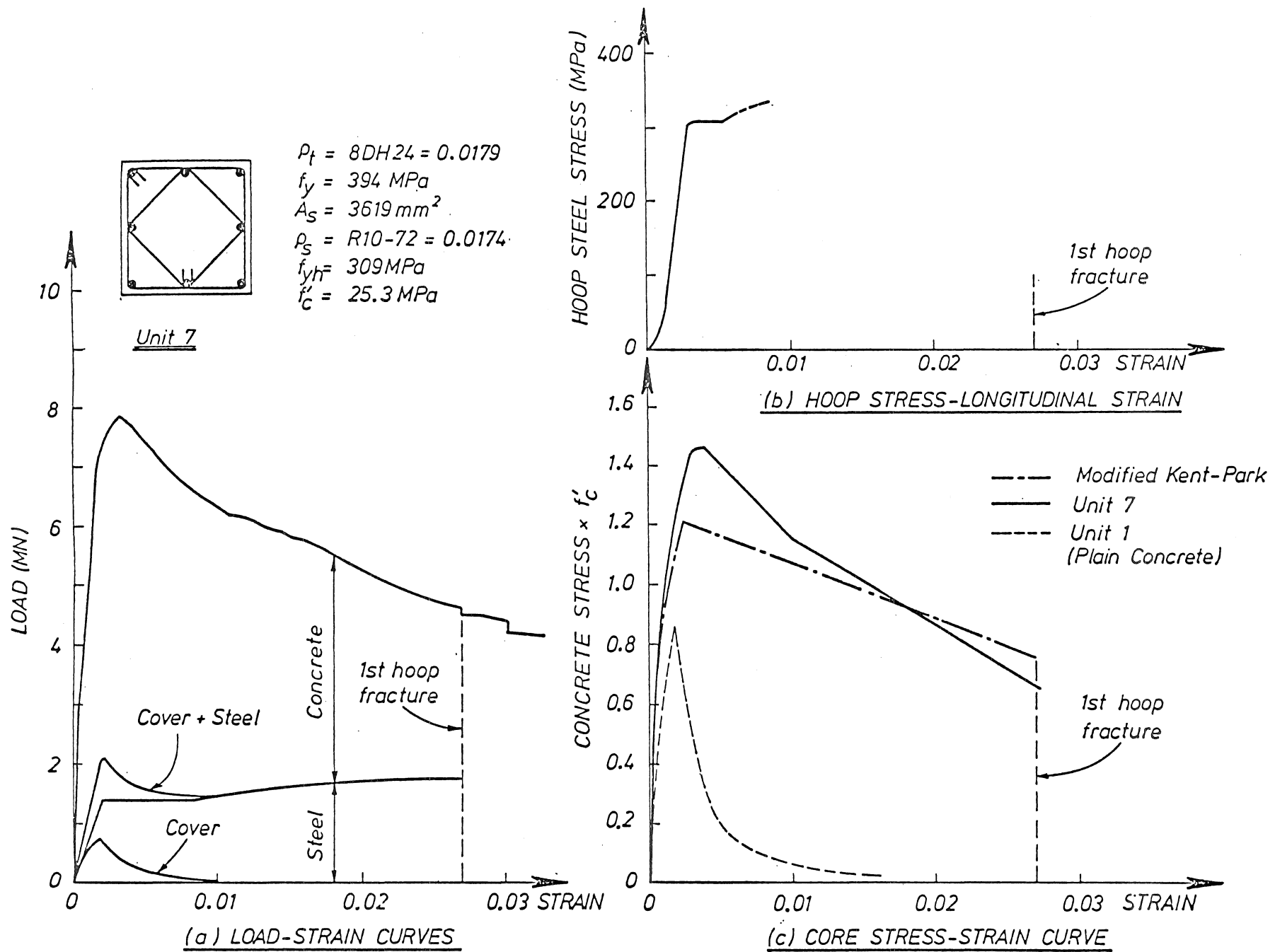


FIGURE 5.14 : UNIT 7 AXIAL LOAD, HIGH SPEED

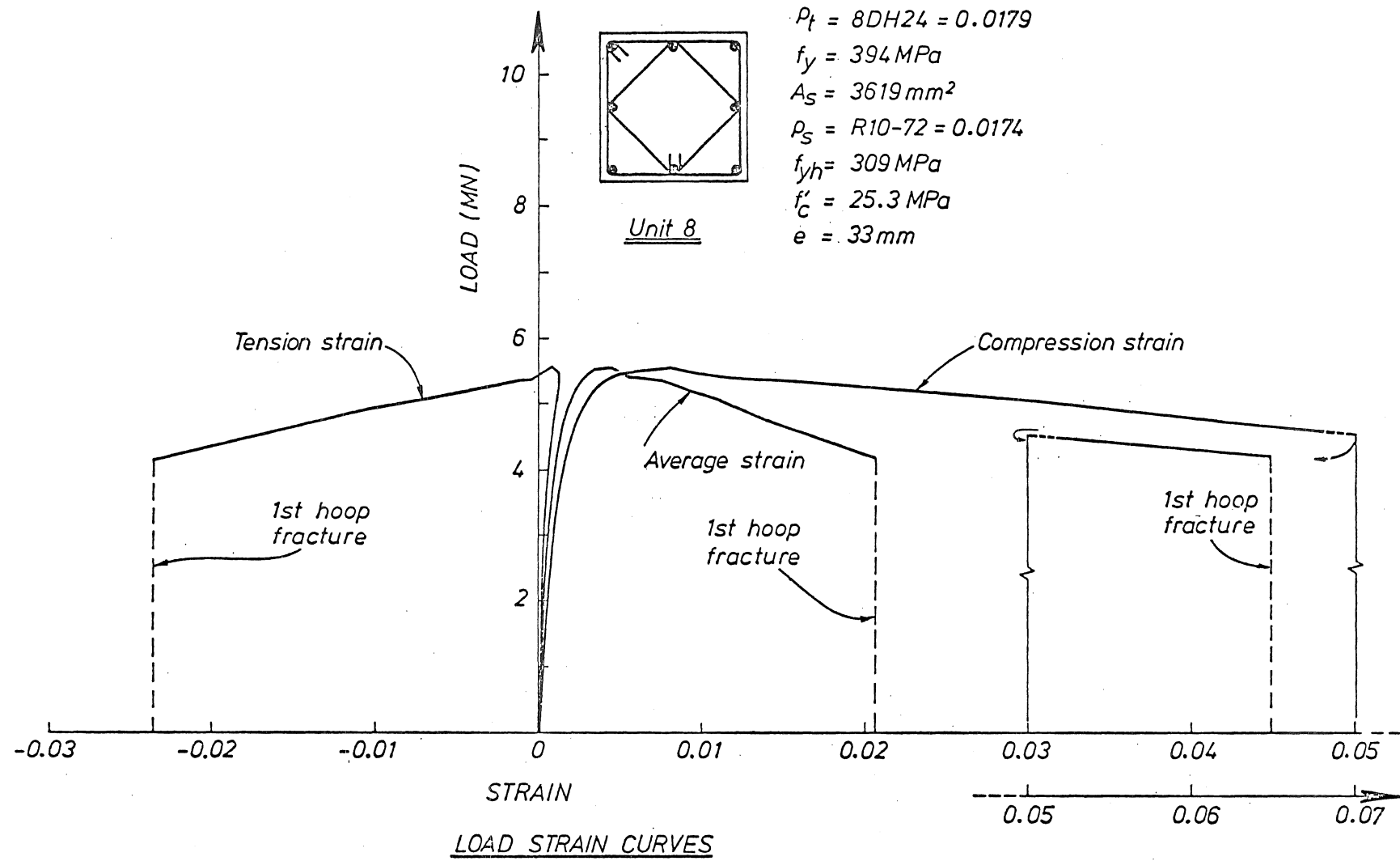


FIGURE 5.15 : UNIT 8 ECCENTRIC LOAD, SLOW SPEED

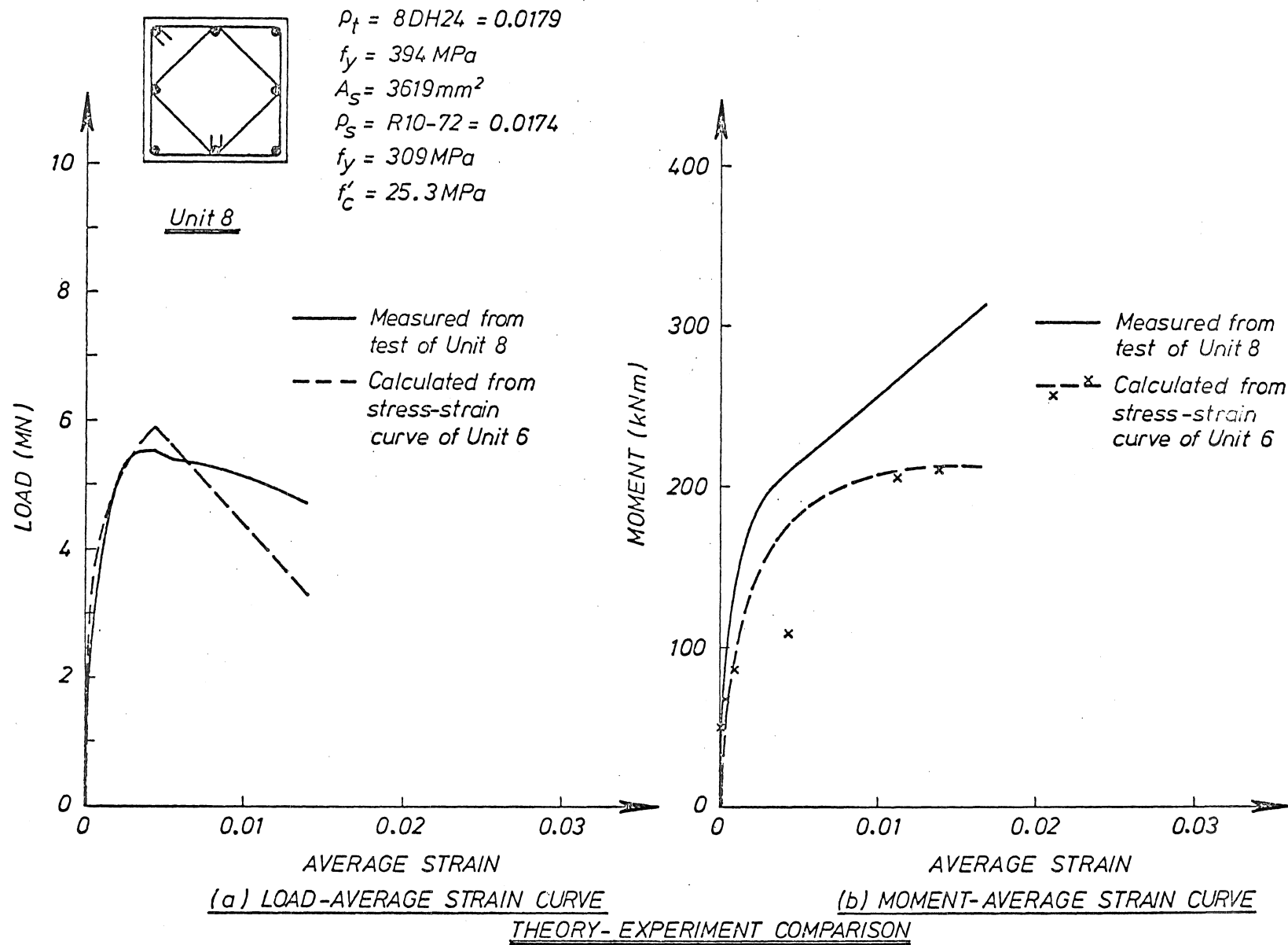


FIGURE 5.16 : UNIT 8 ECCENTRIC LOAD, SLOW SPEED

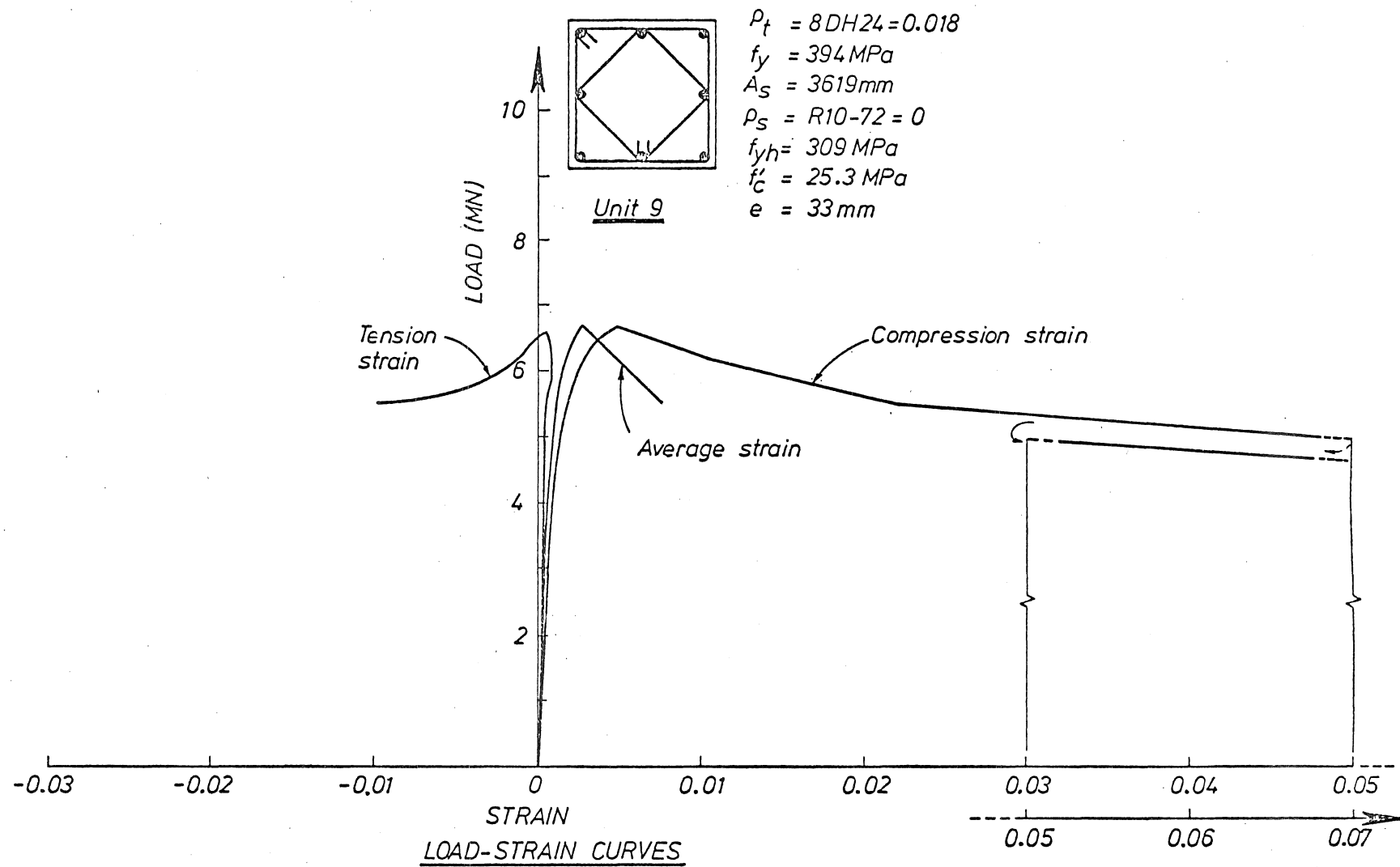


FIGURE 5.17 : UNIT 9 ECCENTRIC LOAD, HIGH SPEED

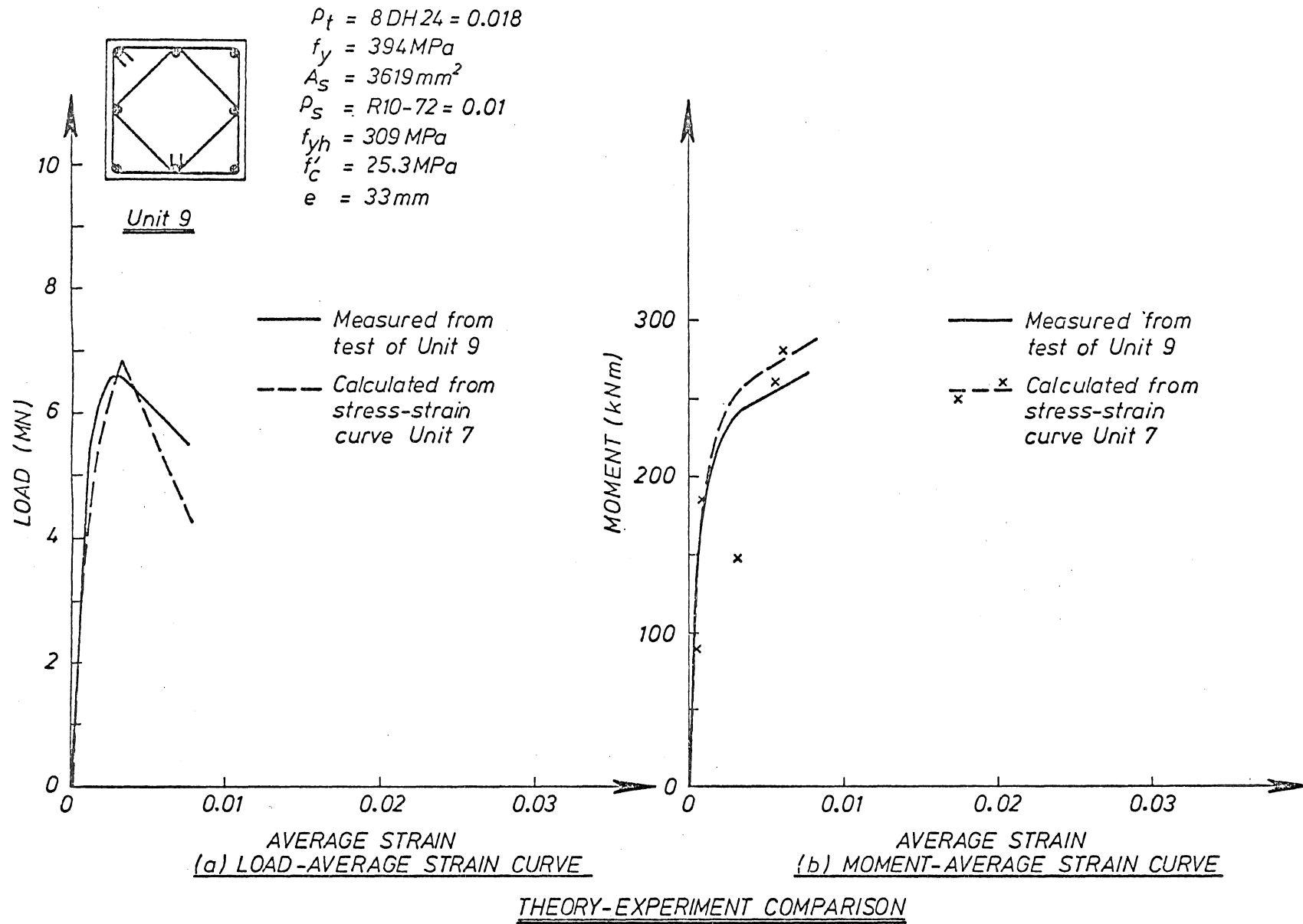


FIGURE 5.18 : UNIT 9 ECCENTRIC LOAD, HIGH SPEED

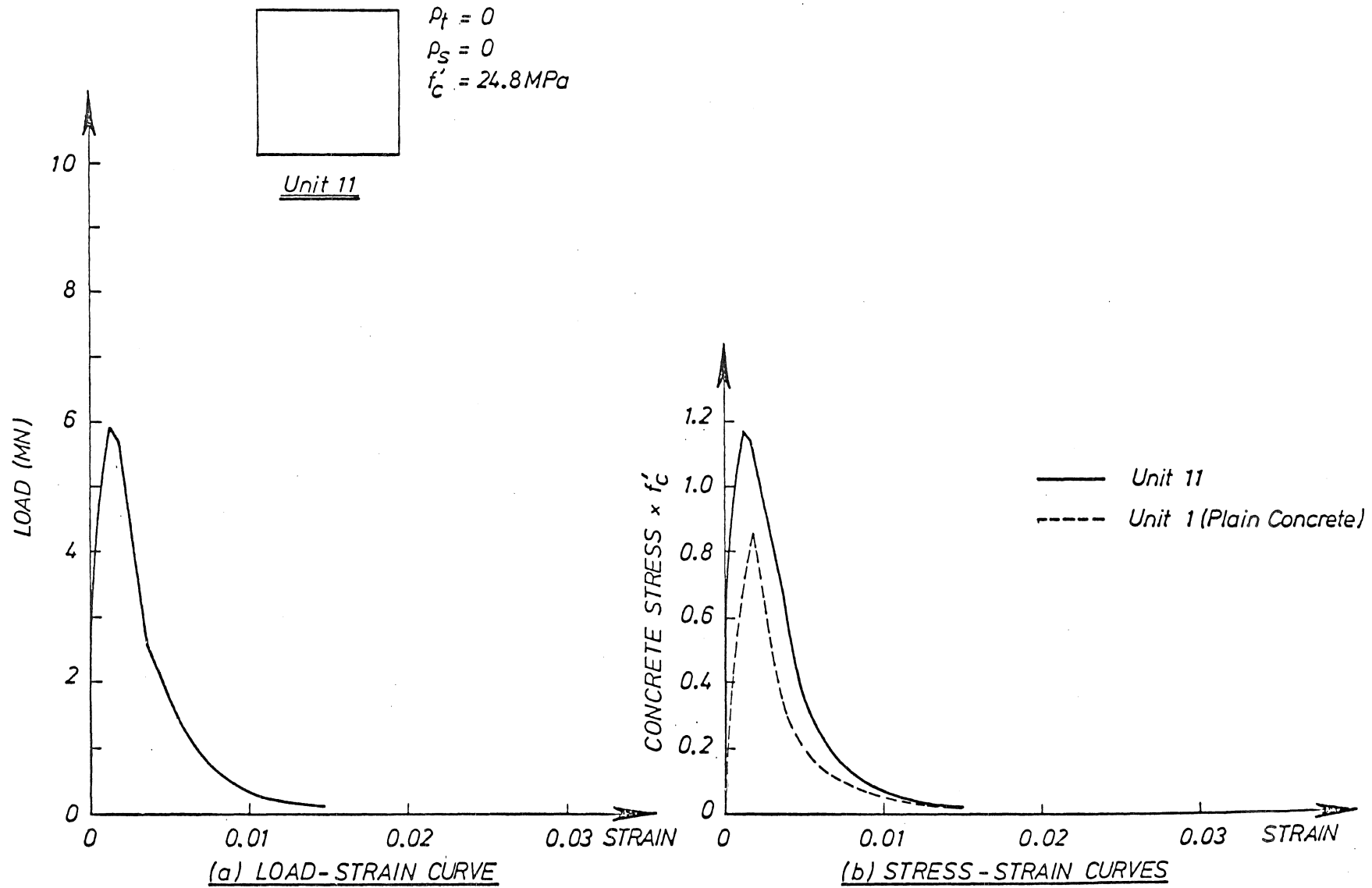


FIGURE 5.19 : UNIT 11 AXIAL LOAD, HIGH SPEED

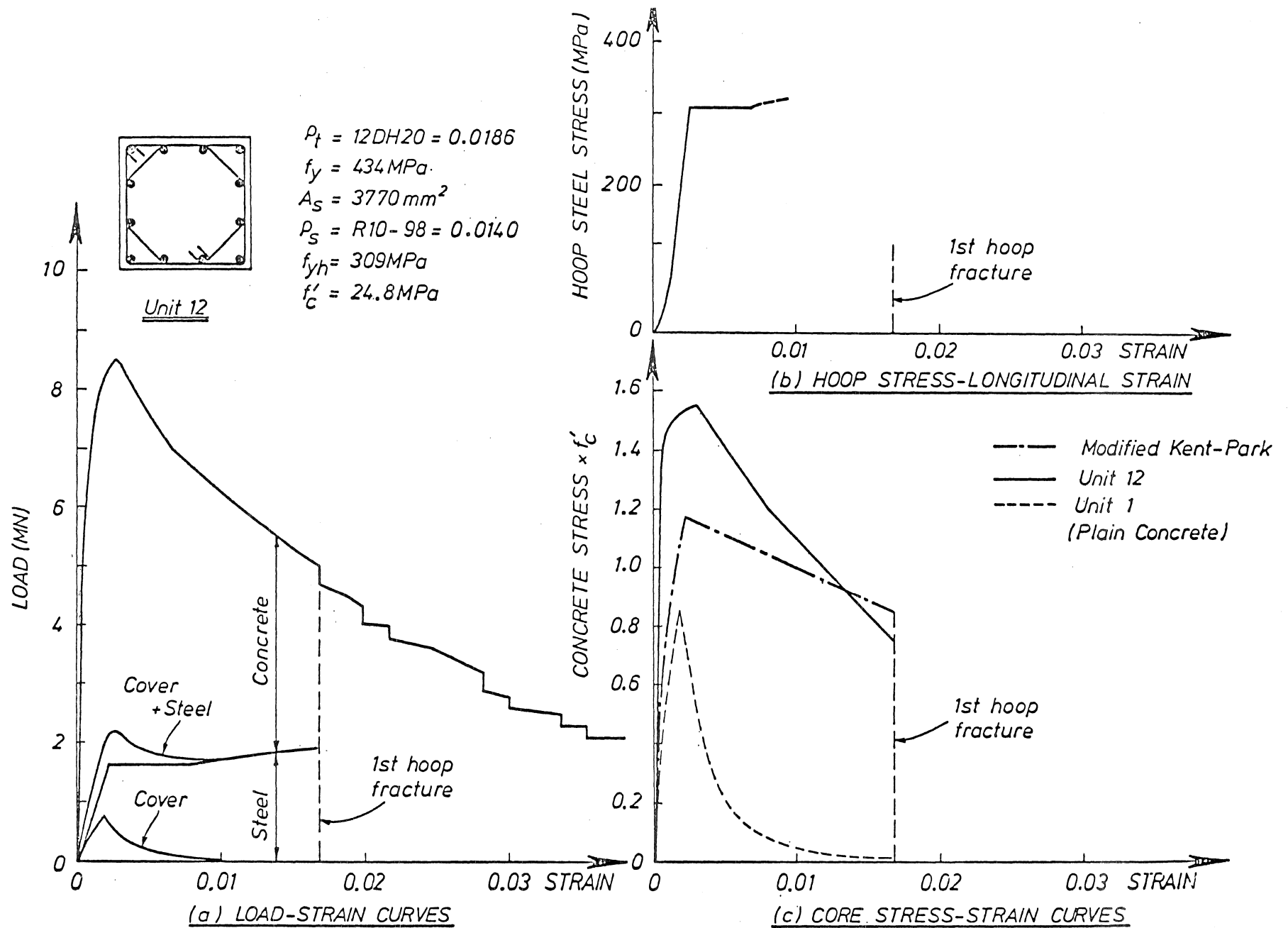


FIGURE 5.20 : UNIT 12 AXIAL LOAD, HIGH SPEED

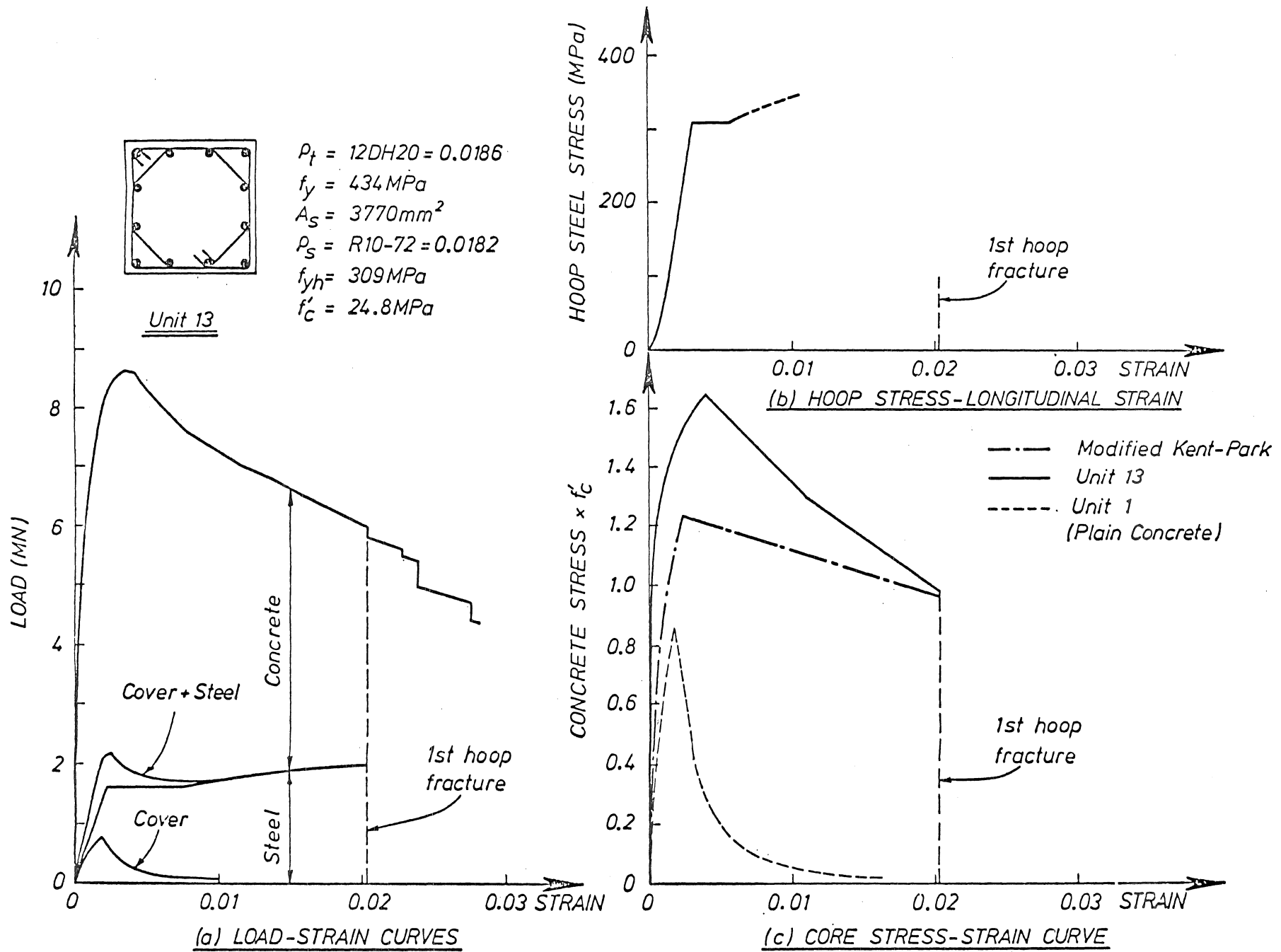


FIGURE 5.21 : UNIT 13 AXIAL LOAD, HIGH SPEED

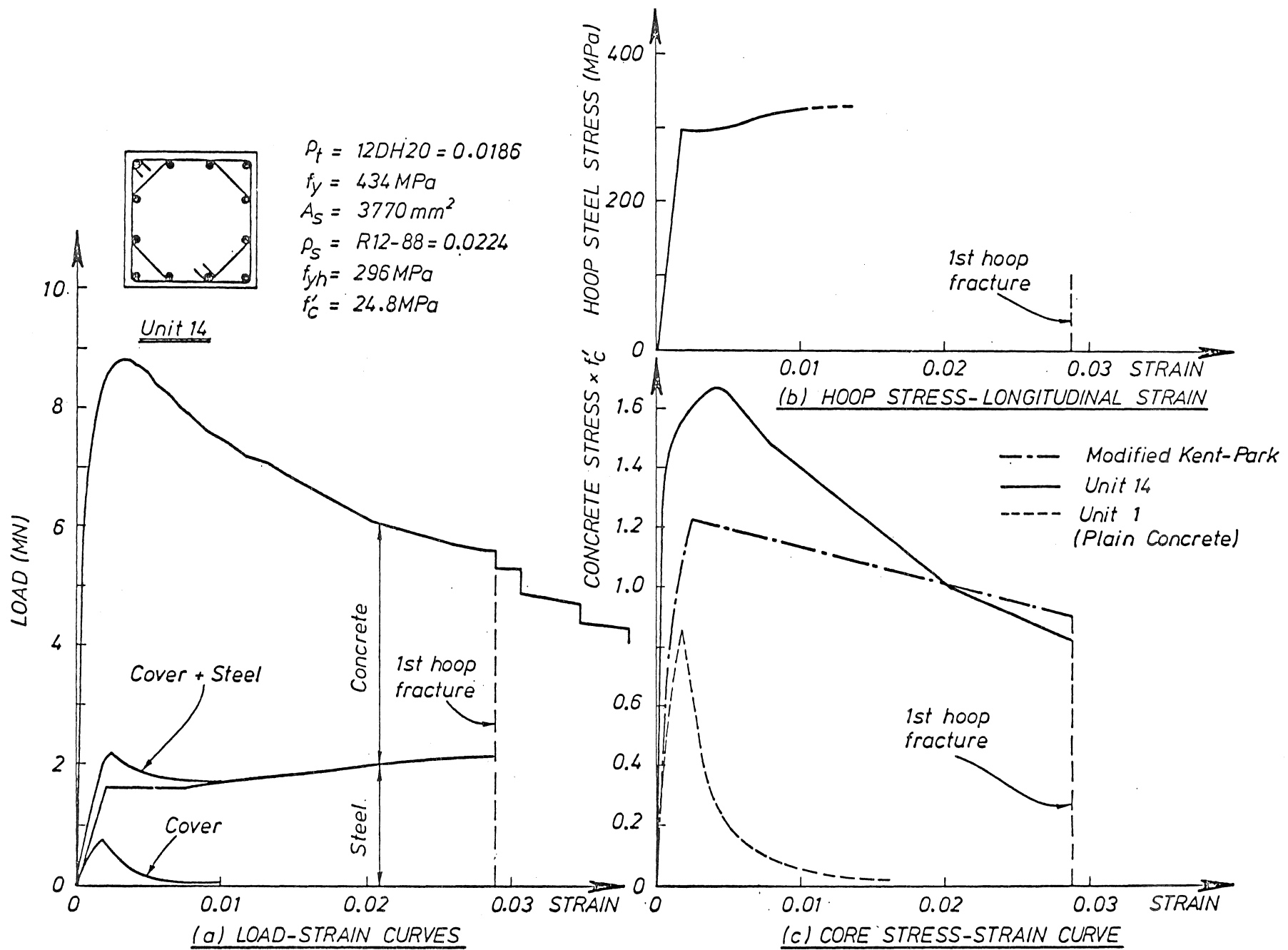


FIGURE 5.22 : UNIT 14 AXIAL LOAD, HIGH SPEED

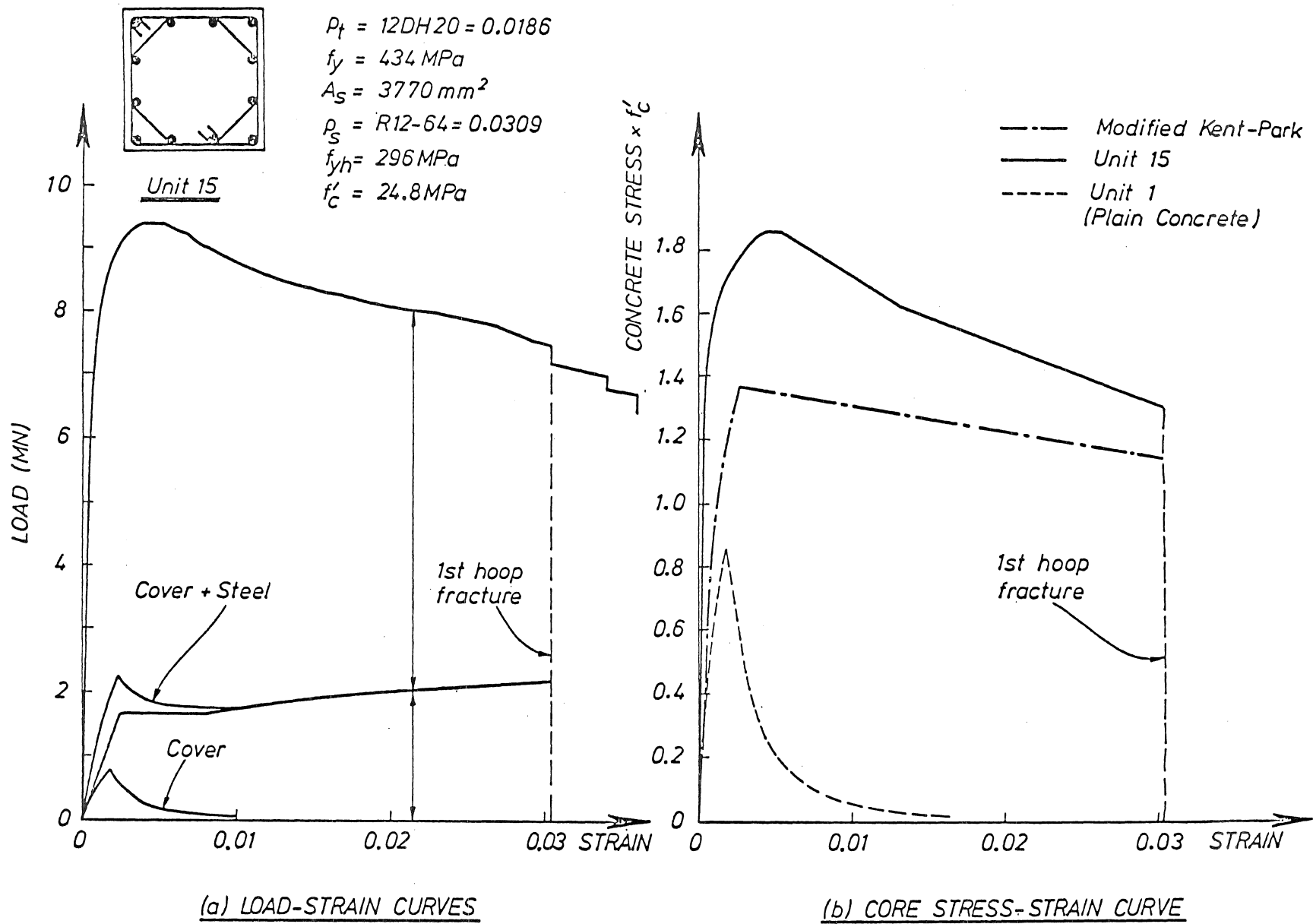


FIGURE 5.23 : UNIT 15 AXIAL LOAD, HIGH SPEED

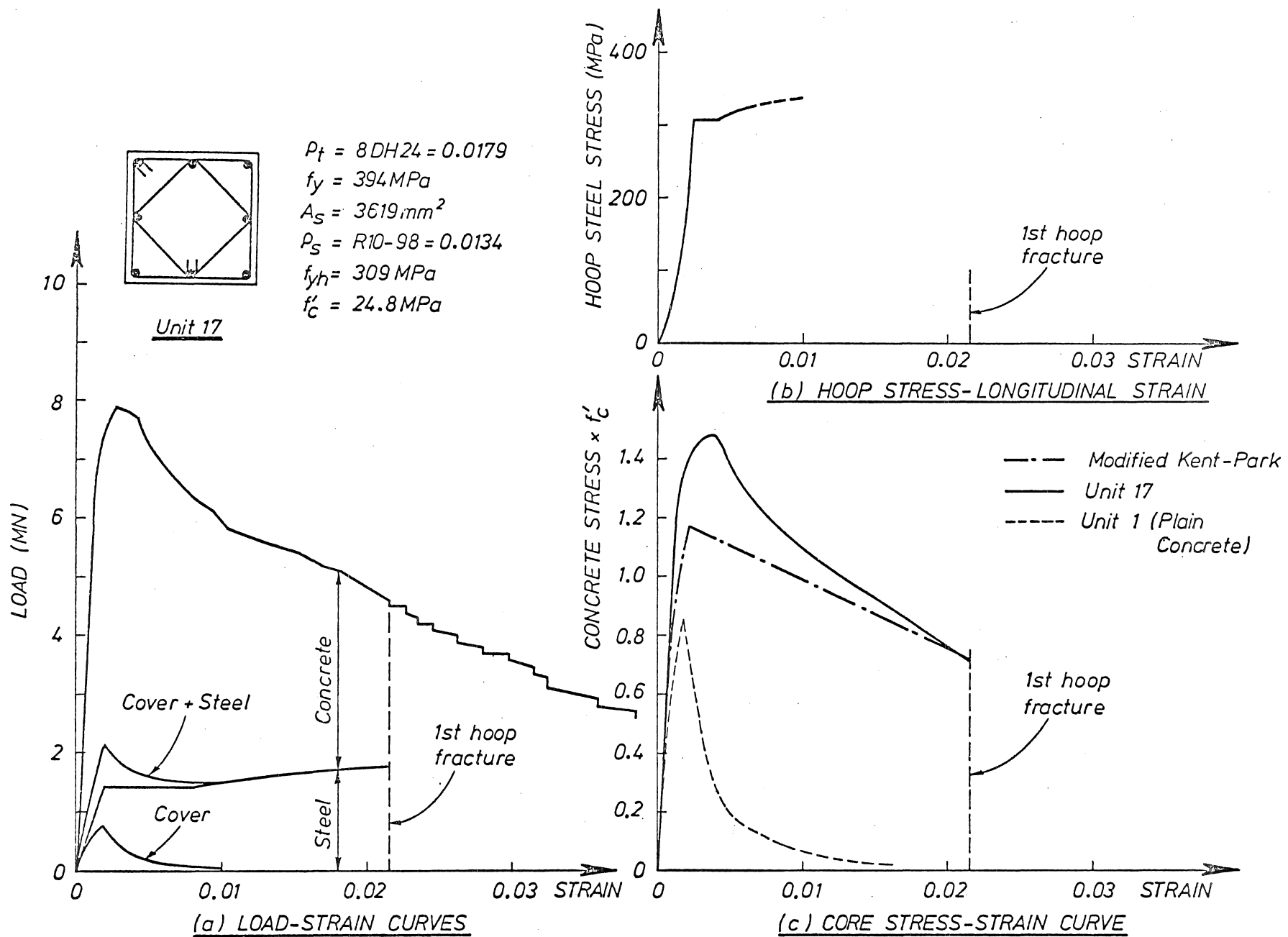


FIGURE 5.24 : UNIT 17 AXIAL LOAD, HIGH SPEED

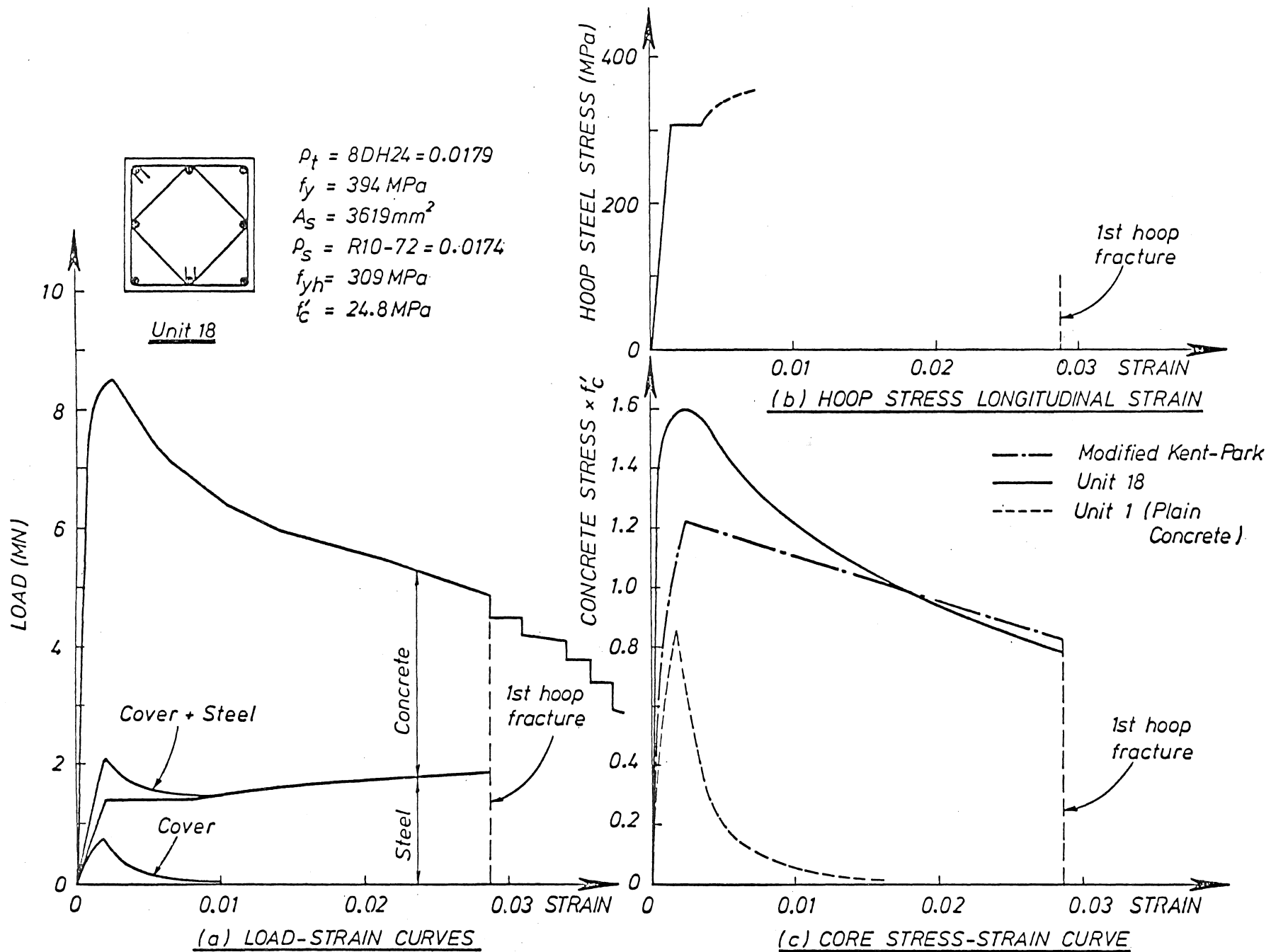


FIGURE 5.25 : UNIT 18 AXIAL LOAD, HIGH SPEED

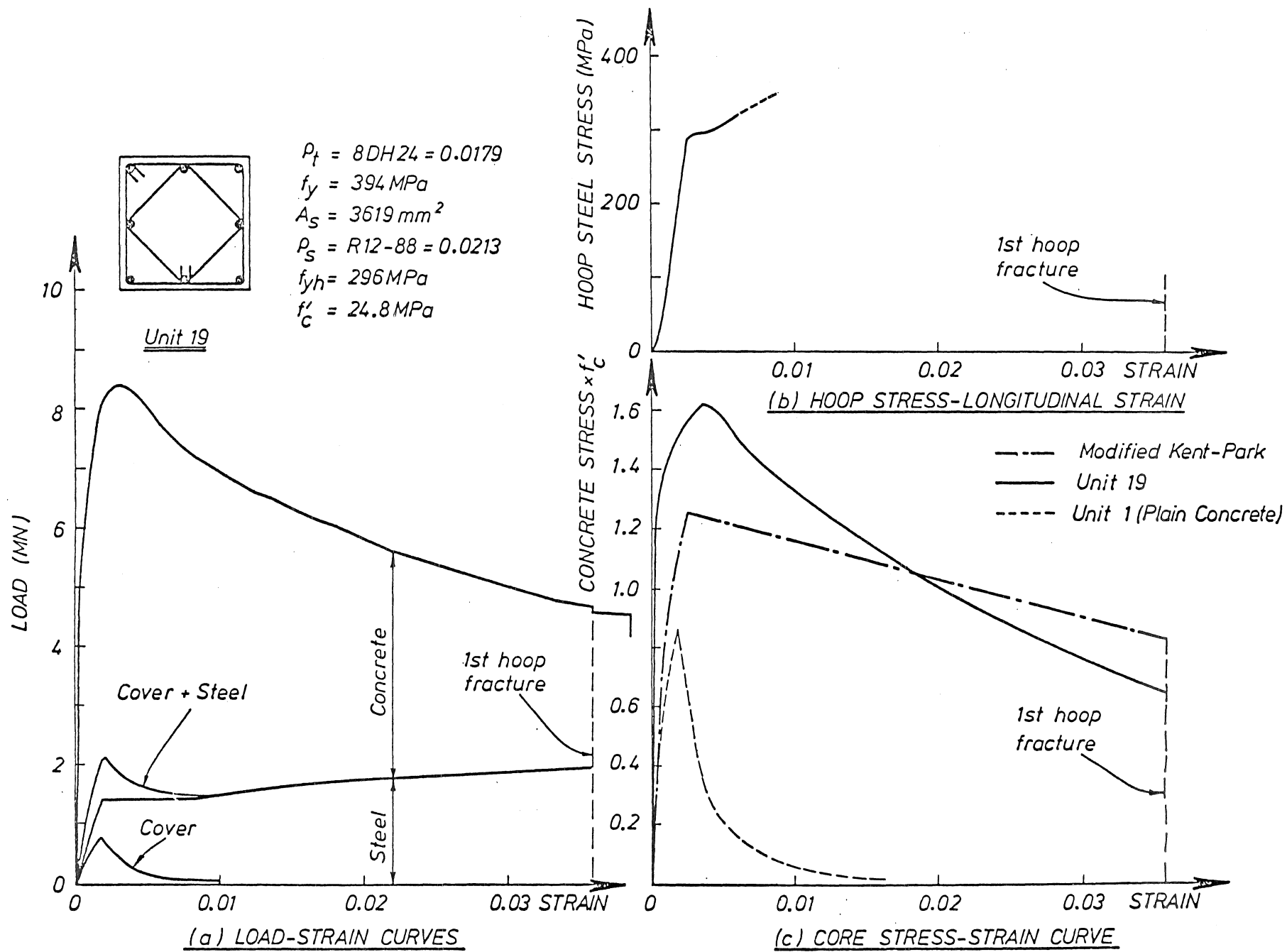


FIGURE 5.26 : UNIT 19 AXIAL LOAD, HIGH SPEED

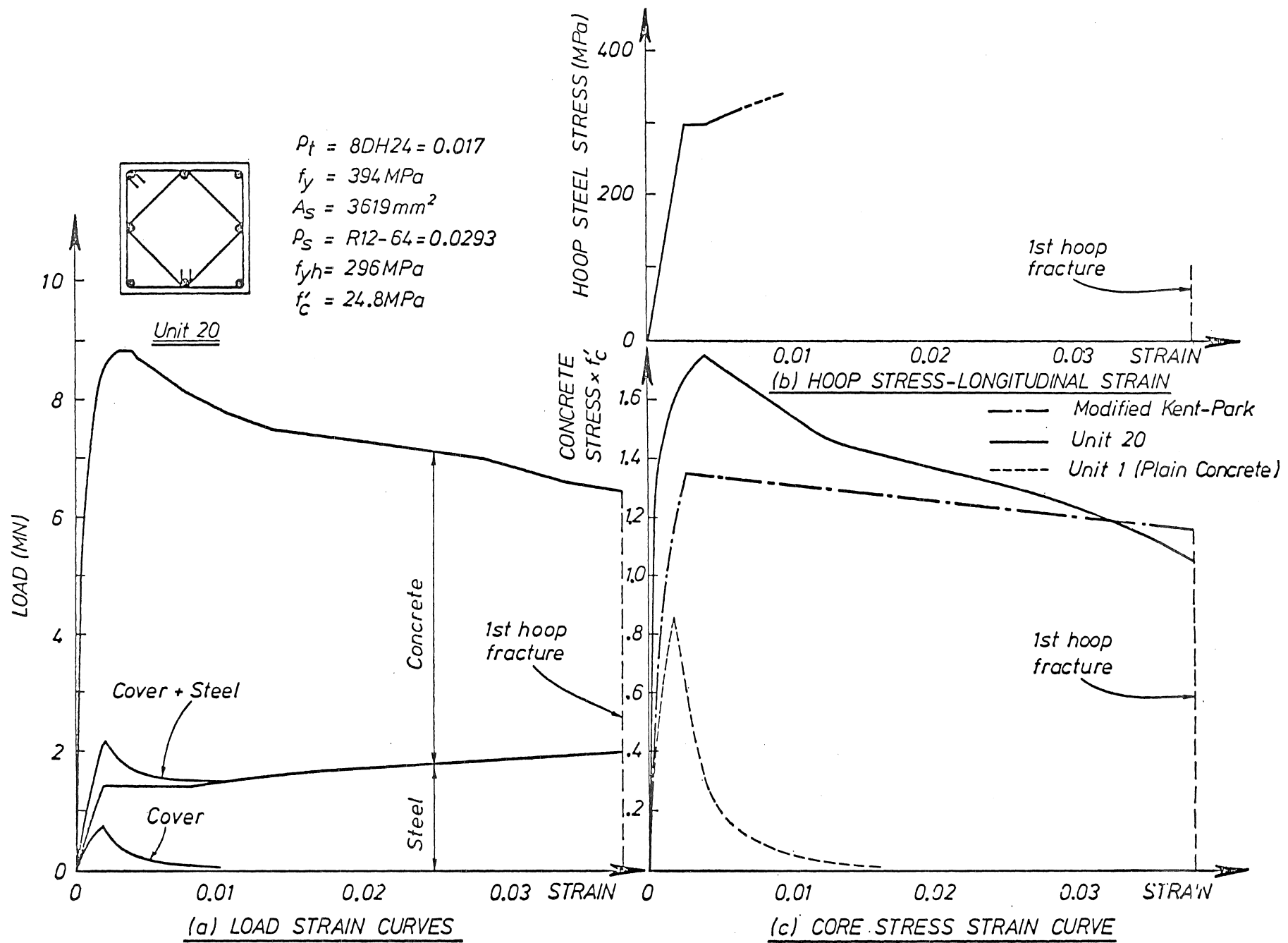


FIGURE 5.27 : UNIT 20 AXIAL LOAD, HIGH SPEED

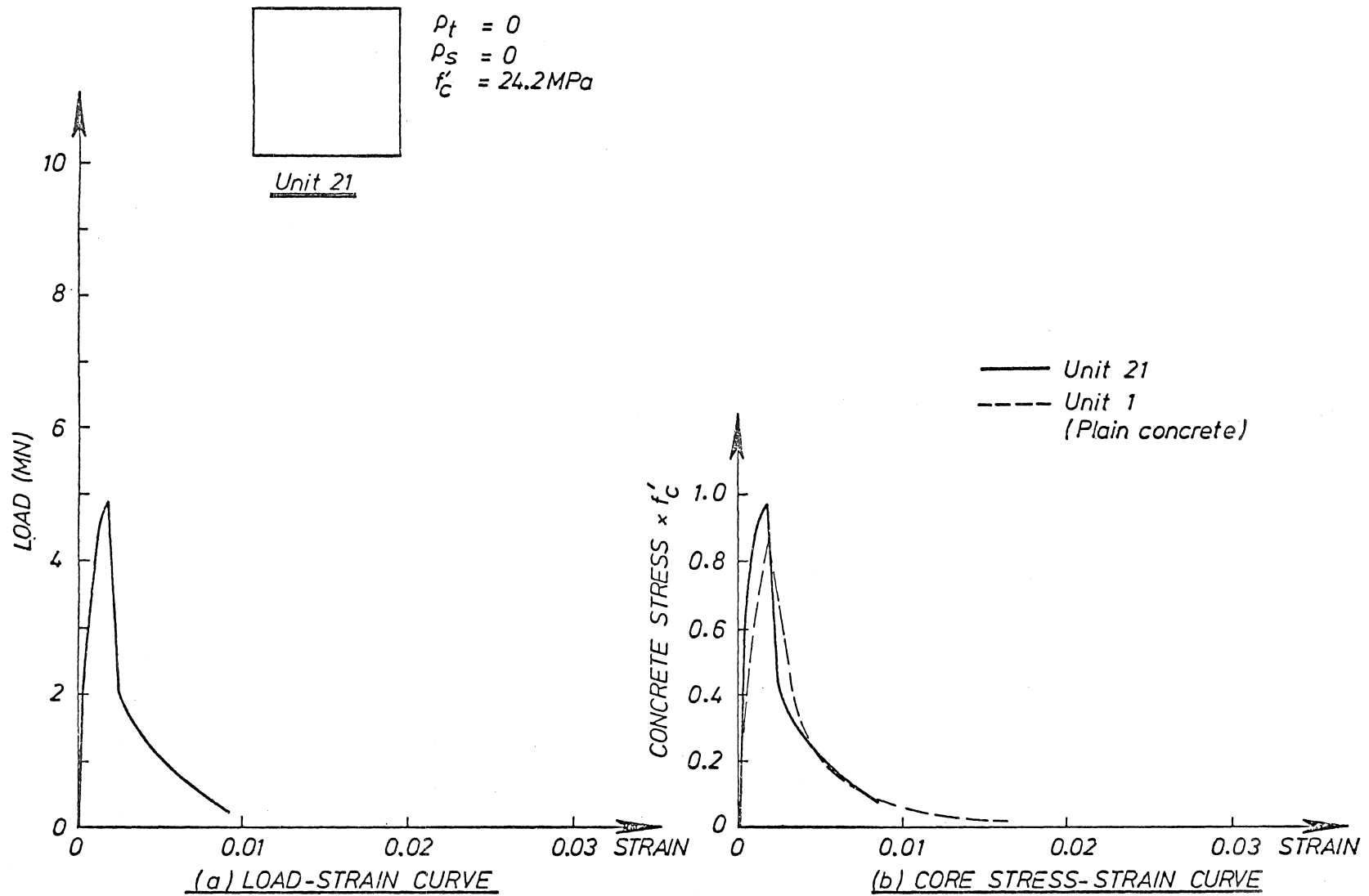


FIGURE 5.28 : UNIT 21 AXIAL LOAD, SLOW SPEED

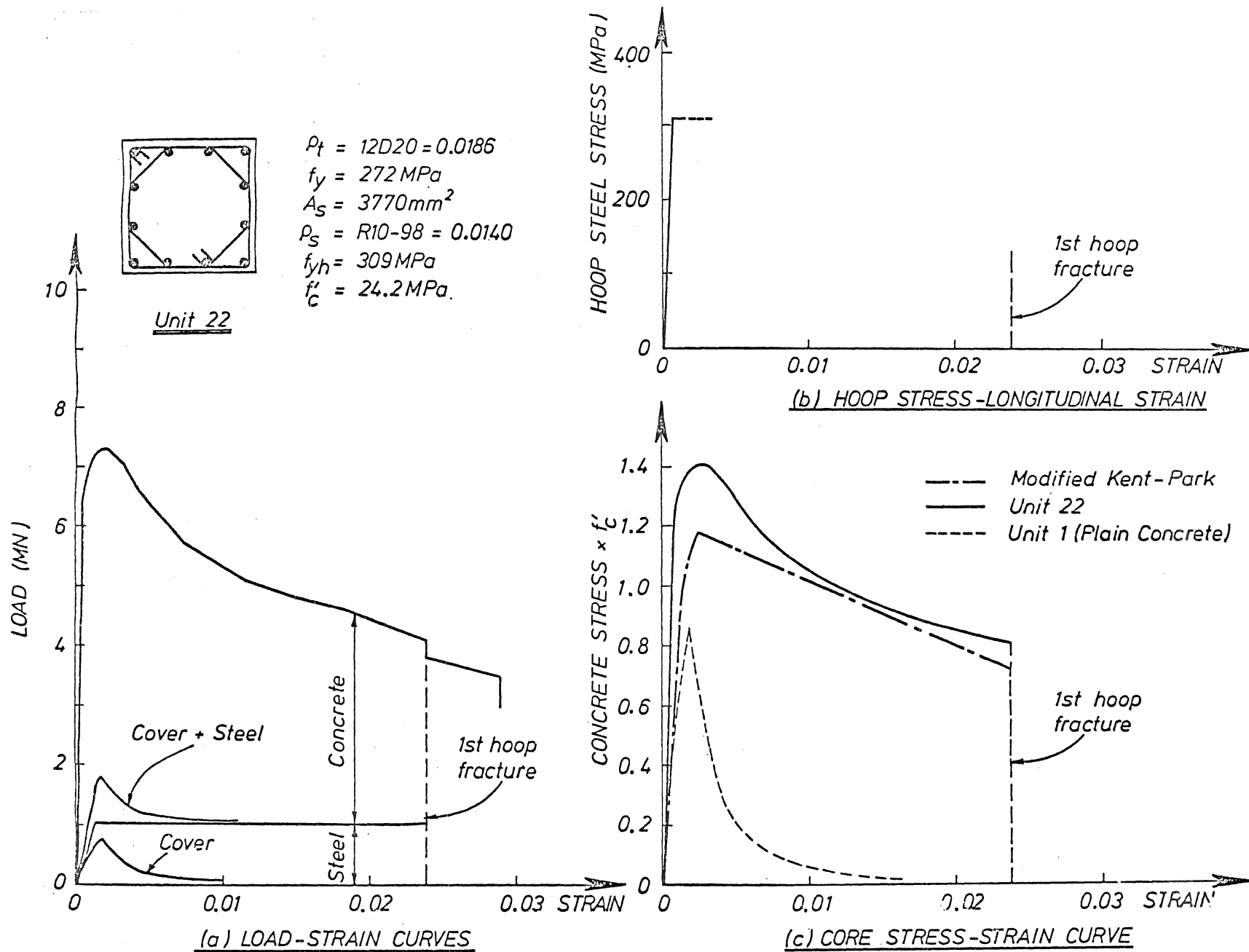


FIGURE 5.29 : UNIT 22 AXIAL LOAD, HIGH SPEED

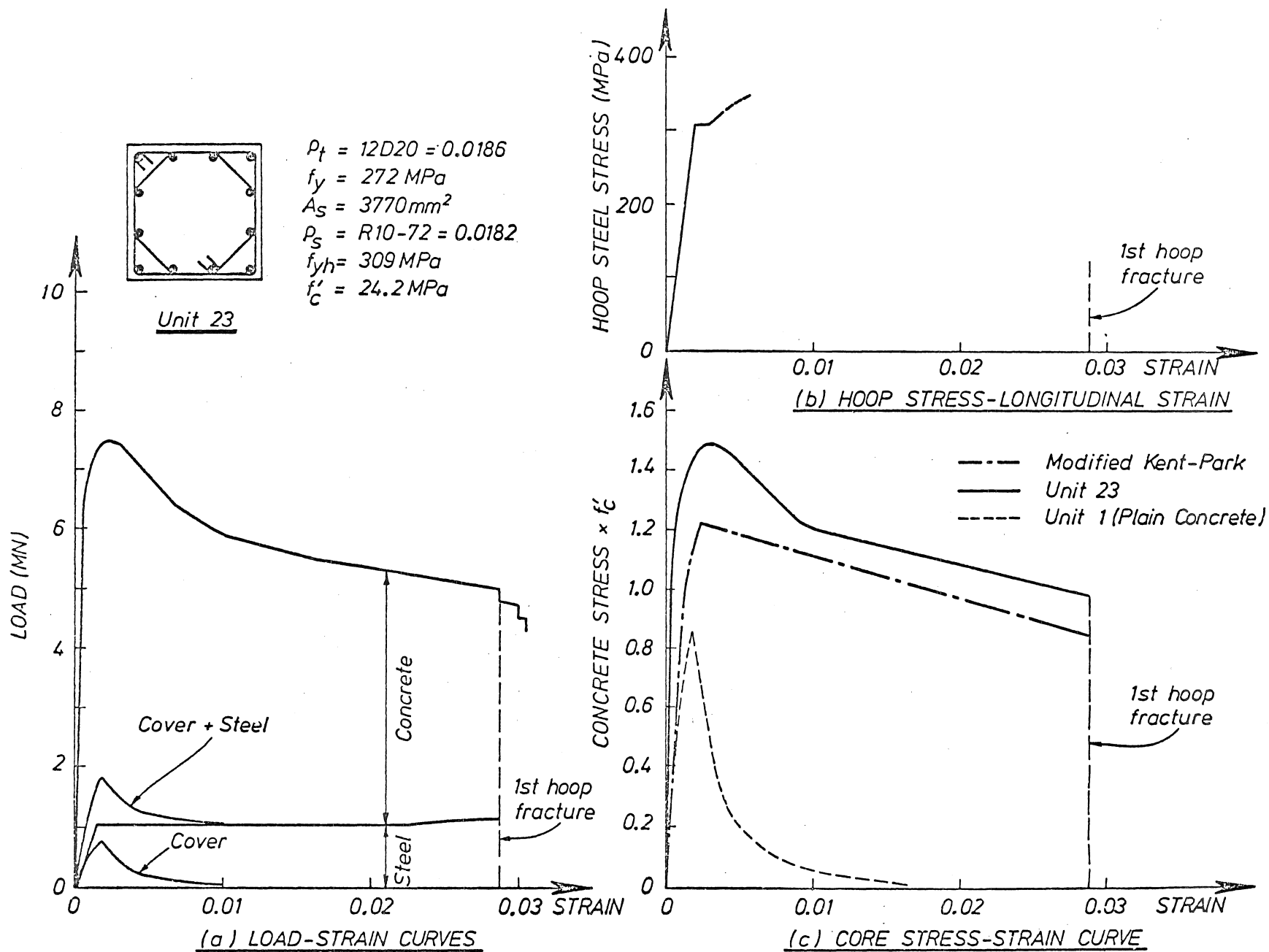


FIGURE 5.30 : UNIT 23 AXIAL LOAD, HIGH SPEED

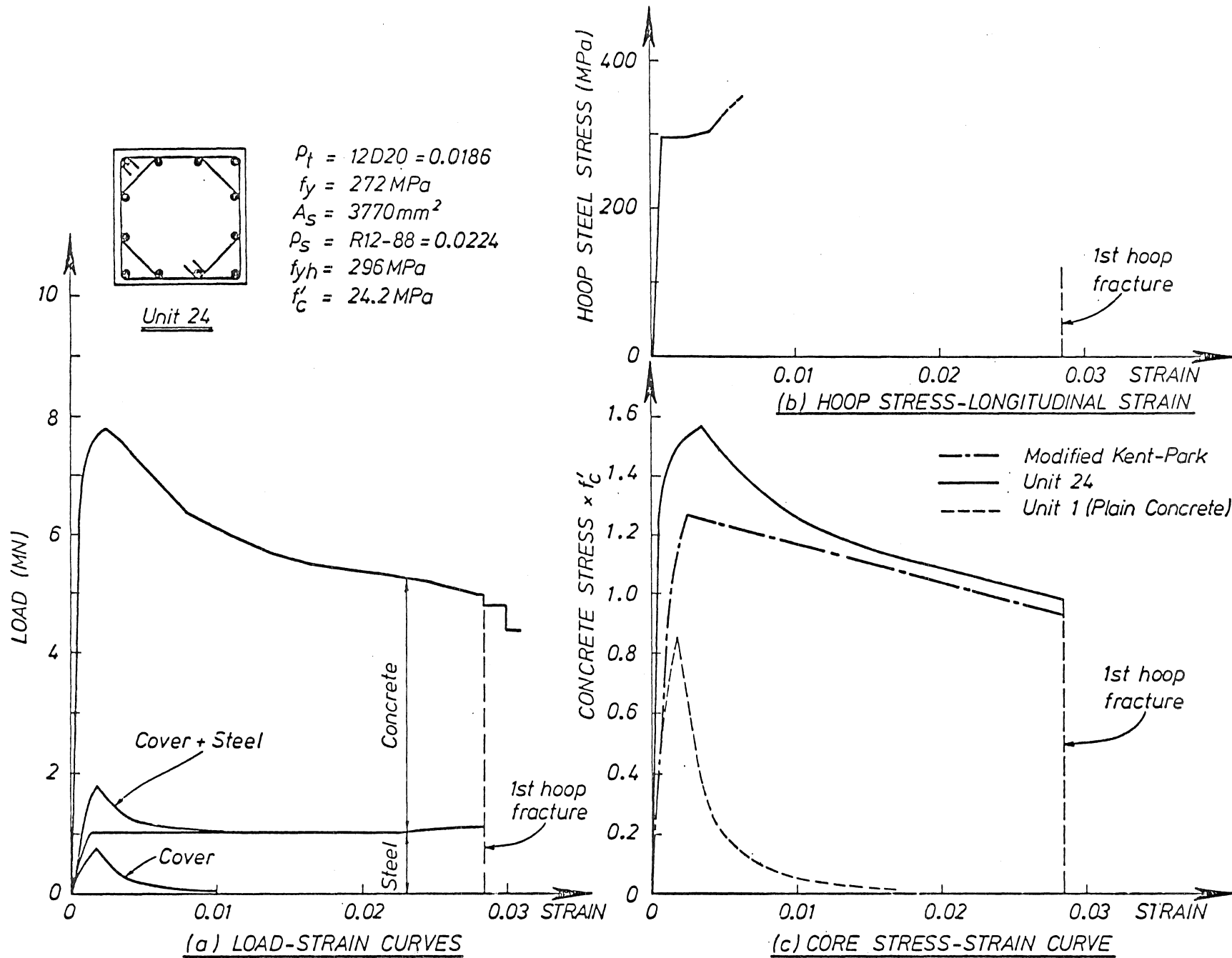


FIGURE 5.31 : UNIT 24 AXIAL LOAD, HIGH SPEED

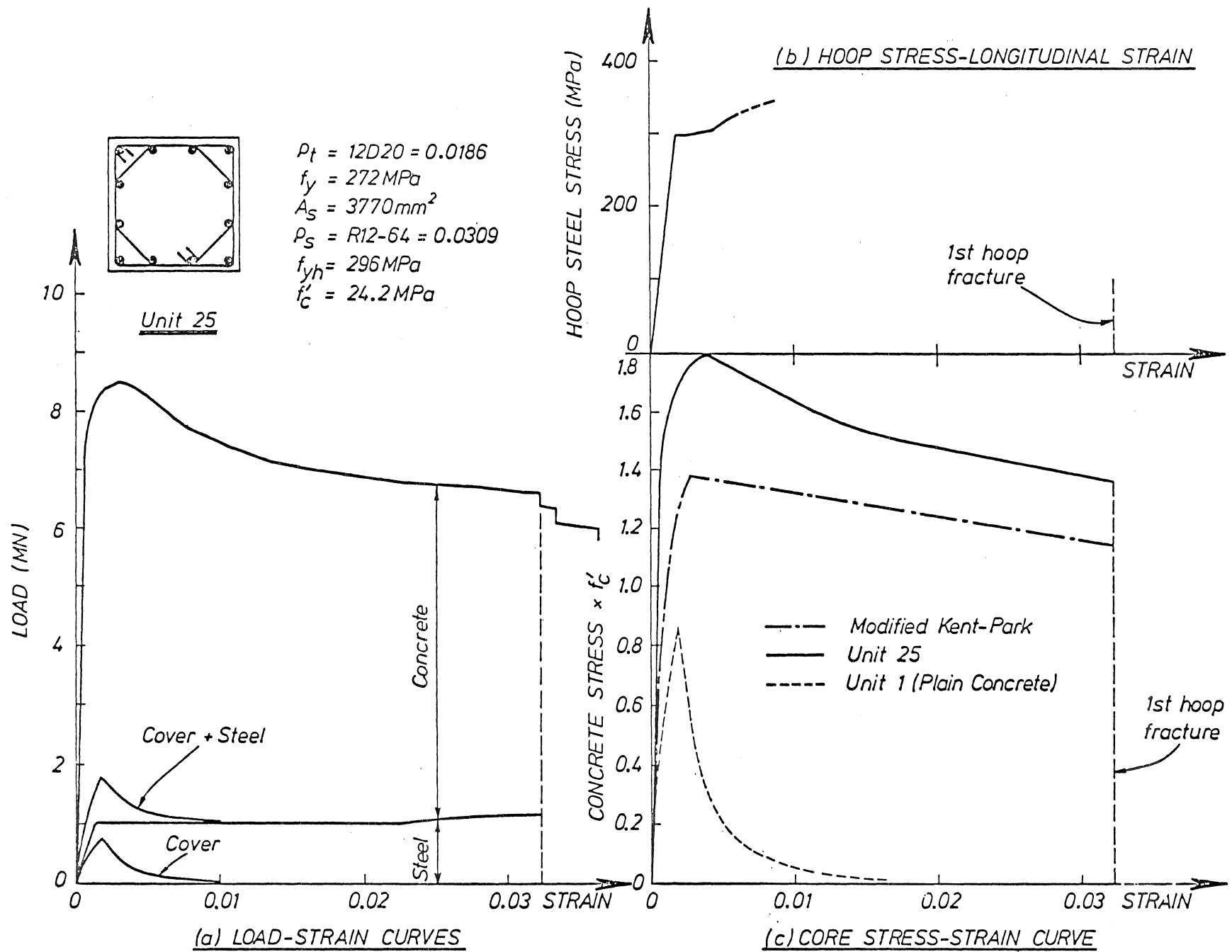


FIGURE 5.32 : UNIT 25 AXIAL LOAD, HIGH SPEED

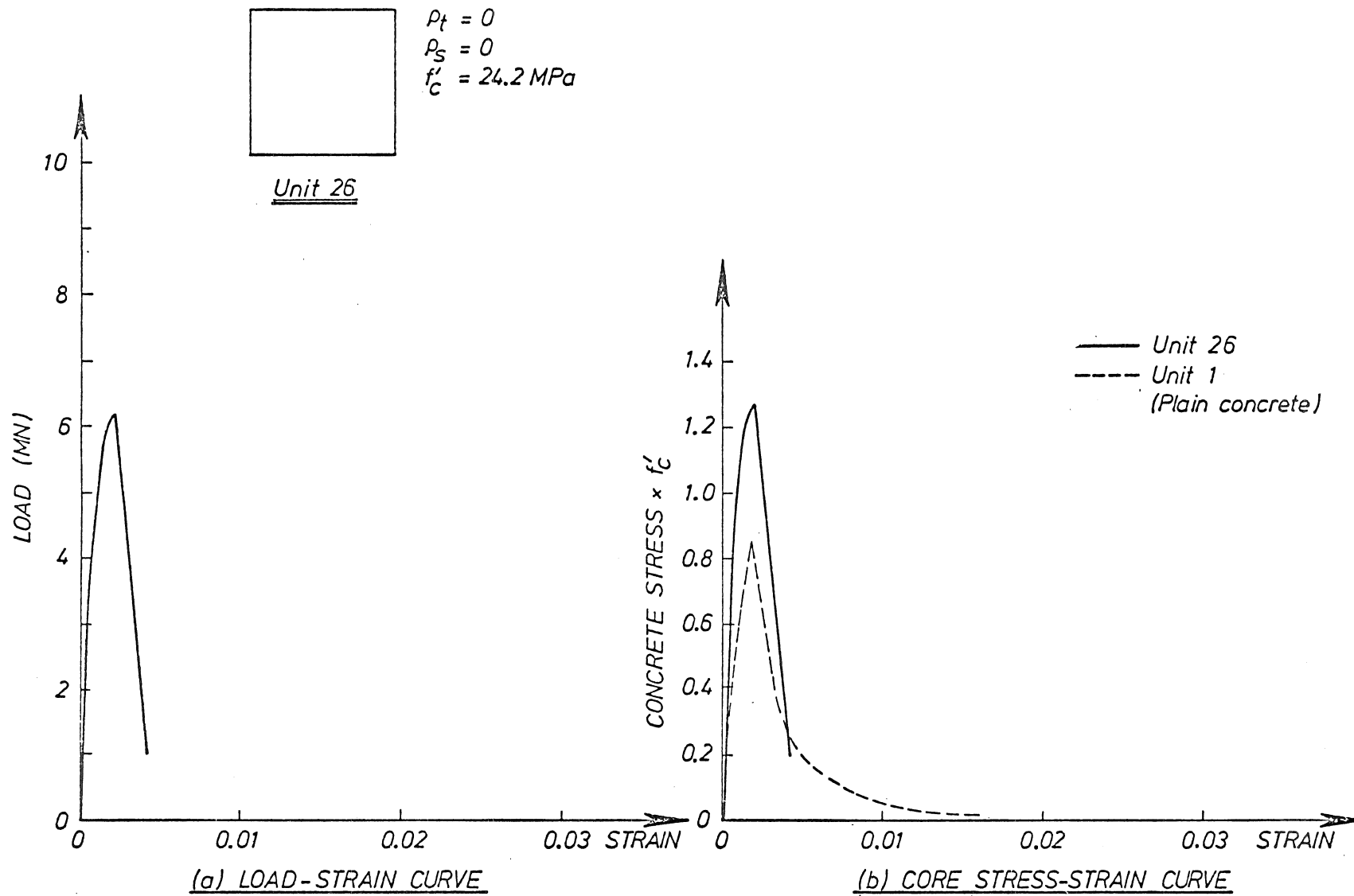


FIGURE 5.33 : UNIT 26 AXIAL LOAD, HIGH SPEED

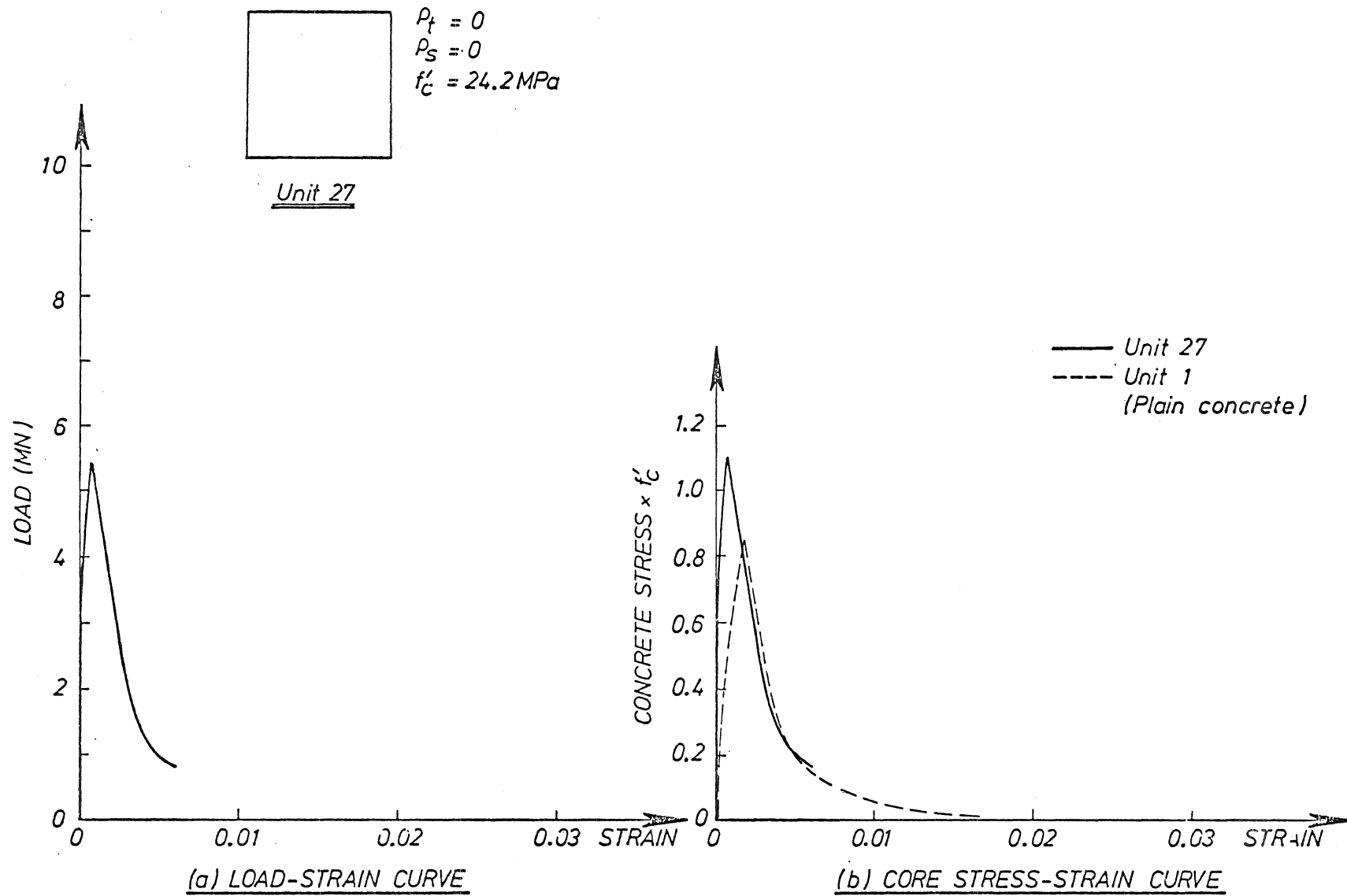


FIGURE 5.34 : UNIT 27 AXIAL LOAD, MEDIUM SPEED

5.3 DISCUSSION OF RESULTS

5.3.1 Rate of Loading

Figures 5.35, 5.36 and 5.37 illustrate the influence of loading rate on the core compressive stress-strain curve for plain concrete (units 21, 26, 27), 8 bar (units 6, 7, 17), and 12 bar (units 2, 3, 13) units respectively. Table 5.2 shows that strength increase due to rate of loading is typically 25% at peak stress but by a strain of $1\frac{1}{2} \sim 2\%$ this may have fallen to (say) 10%. The falling branch in this region (peak stress to (say) 2% strain) is much steeper than the slow test and at larger strains tends towards the curve of the corresponding slow test.

The slow rate ($0.000003 = .004 \text{ mm/s}$) was representative of that rate at which cylinders were loaded in a load controlled, standard cylinder test; and of previous research tests which took (say) 30 minutes to complete. The fast rate ($0.0167/\text{s} = 20 \text{ mm/s}$), as indicated, was representative of the loading rate expected during a seismic attack and the medium rate ($0.00167/\text{s} = 2 \text{ mm/s}$) to indicate the sensitivity of strength increase to changes of loading rate.

Note in this series of tests the fast loading rate was only indicative of that expected during an earthquake and may be exceeded in reality. However, the influence of small changes in loading rate (i.e. factors of 2 or 3) are likely to be small in comparison with the variation from slow to fast within these tests (i.e. a factor of 5000) as shown in the figures mentioned above.

TABLE 5.2 : The Effect of Loading Rate on Peak Stress

UNIT	RATE $\frac{\epsilon/s}{\frac{mm/s}{1200}}$	RELATIVE	f_{cc}/f'_c	RATIO	ARITHMETIC AVERAGE FOR FAST TESTS
PLAIN UNITS					
1	.0000033	0.0002	.86	.89	1.260
11	.0167	1.00	1.17	1.21	
21	.0000033	0.0002	.97	1.00(base)	
26	.0167	1.00	1.27	1.31	
27	.00167	0.10	1.10	1.13	
8 BAR UNITS					
6	.0000033	0.0002	1.22	1.00(base)	1.250
7	.0167	1.00	1.47	1.20	
18	.0167	1.00	1.60	1.30	
12 BAR UNITS					
2	.0000033	0.0002	1.24	1.00(base)	1.245
3	.0167	1.00	1.54	1.24	
13	.0167	1.00	1.55	1.25	
Overall (Fast) Average 1.252					

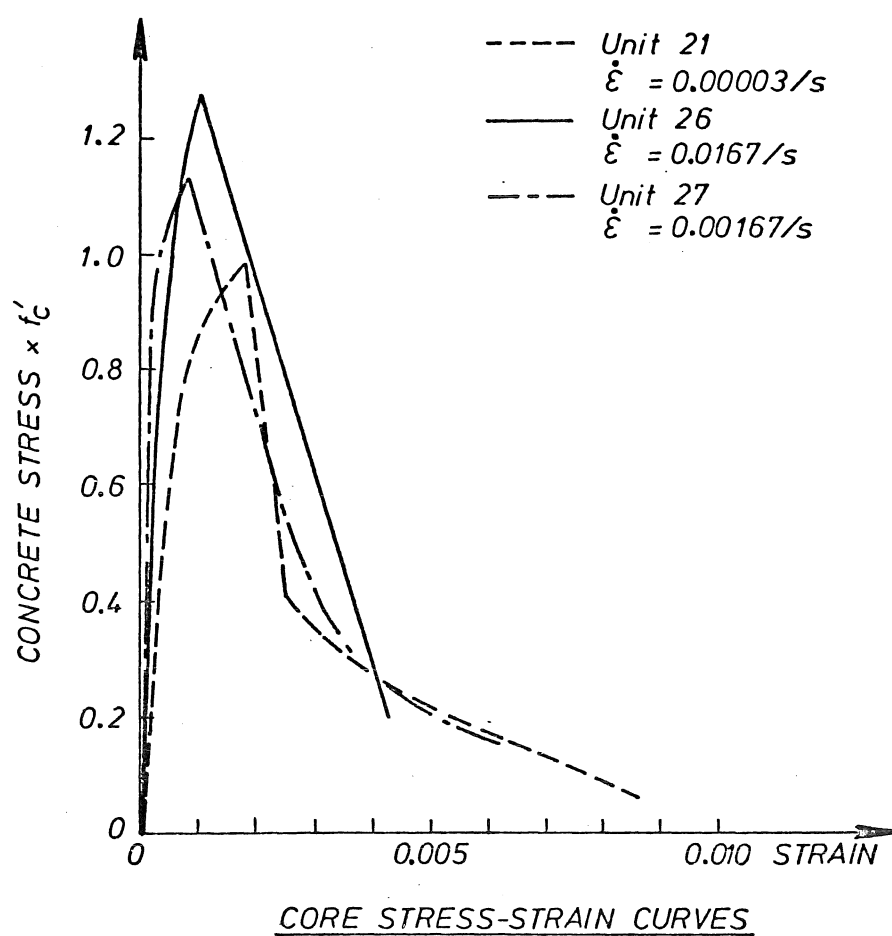


FIGURE 5.35 : Plain Concrete Units Loaded at Different Rates

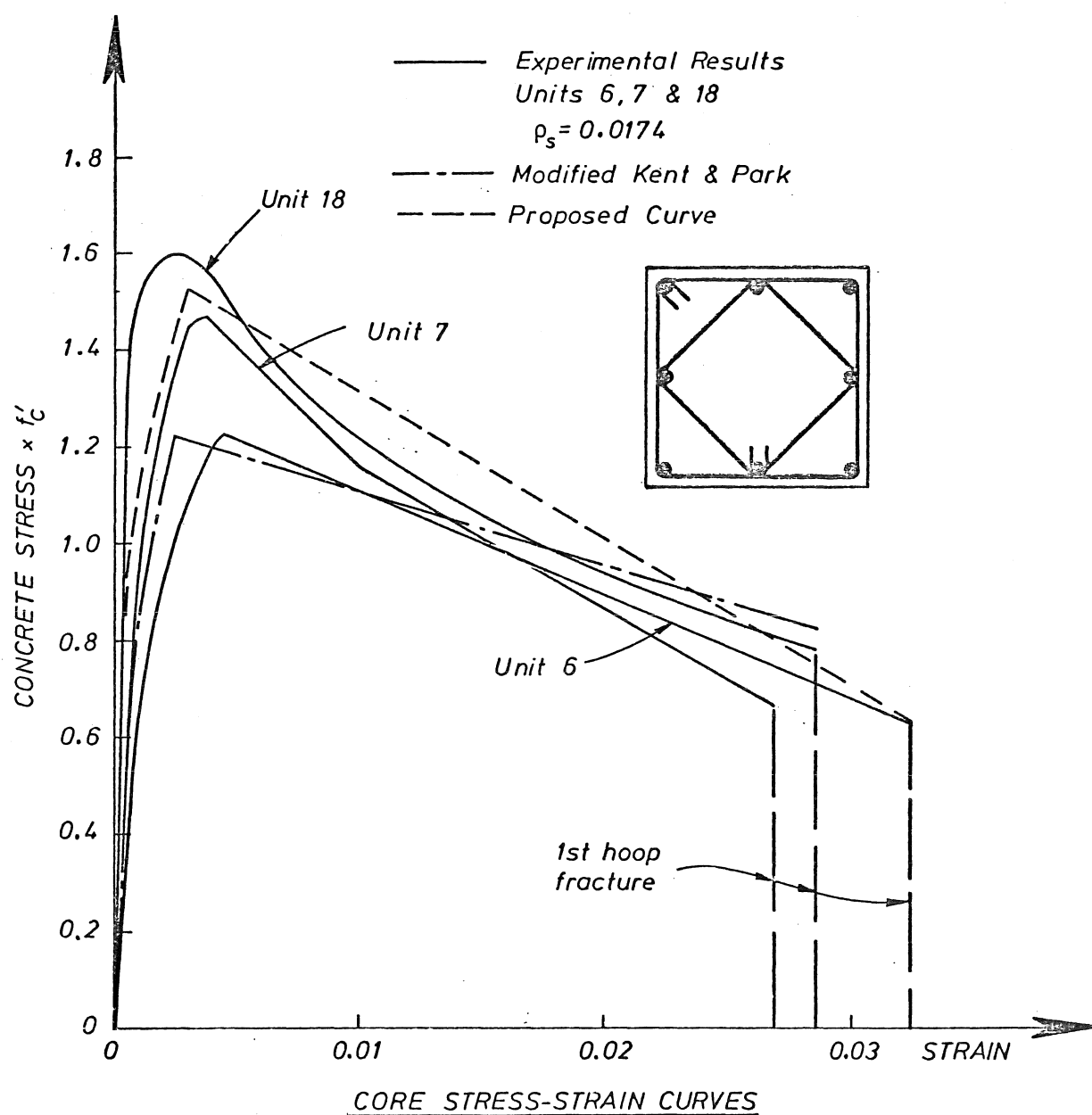


FIGURE 5.36 : 8 Bar Units Loaded at Different Rates

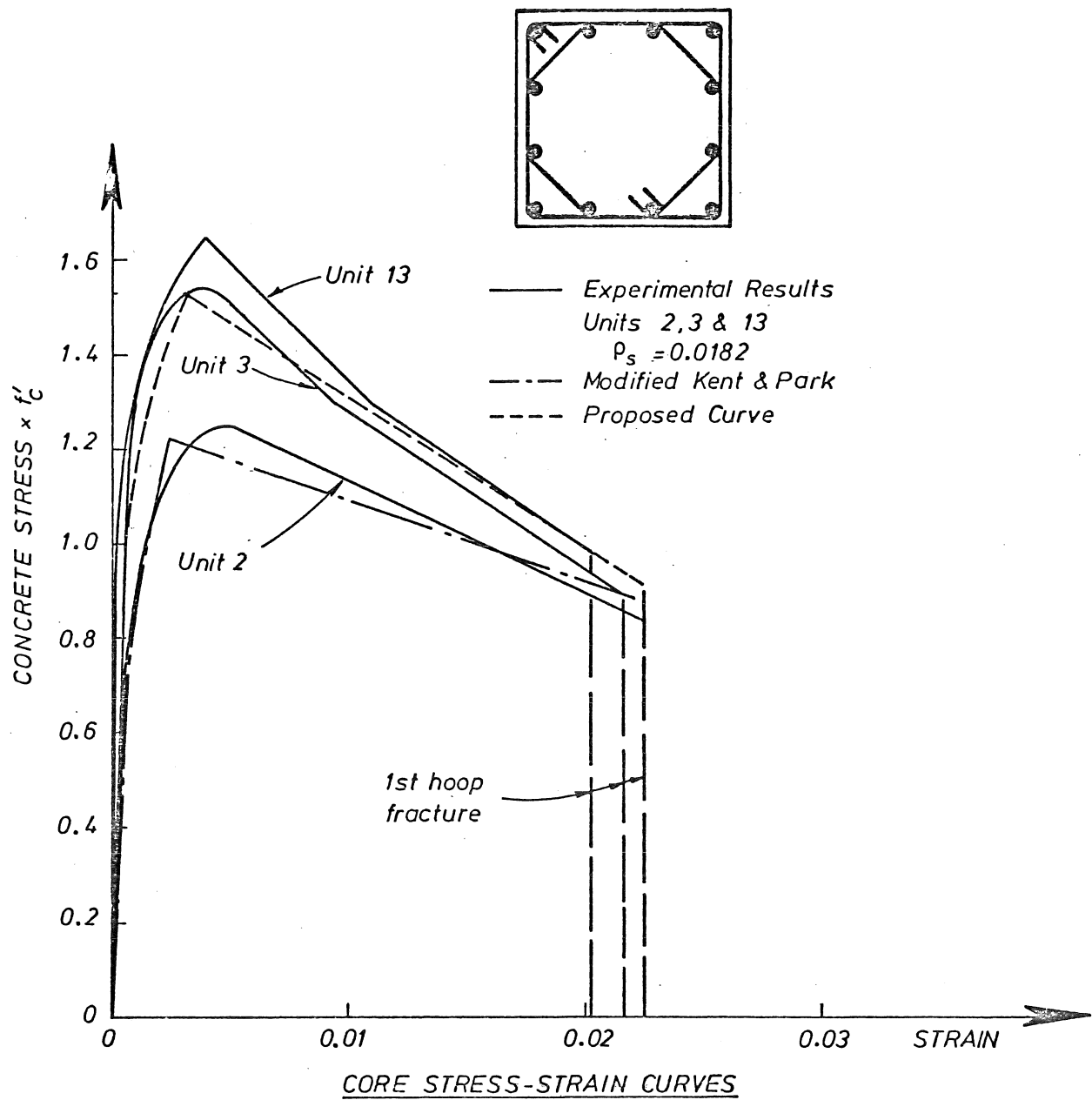


FIGURE 5.37 ; 12 Bar Units Loaded at Different Rates

A proposed alteration to the Modified Kent and Park curve for confined concrete is shown in Figures 5.36 and 5.37 to account for the influence of dynamic loading rates. This is achieved by applying a factor of 1.25 to the peak stress, the strain at peak stress and the slope of the falling branch of the modified Kent and Park curve. The stress-strain curve for dynamic axial loading then becomes : (refer figure 1.8)

Region AB : $\epsilon_c \leq 0.002K$

$$f_c = K f'_c \left[\frac{2\epsilon_c}{0.002K} + \left(\frac{\epsilon_c}{0.002K} \right)^2 \right] \quad \dots \quad 5.1$$

$$\text{where } K = 1.25 \left(1 + \rho_s \frac{f_{yh}}{f'_c} \right) \quad \dots \quad 5.2$$

Region BC

$$f_c = K f'_c \left[1 - Z_m (\epsilon_c - 0.002K) \right] \quad \dots \quad 5.3$$

but not less than $0.2Kf'_c$, where

$$Z_m = \frac{0.625}{\frac{3 + 0.29f'_c}{145f'_c - 1000} + \frac{3}{4} \rho_s \sqrt{\frac{h''}{s_h}} - 0.002K} \quad \dots \quad 5.4$$

The proposed curve is also shown in Figures 5.38 and 5.39 with the different levels of confinement for the 8 and 12 bar units respectively.

5.3.2 Confinement Ratio

The effects of confinement ratio on the behaviour of the units tested at the fast loading rate is shown in Figures 5.38 and 5.39 for 8 and 12 bar units respectively. The proposed curves based on Equations 5.1 to 5.4 are included for comparison.

Note from these figures the large increases in strength obtained from the rapid loading rates (as discussed above) and confinement of the core concrete.

For a quite modest confinement ratio (ρ_s about 0.018) an average increase in core strength of 23% was obtained for the slow tests while a strength

increase of about 55% was obtained for corresponding units under rapid loading. For high confinement ratios (ρ_s about 0.030) strength increases of about 80% were obtained.

The confinement ratios are 0.0134, 0.0174, 0.0213 and 0.0293 for the 8 bar units, and 0.0140, 0.0182, 0.0224, and 0.0309 for the 12 bar units for hoop set spacings of 98, 72, 88 and 64 mm respectively. It will be noted from the similarity between the two centremost curves in each figure that the strength increase from confinement has been largely offset by a reduction resulting from increased spacing of the larger diameter hoop steel used for the units with the higher confinement ratio.

It will be seen that the proposed curve represents the dynamic tests as accurately as the Modified Kent and Park curve represents the static tests. Time in this study does not permit a full regression analysis of the variables but the proposed curve is considered to give a good representation of behaviour at this stage. The proposed curve, like the modified Kent and Park curve, peaks at a lower strain than generally obtained during testing, which, as previously mentioned, was noted by its authors, and is also accepted here on the basis that the influence on moment-curvature calculations is insignificant.

The effectiveness of the transverse reinforcement is seen in both the increase in strength and by the maintenance of a large proportion of the load at high longitudinal strains. Figure 5.40 plots the peak stress against confinement ratio. It will be seen that a factor of 1.25 applied to the Modified Kent and Park equation appears to be a good conservative estimate of the influence of loading rate. Shown also is the strength increase K_s predicted by Sheikh and Uzumeri (Equation 1.18). This was calculated for a 12 bar unit with a hoop spacing of 72 mm and hoop steel stress of 309 MPa, at various confinement ratios. It will be seen in Figure 5.40 that K_s gives a good estimate of strength increase for rapidly loaded units at medium levels of confinement but appears to err at high and low levels of confinement. However, no allowance has been made for dynamic loading rates, and would therefore overestimate the strength increase obtained from slow loading rates.

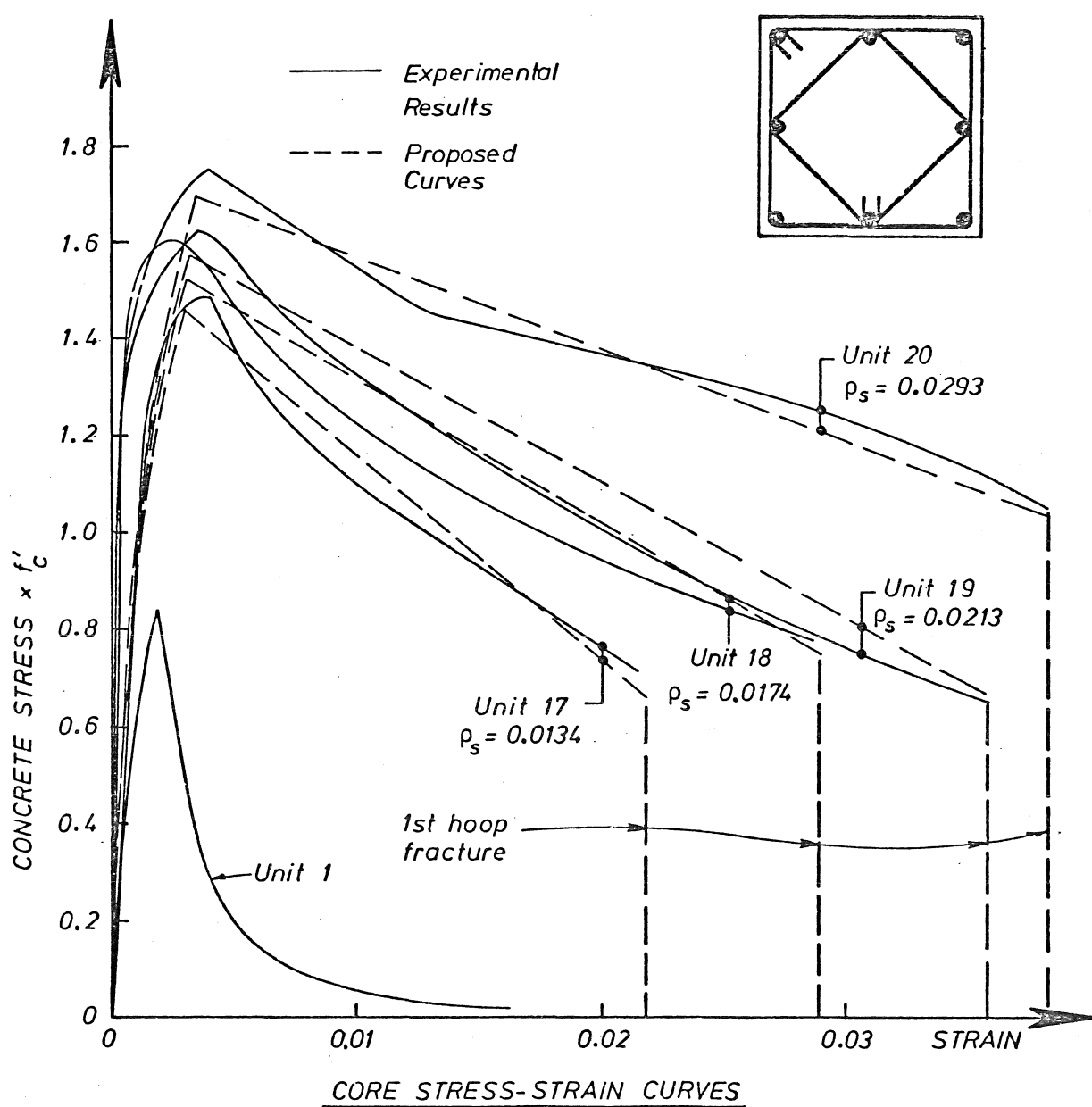


FIGURE 5.38 : Effect of Confinement Ratio for an 8 Bar Unit

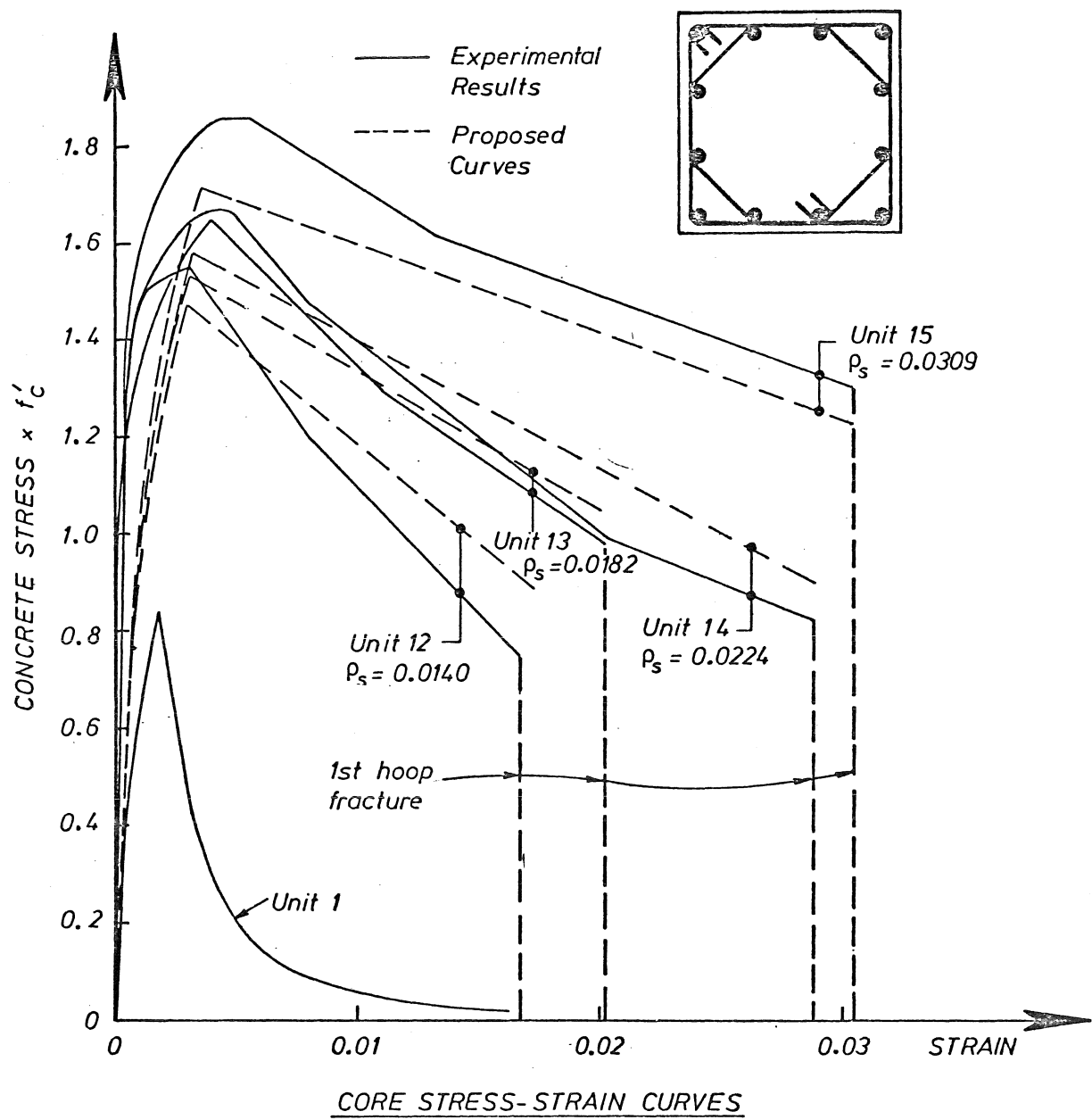
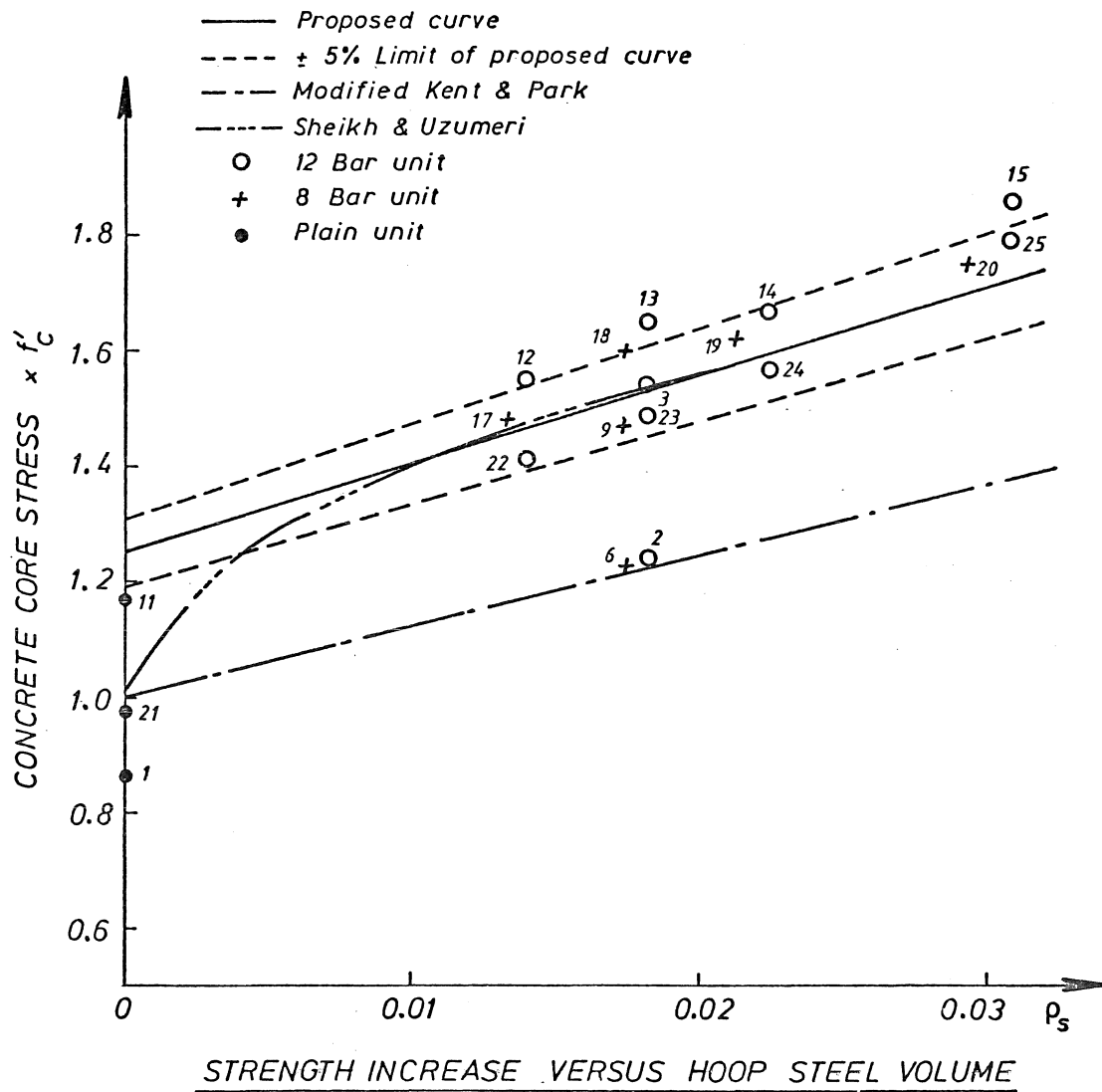


FIGURE 5.39 : Effect of Confinement Ratio for a 12 Bar Unit



Note that Units 1, 2, 6 and 21 were tested at slow speed while the remainder of experimental results refer to high speed tests.

FIGURE 5.40 : Strength Increase Versus Confinement Ratio

5.3.3 Distribution of Longitudinal Steel

Figure 5.41 shows comparative curves for 8 and 12 bar units with similar amounts of longitudinal and confining steel. In each case the curve for a 12 bar unit lies above the curve for the comparable 8 bar unit, indicating that better confinement is obtained from wider distribution of the required longitudinal steel.

5.3.4 Ultimate Compression Strain

Examination of Figure 5.41 indicates that the ultimate compressive strain (at first hoop fracture) is greater in each case in the 8 bar unit than the 12 bar units. This appears to be because the length over which yield penetration can spread is greater in the internal diamond of an 8 bar unit than the internal octagon of a 12 bar unit. This would also be the reason for first fracture of an inner hoop rather than an outer hoop.

A comparison of the theoretical and experimental ultimate compressive strains can be seen in Table 5.3. The theoretical ultimate concrete strain was calculated from Baker (Equation 5.4) and Corley (Equation 5.5):

Baker

$$\epsilon_{cu} = 0.0015 \left[1 + 150\rho_s + (0.7 - 10\rho_s) \frac{d}{c} \right] \leq 0.01 \quad (5.4)$$

Corley

$$\epsilon_{cu} = 0.003 + 0.02 \frac{b}{Z} + \left(\frac{\rho_s f_{yh}}{137.8} \right)^2 \quad (5.5)$$

where ρ_s = volumetric hoop steel ratio

d = effective depth of section

c = neutral axis depth (at the ultimate moment)

b = width of beam

Z = distance from the critical section to the point of contraflexure.

The ratios of $\frac{d}{c}$ and $\frac{b}{Z}$ were considered to be 1.0 and zero respectively for the eccentric units, and of course zero for the axially loaded units.

These equations were developed from test results on simply supported beams (Corley) and have resulted in different criteria to govern what should be designated as ultimate concrete strain.

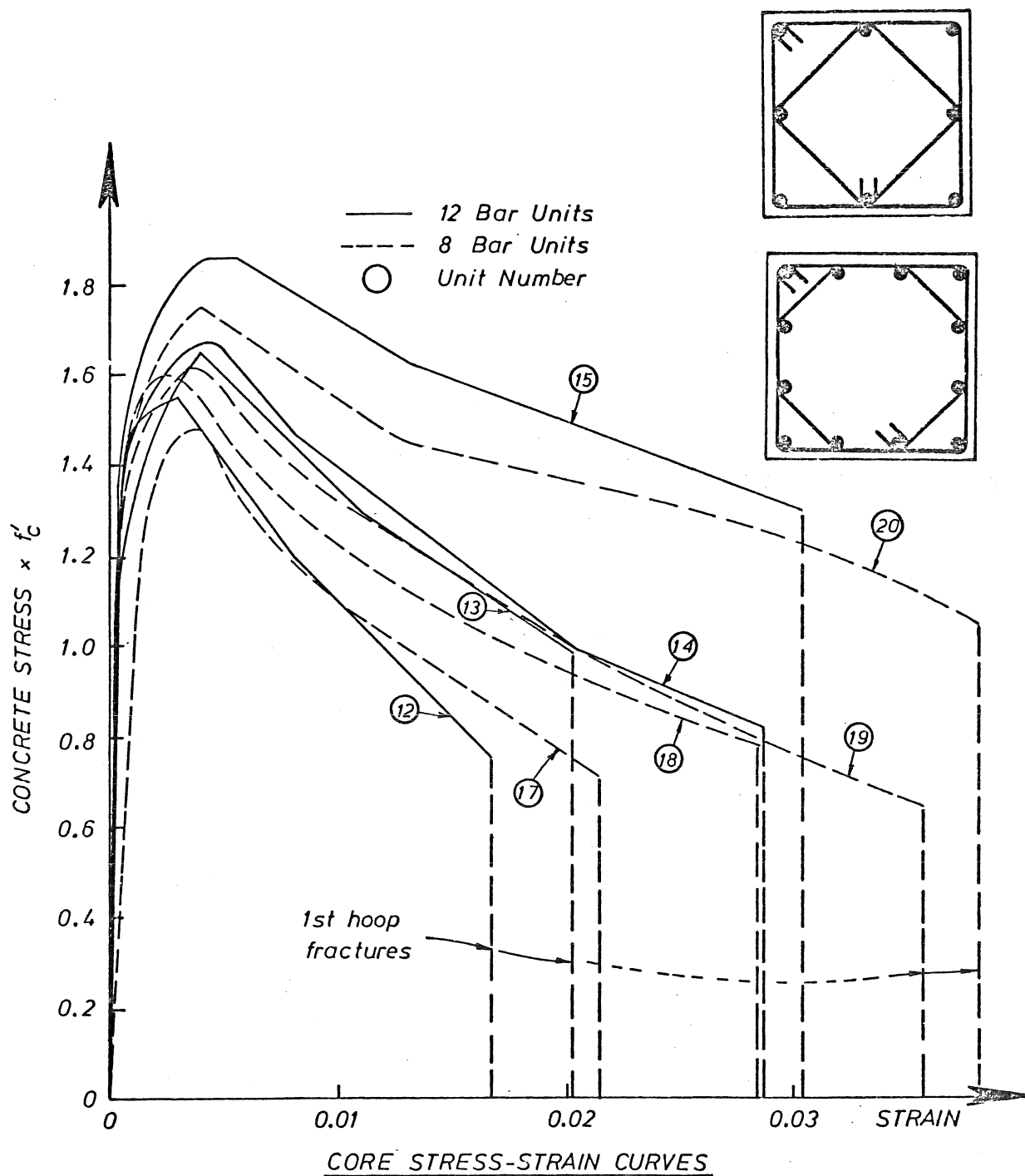


FIGURE 5.41 : Confinement Due to Distribution of Longitudinal Steel

TABLE 5.3 : Comparison of Ultimate Concrete Strains

UNIT	ρ_s	f_{yh}	Baker Eq. 5.4	Corley Eq. 5.5	Exp.	Exp. Baker	Exp. Corley
2	.0182	309	.0056	.0047	.0223	3.98	4.74
3	"	"	"	.0047	.0215	3.84	4.57
4	"	"	.0064	.0047	.0743*	11.61	15.81
5	"	"	"	.0047	.0609*	9.52	12.96
6	.0174	"	.0054	.0045	.0325	6.02	7.22
7	"	"	"	.0045	.0271	5.02	6.02
8	"	"	.0062	.0045	.0649*	10.47	14.42
12	.0140	309	.0047	.0040	.0167	3.55	4.18
13	.0182	"	.0056	.0047	.0203	3.63	4.32
14	.0224	296	.0065	.0053	.0289	4.45	5.45
15	.0309	"	.0085	.0074	.0304	3.58	4.11
17	.0134	309	.0045	.0039	.0214	4.76	5.49
18	.0174	"	.0054	.0045	.0287	5.31	6.38
19	.0213	296	.0063	.0051	.0359	5.70	7.04
20	.0293	"	.0081	.0070	.0382	4.72	5.46
22	.0140	309	.0047	.0040	.0238	5.06	5.95
23	.0182	"	.0056	.0047	.0287	5.13	6.11
24	.0224	296	.0065	.0053	.0284	4.37	5.36
25	.0309	"	.0085	.0074	.0323	3.80	4.36
* Peak strain at 1st hoop fracture for eccentric tests							

The ratios of experiment/theory in Table 5.3 are similar to those found by Gill, Park, and Priestley⁽²⁸⁾, and Potangaroa, Park and Priestley⁽⁴²⁾, as are the strains at first hoop fracture for the eccentric units. These generally lie between 2 and 3% for the axially loaded units and 6 to 7.5% for the eccentrically loaded units. In each case there is also an increase in strain at first hoop fracture with increasing confinement ratio.

It was impossible to establish a spalling strain for the dynamic tests, however for the slow axial units it was about 0.004 and for the slow eccentric units it was about 0.005.

5.3.5 Strength of Longitudinal Steel

It would seem from Figure 5.40 that the strength of longitudinal steel has only a minor effect on confinement. Because the longitudinal bars buckle earlier with Grade 275 steel the confinement of the core is reduced and a lower peak stress is reached. It was noted that double buckling of these bars occurred more frequently than with the high yield (Grade 380) steel. The individual graphs (Figures 5.29 ~ 5.32) show excellent behaviour of the falling branch and may in some respects be considered better than the high yield steel. Strain at first hoop fracture is also increased slightly with the Grade 275 steel.

5.3.6 Eccentricity of Loading

For the eccentric tests no stress-strain curve is possible but the comparison between theory and experiment in Figures 5.10, 5.12, 5.16 and 5.18 raises some doubts about using results obtained from axially loaded units for analysis under eccentric loading, especially if large flexural deformations are involved. The graphs show the theory to be conservative beyond peak load or moment indicating that a flatter falling branch is appropriate for members with strain gradients.

Figure 5.5(e), with central lateral displacement plotted against longitudinal strain, shows that only small displacements occur at low longitudinal strains. Displacements become quite significant beyond about 0.004 and rise quite rapidly, and almost linearly in this region.

The ultimate compressive strain (at first hoop fracture) at 0.060 to 0.075 was much higher than obtained from the axial load tests. However, the longitudinal strain adopted for the axially loaded units was the average value. As noted earlier, strain gradients existed in the axially loaded units (typically up to $\pm 20\%$ of average at failure) with hoop fracture always occurring on the side with maximum compression. The ultimate compressive strains noted in Tables 5.1 and 5.3 for axially loaded units are thus conservative.

Although Baker and Corley both make allowances for the presence of strain gradient when predicting ultimate concrete strain the ratios shown in Table 5.3 for experiment/theory are still of the same order of magnitude for eccentrically loaded units as for axially loaded units.

CHAPTER SIX

CONCLUSIONS AND FUTURE RESEARCH

6.0 SUMMARY

This chapter draws together the conclusions for the research carried out and makes recommendations for future research.

6.1 CONCLUSIONS

(a) Large strength increases were obtained from the effective confinement of core concrete and rapid loading rates. Concrete core strengths up to 186% of cylinder strength were obtained from these tests

(b) The confinement requirements of DZ 3101⁽¹⁾ Chapter 17 provided excellent confinement of the core concrete for the various axial load levels considered.

(c) Loading rate influenced both peak stress and slope of the falling branch of the core stress-strain curve. For the fast loading rate in these tests (0.0167/s) peak stress and slope of the falling branch were increased by about 25%.

(d) An increase in confinement ratio increased the peak stress attained, the strain at first hoop fracture, and decreased the slope of the falling branch. An increase in hoop set spacing tended to reduce the efficiency of confinement.

(e) The presence of a strain gradient increased the strain at first hoop fracture quite significantly (2 to 3 times the strain in axial load tests). It also resulted in a slower decrease in load and moment with increasing strain which may be considered a better behaviour than predicted by analysis using stress-strain curves from axially loaded tests.

(f) Theoretical predictions of ultimate concrete strain based on accepted equations by Baker and Corley are unrealistic and unduly conservative. Ultimate concrete strain of axially loaded units in these tests ranged from 1.67% to 3.82% and increased with increasing confinement ratio.

A definition of ultimate concrete strain of "the strain at first hoop fracture" is felt to be appropriate for columns.

(g) Early buckling of Grade 275 longitudinal steel reduces the effective confinement of the core concrete, when compared with Grade 380 steel, resulting in a lower peak stress (about 10%), and an increase in strain at first hoop fracture (also about 10%).

(h) An increase in the number of longitudinal steel bars resulted in a better confinement of the core concrete for a given total steel area.

6.2 RECOMMENDATIONS FOR FUTURE RESEARCH

(a) There still remains a need for experimental work to be carried out on full size or near full size test units.

(b) The presence of a strain gradient is not fully understood and its influence, while it appears to be beneficial, needs to be examined.

(c) The increase in cylinder strength of confined core concrete has been established experimentally but a rational theoretical analysis needs to be developed, for both circular and rectangular sections if possible. Such an analysis would need to include the effects evident in these tests such as loading rate, confinement ratio, presence of a strain gradient and distribution of longitudinal steel.

(d) All the units tested had very similar concrete cylinder strengths. Further investigation is necessary to establish the influence of concrete strength on the stress strain relationship for confined concrete.

(e) Five units in this series of tests have been left to be tested at some later date in order to establish the influence of the age of concrete at the time of testing. Particular attention should be paid to any change of stiffness or a more brittle behaviour with age.

APPENDIX AREFERENCES

1. "Draft Code of Practice for the Design of Concrete Structures (DZ 3101)", Standards Association of New Zealand, 1978.
2. SHEIKH, S.A., "Effectiveness of Rectangular Ties as Confinement Steel in Reinforced Concrete Columns", Ph.D. Thesis, University of Toronto, Canada, 1978.
3. KING, J.W.H., "The Effect of Lateral Reinforcement in Reinforced Concrete Columns", The Structural Engineer, Vol. 24, No. 7, July 1946, pp.355-388.
4. KING, J.W.H., "Further Notes on Reinforced Concrete Columns", The Structural Engineer, Vol. 24, Nov. 1946, pp.609-616.
5. KING, J.W.H., "Some Investigations of Effect of Core Size and Steel and Concrete Quality in Short Reinforced Concrete Columns", Magazine of Concrete Research, Vol. 2, Jan. 1949.
6. CHAN, W.W.L., "The Ultimate Strength and Deformation of Plastic Hinges in Reinforced Concrete Frameworks", Magazine of Concrete Research, Vol. 7, No. 21, Nov. 1955, pp. 121-132.
7. BRESLER, B., and GILBERT, P.H., "Tie Requirements for Reinforced Concrete Columns", ACI Journal, Proceedings Vol. 58, No. 5, November, 1961, pp.555-569.
8. PFISTER, J.F., "Influence of Ties on the Behaviour of Reinforced Concrete Columns", ACI Journal, Proceedings Vol. 61, No. 5, May 1964, pp.521-536.
9. SZULCYNISKI, T., and SOZEN, M.A., "Load-Deformation Characteristics of Reinforced Concrete Prisms with Rectilinear Transverse Reinforcement", Structural Research Series No. 224, Civil Engineering Studies, University of Illinois, Urbana, Sept. 1961, 54 pp.
10. ROY, H.E.H., and SOZEN, M.A., "A Model to Simulate the Responses of Concrete to Multi-Axial Loading", Structural Research Series No.268, Civil Engineering Studies, University of Illinois, Urbana, June 1963.
11. ROY, H.E.H., and SOZEN, M.A., "Ductility of Concrete", Proceedings of the International Symposium on the Flexural Mechanics of Reinforced Concrete, ASCE - ACI, Miami, November 1964, pp. 2130-224.

12. BERTERO, V.V., and FELIPPA, C., "Discussion of 'Ductility of Concrete', by H.E.H. Roy and M.A. Sozen", Proceedings of the International Symposium on the Flexural Mechanics of Reinforced Concrete, ASCE - ACI, Miami, November 1964, pp. 227-234.
13. STOCKL, S., "Discussion of 'Ductility of Concrete', by H.E.H. Roy and M.A. Sozen", Proceedings of the International Symposium on the Flexural Mechanics of Reinforced Concrete, ASCE - ACI, Miami, November 1964, pp. 225-227.
14. HUDSON, Fred M., "Reinforced Concrete Columns: Effects of Lateral Tie Spacing on Ultimate Strength", Paper No. 10, Symposium on Reinforced Concrete Columns, ACI Special Publication SP.13, 1966, pp. 235-244.
15. SOLIMAN, M.T.M., YU, C.W., "The Flexural Stress-Strain Relationship of Concrete Confined by Rectangular Transverse Reinforcement", Magazine of Concrete Research, Vol. 19, No. 61, Dec. 1967, pp. 223-238.
16. SHAH, S., and RANGAN, B.V., "Effects of Reinforcement on Ductility of Concrete", Journal of the Structural Division, ASCE, ST6, June 1970, pp.1167-1184.
17. SOMES, Normal F., "Compression Tests on Hoop-Reinforced Concrete", Journal of the Structural Division, Proceedings of the American Society of Civil Engineers, ST7, July 1970, pp.1495-1509.
18. KENT, D.C., PARK, R., "Flexural Members with Confined Concrete", Journal of the Structural Division, ASCE, Vol. 97, ST7, July 1971, pp.1969-1990.
19. SARGIN, M., "Stress-Strain Relationships for Concrete and the Analysis of Structural Concrete Sections", Study No. 4, Solid Mechanics Division, University of Waterloo, Waterloo, Canada, 1971, 167 pp.
20. SARGIN, M., GHOSH, S.K., and HANDA, U.K., "Effects of Lateral Reinforcement Upon the Strength and Deformation Properties of Concrete", Magazine of Concrete Research, Vol. 28, No.75-76, June-Sept., 1971, pp. 99-110.
21. BURDETTE, Edwin G., and HILSDORF, Hubert K., "Behaviour of Laterally Reinforced Concrete Columns", Journal of the Structural Division, Proceedings of the American Society of Civil Engineers, ST2, February 1971, pp.587-602.
22. BUNNI, N.G., "Rectangular Ties in Reinforced Concrete Columns", ACI Special Publication SP50-8, 1975, pp.193-210.
23. KAAR, P.H., FIORATO, A.E., CARPENTER, J.E., and CORLEY, W.G., "Limiting Strains of Concrete Confined by Rectangular Hoops", Tentative Report, Research and Development, Construction Technology Laboratories, Portland Cement Association, PCA R/D Ser. 1557, January 1977.

24. VALLENAS, J., BERTERO, V.V., and POPOV, E.P., "Concrete Confined by Rectangular Hoops and Subjected to Axial Loads", Earthquake Engineering Research Centre, College of Engineering, University of California, Berkeley, California, Report No. UCB/EERC-77/13, August 1977, 114 pp.
25. LESLIE, P.D., "Ductility of Reinforced Concrete Bridge Piers", Master of Engineering Report, University of Canterbury, New Zealand, 1974.
26. STURMAN, G.M., SHAH, S.P., and WINTER, G., "Effect of Flexural Strain Gradients on Microcracking and Stress-Strain Behaviour of Concrete", ACI Journal, Proceedings Vol. 62, No. 7, July 1965, pp. 805-822.
27. HOGNESTAD, E., HANSON, N.W., and MCHENRY, D., "Concrete Stress Distribution in Ultimate Strength Design", ACI Journal, Proceedings Vol. 52, No. 12, Dec. 1955, pp. 455-579.
28. GILL, W.D., PARK, R., and PRIESTLEY, M.J.N., "Ductility of Rectangular Reinforced Concrete Columns With Axial Load", Research Report 79-1, Department of Civil Engineering, University of Canterbury, February 1979.
29. PARK, R., PRIESTLEY, M.J.N., and GILL, W.D., "Ductility of Square Confined Reinforced Concrete Columns", Paper submitted to ASCE.
30. PARK, R., and PRIESTLEY, M.J.N., "Code Provisions for Confining Steel in Potential Plastic Hinge Regions of Columns in Seismic Design".
31. "Building Code Requirements for Reinforced Concrete (ACI 318-77)" American Concrete Institute, Detroit, 1977, 102 pp.
32. "Recommended Lateral Force Requirements and Commentary", Seismology Committee, Structural Engineers Association of California, 1975, 21 pp plus commentary and appendices.
33. "Tentative Provisions for the Development of Seismic Regulations for Buildings", Applied Technology Council, US Government Printing Office, Washington, 1978, 505 pp.
34. "Analysis and Design of Reinforced Concrete Bridge Structures", ACI Committee 343, American Concrete Institute, Detroit, 1977, 116 pp.
35. OKUBO, T., and IWASAKI, T., "Summary of Experimental and Analytical Seismic Research Recently Performed on Highway Bridges", Proceedings of a Workshop on Seismic Problems Related to Bridges, Applied Technology Council, Palo Alto, California, January 1979.
36. "Design Essentials in Earthquake Resistant Buildings", Architectural Institute of Japan, Tokyo, 1970, 295 pp.

37. "Ductility of Bridges with Reinforced Concrete Piers", CDP 810/A, Ministry of Works and Development, April 1975 (plus December 1977 amendment), 109 pp.
38. "Highway Design Brief", CDP 701/D, Ministry of Works and Development, September 1978 (plus November 1978 addendum), 52 pp.
39. BAKER, A.L.L., and AMARKONE, A.M.N., "Inelastic Hyperstatic Frames Analysis", Proceedings of International Symposium on the Flexural Mechanics of Reinforced Concrete", ASCE - ACI, Miami, Nov. 1964, pp. 85-142.
40. PRIESTLEY, M.J.N., PARK, R., and NG, K.H., "Seismic Behaviour of Reinforced Concrete Bridge Piers", Master of Engineering Report, University of Canterbury, New Zealand, 1976.
41. PARK, R., and PAULAY, T., "Reinforced Concrete Structures", John Wiley and Sons, New York, 1975, 769 pp.
42. POTANGAROA, R., PARK, R., and PRIESTLEY, M.J.N., "Ductility of Spirally Reinforced Concrete Columns Under Seismic Loading", Master of Engineering Report, University of Canterbury, New Zealand, 1979.

Classn:

THE STRESS STRAIN RELATIONSHIP FOR CONFINED CONCRETE :
RECTANGULAR SECTIONS.

Bryan D. Scott

ABSTRACT:

An experimental investigation of square confined concrete columns subjected to concentric or eccentric axial loads to failure at slow or dynamic loading rates. Results are presented for 25 units tested and conclusions made about loading rate, eccentricity, distribution of longitudinal steel and confinement ratio.

Department of Civil Engineering, University of Canterbury,
Master of Engineering Report, 1980.